CANADIAN THESES ON MICROFICHE

I.S.B.N.

THESES CANADIENNES SUR MICROFICHE

National Library of Canada
Collections Development Branch

Canadian Theses on
Microfiche Service

Ottawa, Canada
K1A 0N4

Bibliothèque nationale du Canada
Direction du développement des collections

Service des thèses canadiennes
sur microfiche

## NOTICE

The quality of this microfiche is heavily dependent upon the quality of the original thesis submitted for microfilming. Every effort has been made to ensure the highest quality of reproduction possible.

If pages are missing, contact the university which granted the degree.

Some pages may have indistinct print especially if the original pages were typed with a poor typewriter ribbon or if the university sent us a poor photocopy.

Previously copyrighted materials (journal articles, published tests, etc.) are not filmed.

Reproduction in full or in part of this film is governed by the Canadian Copyright Act, R.S.C. 1970, c. C-30. Please read the authorization forms which accompany this thesis.

THIS DISSERTATION
HAS BEEN MICROFILMED
EXACTLY AS RECEIVED

## AVIS

La qualité de cette microfiche dépend grandement de la qualité de la thèse soumise au microfilmage. Nous avons tout fait pour assurer une qualité supérieure de reproduction.

S'il manque des pages, veuillez communiquer avec l'université qui a conféré le grade.

La qualité d'impression de certaines pages peut laisser à désirer, surtout si les pages originales ont été dactylographiées à l'aide d'un ruban usé ou si l'université nous a fait parvenir une photocopie de mauvaise qualité.

Les documents qui font déjà l'objet d'un droit d'auteur (articles de revue, examens publiés, etc.) ne sont pas microfilmés.

La reproduction, même partielle, de ce microfilm est soumise à la Loi canadienne sur le droit d'auteur, SRC 1970, c. C-30. Veuillez prendre connaissance des formules d'autorisation qui accompagnent cette thèse.

LA THÈSE A ÉTÉ
MICROFILMÉE TELLE QUE
NOUS L'AVONS REÇUE

NL-339 (r. 82/08)

Canada

0-315-06041-7

National Library of Canada | Bibliothèque nationale du Canada

Canadian Theses Division | Division des thèses canadiennes

Ottawa, Canada
K1A 0N4

53961

## PERMISSION TO MICROFILM — AUTORISATION DE MICROFILMER

• Please print or type — Écrire en lettres moulées ou dactylographier

Full Name of Author — Nom complet de l'auteur

DRAGAN KRSTIC

Date of Birth — Date de naissance

NOV. 25, 41

Country of Birth — Lieu de naissance

YUGOSLAVIA

Permanent Address — Résidence fixe

1604-89ST
EDMONTON
T6K 2A9

Title of Thesis — Titre de la thèse

GEOCHRONOLOGY OF THE CHARLEBOIS LAKE AREA, NORTHEASTERN SASK.

University — Université

U OF A

Degree for which thesis was presented — Grade pour lequel cette thèse fut présentée

M. Sc

Year this degree conferred — Année d'obtention de ce grade

1982

Name of Supervisor — Nom du directeur de thèse

DR H. BAADSGAARD

Permission is hereby granted to the NATIONAL LIBRARY OF CANADA to microfilm this thesis and to lend or sell copies of the film.

The author reserves other publication rights, and neither the thesis nor extensive extracts from it may be printed or otherwise reproduced without the author's written permission.

L'autorisation est, par la présente, accordée à la BIBLIOTHÈQUE NATIONALE DU CANADA de microfilmer cette thèse et de prêter ou de vendre des exemplaires du film.

L'auteur se réserve les autres droits de publication; ni la thèse ni de longs extraits de celle-ci ne doivent être imprimés ou autrement reproduits sans l'autorisation écrite de l'auteur.

SEPT. 28, 81

Date

Signature

NL-91 (4/77)

THE UNIVERSITY OF ALBERTA

# GEOCHRONOLOGY OF THE CHARLEBOIS LAKE AREA, NORTHEASTERN SASKATCHEWAN

by

© DRAGAN KRSTIC

A THESIS

SUBMITTED TO THE FACULTY OF GRADUATE STUDIES AND RESEARCH

IN PARTIAL FULFILMENT OF THE REQUIREMENTS FOR THE DEGREE

OF MASTER OF SCIENCE IN GEOLOGY

DEPARTMENT OF GEOLOGY

EDMONTON, ALBERTA

FALL, 1981

THE UNIVERSITY OF ALBERTA

RELEASE FORM

NAME OF AUTHOR ....DRAGAN KRSTIC.....

TITLE OF THESIS ....GEOCHRONOLOGY OF THE CHARLEBOIS LAKE AREA, NORTHEASTERN SASKATCHEWAN.....

DEGREE FOR WHICH THESIS WAS PRESENTED ....M.Sc.....

YEAR THIS DEGREE GRANTED .....1981.....

Permission is hereby granted to THE UNIVERSITY OF ALBERTA LIBRARY to reproduce single copies of this thesis and to lend or sell such copies for private, scholarly or scientific research purposes only.

The author reserves other publication rights, and neither the thesis nor extensive extracts from it may be printed or otherwise reproduced without the author's written permission.

(Signed) .....

PERMANENT ADDRESS:

....1604 - 89 Street,.....

....Edmonton, Alberta.....

....T6K 2A9.....

DATED ..July 31,..... 1981

THE UNIVERSITY OF ALBERTA

FACULTY OF GRADUATE STUDIES AND RESEARCH

The undersigned certify that they have read, and recommend to the Faculty of Graduate Studies and Research, for acceptance, a thesis entitled .....
GEOCHRONOLOGY OF THE CHARLEBOIS LAKE AREA,
NORTHEASTERN SASKATCHEWAN
submitted by DRAGAN KRSTIC
in partial fulfilment of the requirement for the degree of MASTER OF SCIENCE IN GEOLOGY.

A. Baadsgaard
Co-Supervisor

G. C. Cummings
Co-Supervisor

J. Thorpe

K. Muehlenbachs

DATE July 31, 1981

## ABSTRACT

Whole rock Pb-Pb and Rb-Sr isotopic results indicate an age of deposition of less than 2400-2470 m.y. for the sedimentary precursors of the Charlebois Lake complex. The data also indicate a major metamorphism of the precursors during the Hudsonian metamorphic event which, in this area, ended 1750 m.y. ago. U-Th-Pb determinations carried out on cogenetic uraninite and monazite-rich mineral fractions from granodioritic granofels and migmatite members of the Charlebois Lake complex establish open system chemical behaviour 1750-1797 m.y. ago. Taken as a whole, the geochronological evidence suggests the uranium mineralization is a result of the local remobilization of uranium-rich sediments during the Hudsonian metamorphic event. The geochronological conclusions agree well with the geological conclusions of Morra (1977).

## ACKNOWLEDGEMENTS

I wish to express my sincere gratitude to Dr. H. Baadsgaard for introducing me to the world of isotope geology, his assistance and continual encouragement. The generosity of Dr. G.L. Cumming for his time, advice and assistance is deeply appreciated. The project was suggested and the majority of samples were provided by Dr. G.L. Cumming who also wrote most of the computer programs used for the data analysis. Without his help the completion of this work would not have been possible. Dr. R.D. Morton prepared a polished section of the Sickle Lake sample and separated uranium mineral fractions. For this and his interest in the progress of this project I am grateful. I am indebted to H. McCullough and L. Tober who provided much support and who were responsible for the excellent condition and performance of the mass spectrometers. Ms. Muriel Tait is acknowledged for her expert typing and deciphering my handwriting.

Special thanks are extended to my wife Milica and to my two daughters Liliana and Sasha for their constant understanding and cooperation and for all their evenings and weekends spent without me, while this project was in progress.

TABLE OF CONTENTS


| CHAPTER | | PAGE |
|---|---|---|
| I | INTRODUCTION | 1 |
| II | REGIONAL AND LOCAL GEOLOGY | 3 |
| III | RESULTS AND DISCUSSION | 23 |
| | U-Th-Pb Results | 27 |
| | Pb-Pb Results | 28 |
| | Rb-Sr Results | 65 |
| IV | SUMMARY AND CONCLUSIONS | 83 |
| | REFERENCES | 89 |
| | APPENDIX I | 95 |
| | U-Th-Pb Systematics | 95 |
| | Pb-Pb Systematics | 99 |
| | Rb-Sr Systematics | 109 |
| | APPENDIX II | 113 |
| | General Laboratory Procedures | 113 |
| | Pb-Pb Analyses | 114 |
| | U-Th-Pb Analyses | 118 |
| | Rb-Sr Analyses | 121 |

## LIST OF TABLES


| TABLE | | PAGE |
|---|---|---|
| I | TABLE OF STRATIGRAPHIC UNITS | 14 |
| II | U-Th-Pb CONCENTRATION DATA | 29 |
| III | U-Th-Pb APPARENT AGE DATA | 30 |
| IV | U-Th-Pb ISOTOPIC RATIO DATA | 31 |
| V | Pb-Pb ANALYTICAL DATA | 39 |
| VI | Rb-Sr ANALYTICAL DATA | 66 |
| VII | GENERALIZED PRECAMBRIAN GEOCHRONOLOGY OF THE CHARLEBOIS LAKE AREA | 84 |
| VIII | ISOTOPIC ANALYSES OF NBS SRM-981 COMMON LEAD STANDARD | 117 |
| IX | ISOTOPIC ANALYSES OF RUBIDIUM AND STRONTIUM STANDARDS | 122 |

## LIST OF FIGURES


| FIGURE | | PAGE |
|---|---|---|
| 1. | Lithostructural subdivision of northern Saskatchewan | 4 |
| 2. | Metamorphic map of northern Saskatchewan | 9 |
| 3. | Geological map of the Charlebois Lake area | 11 |
| 4. | Sample location map | 24 |
| 5. | Concordia diagram for uraninite and monazite-rich mineral fractions | 32 |
| 6. | Pb-Pb diagram for whole rock samples from the "Pegasus Lake Area" | 44 |
| 7. | Pb-Pb diagram for whole rock samples from the "Old Camp Area" | 46 |
| 8. | Pb-Pb diagram for some granodioritic granofels and migmatite whole rock samples | 49 |
| 9. | Pb-Pb diagram for a feldspar-whole rock pair | 52 |
| 10. | Three stage Pb-Pb model history for whole rock systems from the Charlebois Lake area | 57 |
| 11. | Pb-Pb diagram for whole rock samples from the Charlebois Lake area | 60 |
| 12. | Pb-Pb diagram for whole rock late felsic dyke samples | 62 |
| 13. | Pb-Pb diagram for whole rock late felsic dyke samples | 63 |
| 14. | Rb-Sr diagram for whole rock samples from the "Pegasus Lake Area" | 70 |
| 15. | Rb-Sr diagram for whole rock samples from the "Old Camp Area" | 73 |
| 16. | Rb-Sr diagram for combined whole rock data from the "Pegasus Lake Area" and the "Old Camp Area" | 76 |

LIST OF FIGURES (cont'd)


| FIGURE | | PAGE |
|---|---|---|
| 17. | Rb-Sr diagram for whole rock late felsic dyke samples | 81 |
| 18. | Concordia diagram | 98 |
| 19. | Lead growth curve | 101 |
| 20. | Two stage lead evolution system | 104 |
| 21. | Three stage lead evolution system | 106 |
| 22. | Rb-Sr isochron diagram | 110 |
| 23. | Sr growth curve diagram | 111 |

# CHAPTER I

## INTRODUCTION

Because of sharply rising prices of uranium over the last 20 to 30 years, low grade uranium deposits of pegmatite type have become increasingly attractive to uranium exploration companies.

This type of deposit is found in Precambrian Shield areas throughout the world, most commonly occurring in the regionally metamorphosed terrains that have been extensively granitized. The Canadian Shield contains a large number of these sub-economic deposits and although no serious exploitation has been attempted so far, these deposits continue to be studied and assessed as potential uranium producers in the future.

One of the better known U-pegmatite deposits in the Churchill province is in the Charlebois Lake area in northeastern Saskatchewan. The geology of the area has been studied in detail on a few occasions in the past and therefore it is considered that relatively complete geological documentation for the area is available.

The purpose of this study was to investigate the chronology and evolution of the Charlebois Lake area by examining U-Th-Pb, Pb-Pb and Rb-Sr isotope systems from various rock units of the Charlebois Lake complex. It was hoped that these isotopic systems would record events that affected the area and would provide insight into the

origin of the Charlebois Lake complex and associated U-mineralization.

The samples were collected so that they represent the major units of the complex: granitic to tonalitic gneiss, mineralized granodioritic granofels, biotite and hornblende gneiss, amphibolite and late felsic dyke.

## CHAPTER II

## REGIONAL AND LOCAL GEOLOGY

The Charlebois Lake area is located in northeastern Saskatchewan, about 160 km west of the Manitoba border and 50 km south of the Northwest Territories border. Approximate coordinates are 59°50'N and 104°40'W (Figure 1). Although the geological surveys of northern Saskatchewan were initiated at the beginning of this century and intensified after the Second World War, with the increasing need for uranium most of the efforts were concentrated primarily north of Lake Athabasca and west of the Charlebois Lake area.

The first serious reconnaissance work in the area was done by Mawdsley (1950) who described a number of radioactive occurrences. This work was followed by more detailed field work, mapping, petrological and petrographic studies by Mawdsley (1952), Cumming (1952) and Kirkland (1952). From that time on, for a period of about twenty years, not much activity has been reported in this area.

In the meantime regional work on the Saskatchewan Shield continued. Geophysical surveys of northern Saskatchewan were carried out. The gravity and aeromagnetic results suggested that the Saskatchewan crystalline basement was composed of several distinct tectonic units

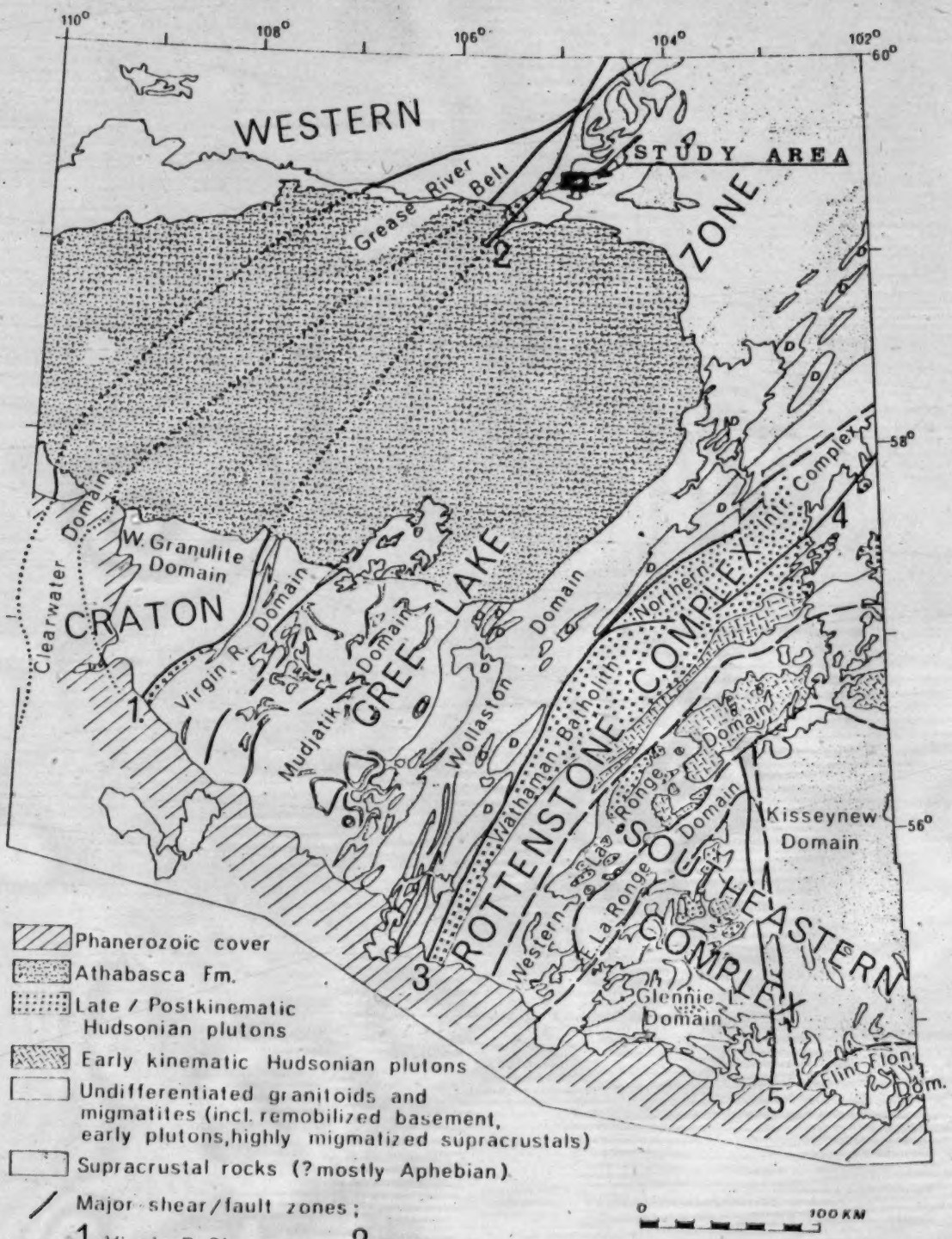


Figure 1. Lithostructural subdivision of Northern Saskatchewan (from Lewrey et al. 1978).

which are traceable to the Cordillerian fold belt. As such they were perceived as deep crustal entities. Further geological studies of the Saskatchewan Precambrian basement were of broader scope and included structural, petrological, geochemical and also a number of geochronological investigations.

Four lithostructural units presently recognized in Saskatchewan were discussed and described in a number of important papers, particularly those by Lewrey et al. (1978), Burwash (1978,1979), Sibbald et al. (1976), Burwash et al. (1962,1969,1970), and Koster et al. (1970). A few of these publications also dealt with main events leading to the final stabilization of this part of the Churchill structural province. As a result it is now certain that much of the Archean craton in Saskatchewan was reactivated during the Hudsonian orogeny which lasted from 1900 m.y. ago to 1700 m.y. ago (Burwash et al. 1969). Reactivation consisting of extensive granitization, K-metasomatism and polymetamorphism affected much of the Saskatchewan Shield.

The four lithostructural units of the Saskatchewan Shield are shown in Figure 1. Significant features of these northeasterly trending units are described in detail in the paper by Lewrey et al. (1978). A brief summary of two of these units will be given here; since the Charlebois Lake area is part of one unit, it is geogra-

phically close to the other and together they contain most of the radioactive anomalies discovered so far in Saskatchewan.

The first is the Western Craton which occupies the northeast corner of Alberta and western Saskatchewan. It is comprised of an Archean basement complex of granitoids, migmatites and other high grade metamorphic rocks. Reactivation of the Craton during the Hudsonian orogeny resulted in a series of younger mobile belts which surround the older stable blocks (Beck 1969). Hudsonian overprinting occurred under conditions of lower amphibolite and greenschist facies metamorphism. Here, depending on the degree of reactivation, a range of ages from 2500 m.y. to 1750 m.y. can be observed (Baadsgaard and Godfrey 1970, Sassano et al. 1972, Koeppel 1968).

In this area a large number of uraniferous pegmatite deposits can be found. Most of them are pegmatite deposits of group A (Trembley 1978). One of the more prominent is the Grease River occurrence which is located only about 30 km west of the Charlebois Lake area. Here uranium occurs in massive to faintly foliated granite and in the pegmatites that form part of the Archean basement gneiss complex. The uraniferous pegmatites are of various dimensions and are erratically distributed. Since the pegmatites occur only in the basement granites and granitic gneisses to which they are closely related in

composition, they are regarded as the anatectic fractions of the basement granitic rocks. They are generally coarse-grained and not related to a single large intrusive granite body.

The central part of the Saskatchewan Shield is occupied by the Cree Lake zone. This zone is flanked to the west by the Virgin River domain and to the east by the Wollaston domain. The zone is comprised of mainly Archean granitoids, migmatites and high grade metamorphic rocks. The whole area is characterized by foliated, folded and boudinaged small scale granitoid segregations which might indicate extensive "in situ" anatexis. It is suggested that pressure-temperature conditions throughout most of the Cree Lake zone during the metamorphism were at least as high as those corresponding to the upper amphibolite facies.

Lewrey et al. (1978) state that in the Cree Lake zone "it is probable that the high grade conditions achieved early in the deformational history were maintained at essentially the same level throughout and beyond the close of the major deformational event. Accompanying anatexis was effectively 'in situ' as there is little evidence of large scale intrusion".

Some reference to this statement will be made again in Chapter III when discussing the ages of uraninites and monazites. Metamorphic grade of the zone falls slightly

in the cooler, more brittle, marginal areas of Virgin River and Wollaston domain (Figure 2).

Geochronological studies, although limited mainly to the Wollaston domain and areas south of Athabasca basin, yield a range of ages from 2700 m.y. to 1570 m.y. (Cumming and Scott 1975, Weber et al. 1975, Money et al. 1970).

Uraniferous pegmatite deposits are numerous in the Cree Lake zone. Both Group A and Group B deposits can be found (Trembley 1978). Group B deposits (Charlebois Lake occurrence is a typical representative of this deposit) are characterized by the concordance of the pegmatite layer with stratigraphically lower granitic gneisses and stratigraphically higher mafic-rich gneisses, gradational contacts between the pegmatite and other rock units and much more variable grain size and composition than exhibited by Group A.

In 1974, Fosago Exploration Ltd. carried out an extensive exploration program in the Charlebois-Higginson Lake area, consisting of detailed geological mapping and radioactive surveys in order to study the relative stratigraphic position of the radioactive occurrences. In 1977 F. Morra completed an M.Sc. thesis in which he described the geology and uranium deposits of the Charlebois Lake area. This thesis (along with the work of Cumming (1952), Kirkland (1952) and Mawdsley (1952)) was used as a major source of geological reference in the present study.

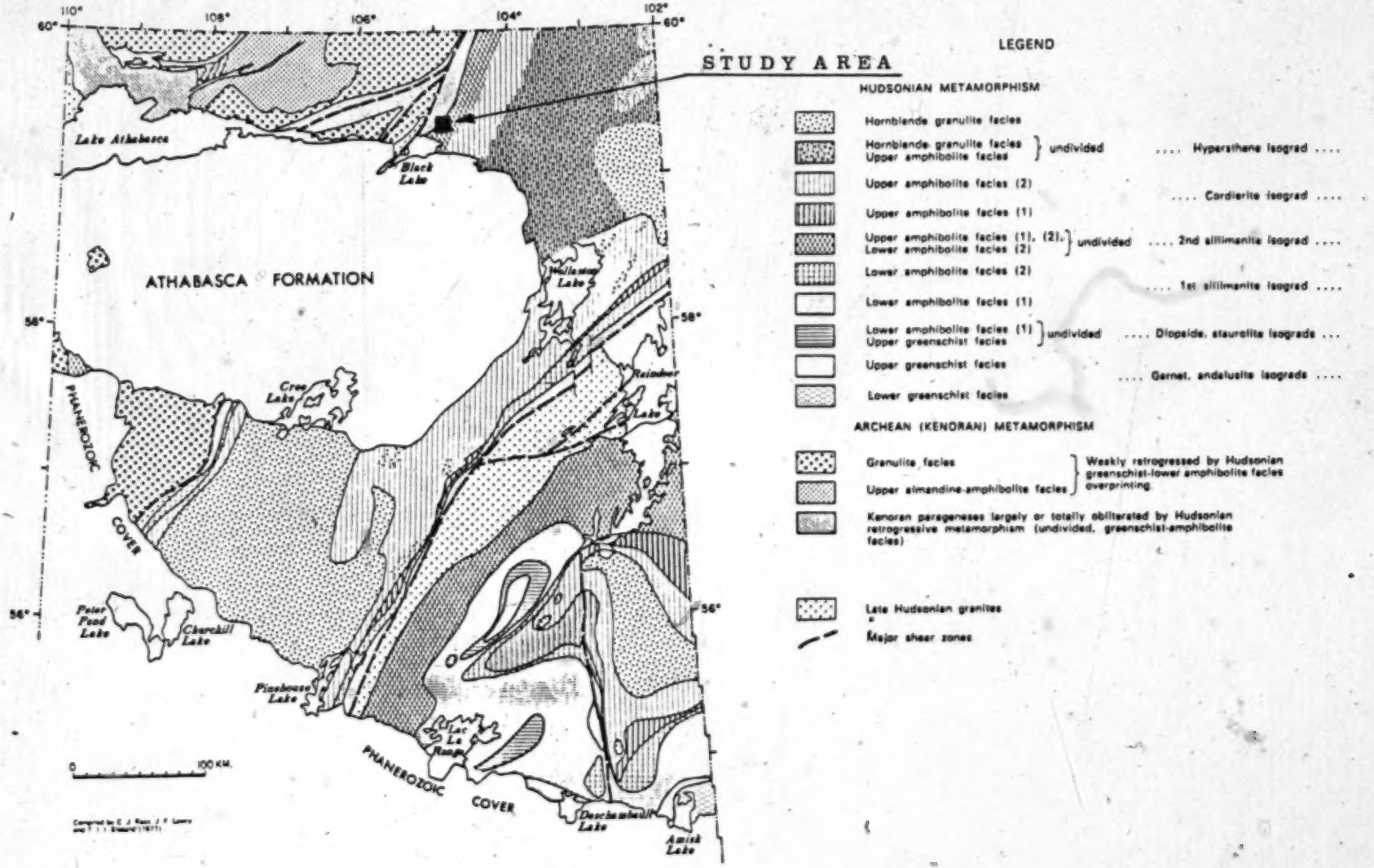


Figure 2. Metamorphic map of the Saskatchewan Shield (from Lewrey et al. 1978).

Most of the Charlebois Lake area which is situated in the northwestern part of the Cree Lake zone and which appears to be the northern extension of the Virgin River domain, is underlain by massive and foliated granitic to tonalitic gneiss. Other lesser rock units are migmatite, granodioritic granofels (or younger intrusive pegmatite, as called by Cumming, 1952), calc-silicate rocks, hornblende gneiss, amphibolite, biotite gneiss and quartzite. Figure 3 (a map adopted from Morra (1977)) gives the relative distribution of these rock units.

All of the rock units in the area are gently to strongly folded with few poorly-exposed faults. The most prominent lineament is represented by the Higginson Lake fault which is believed to be an offset extension of the regionally important Clut Lake fault. North of this fault there are possibly a few more parallel faults: one through Dramnitzke Bay, one immediately north of it, one from Heisler Lake to Sprekley Lake, and others. One of the rare occurrences of the mylonite zone has been observed by Cumming (1952) on the granitic gneiss on the west shore of Sprekley Lake. This area is presumably an extension of the east-west trending fault that originates at Heisler Lake.

The largest number of folds follows the general regional and local fault trends, i.e. axes of the folds have a northeast-southwest direction. The cores of the

SPREKLEY LAKE
UNMAPPED
LENIUK LAKE
UNMAPPED
1a
1c
1b
SPREKLEY LAKE
POCHARLEBOIS LAKE
FOX BAY
CHESHAM LAKE
DRAMMEN LAKE BAY
MACHETE LAKE
OTT LAKE
PEGASUS LAKE
UNMAPPED
104° 50'
58° 30'
58° 25'

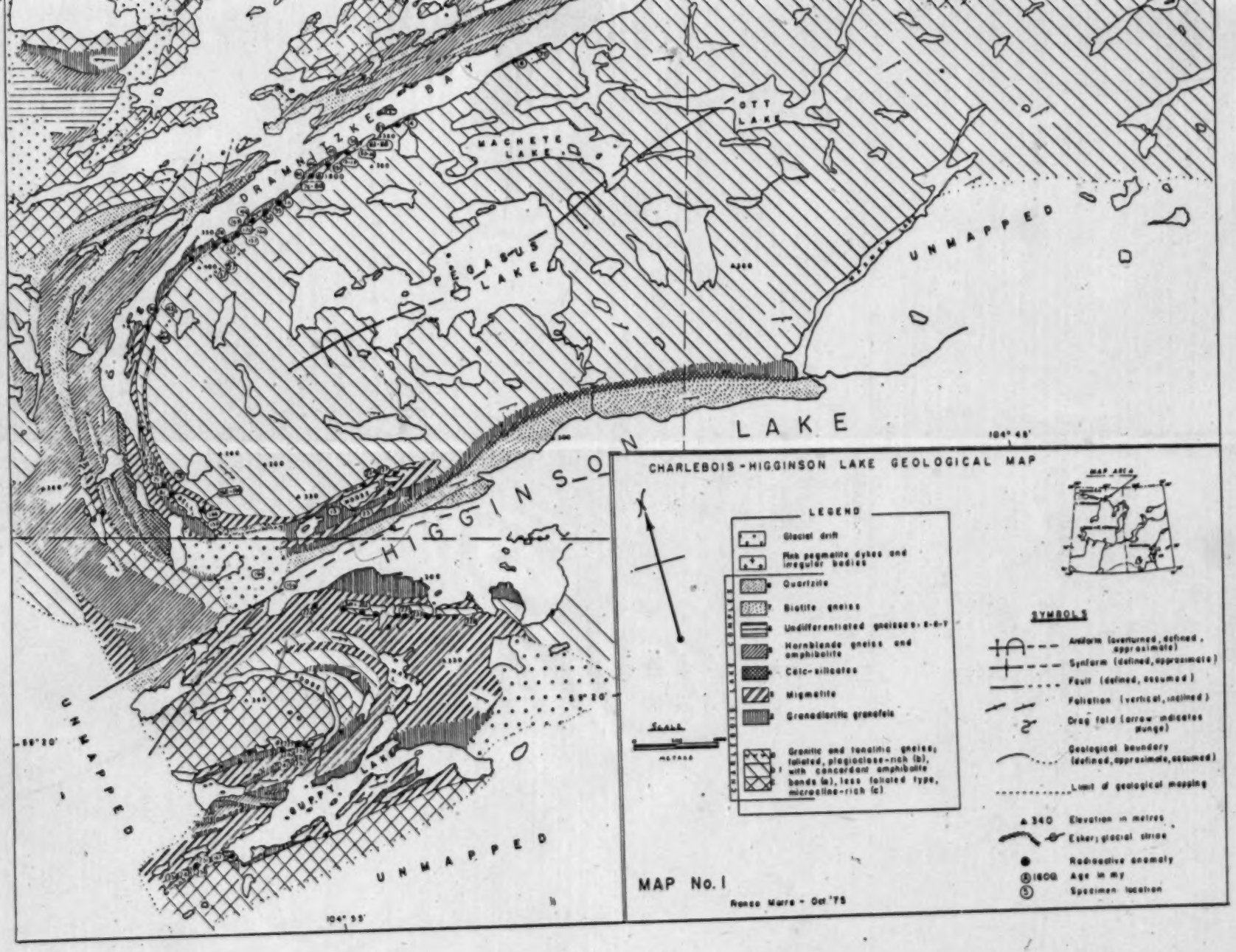


Figure 3. Geological map of the Charlebois Lake Area (from Morra, 1977).

anticlines are occupied by the granitic to tonalitic gneisses while synforms are generally occupied by other rock units, such as biotite, hornblende gneisses, calc-silicates and quartzites.

The granitic to tonalitic gneiss is best represented south of Dramnitzke Bay where it forms the core of the overturned Pegasus Lake anticline. The anticline is flanked on both sides by a metasedimentary sequence which is continuous and regular.

In an unpublished report, Sassano (1974) attempted to correlate the granitic to tonalitic gneiss of this area with the Donaldson Lake gneiss (of Middle Tazin age) from the Beaverlodge area (Sassano 1972). He also suggested that an unconformity separates the granitic and tonalitic gneiss from the rest of the metasedimentary sequence, which he tentatively correlated to the Fay Mine sequence (of Upper Tazin age). Cumming (1952) suggested that the coarse to very coarse grained, mineralized rock which outcrops around Pegasus Lake granitic gneiss is in fact younger intrusive pegmatite.

Based on field observations, stratigraphic and structural characteristics such as concordance of the contacts, regularity of the sequence of the rock units in the antiforms and synforms, petrographic and other laboratory studies, Morra (1977) concluded that "young intrusive pegmatite" (which he calls granodioritic granofels) is a

part of the metasedimentary sequence. He also concluded that the granitic to tonalitic gneiss is the oldest, basal and integral part of the Charlebois Lake metasedimentary complex.

A list of stratigraphic units, as summarized by Morra (1977), is given in Table I.

Since the lower contact of granitic and tonalitic gneiss is not visible in the area, it is believed that the Charlebois Lake complex could have a thickness of up to 3000 meters and that the crystalline basement rocks are not exposed.

The rocks of the area have undergone regional metamorphism in the intermediate amphibolite facies. The presence of sillimanite and garnet associated with biotite, microcline and oliogoclase, along with other metamorphic assemblages, is widespread (Cumming 1952, Morra 1977). This paragenesis was described by Winkler (1967) as the sillimanite-almandine-orthoclase subfacies of the amphibolite facies. Mineral assemblages belonging to the upper limit of amphibolite facies, although not very common, were also found by Morra (1977). This seems to be in good agreement with regional metamorphic patterns. Lewrey et al. (1978) suggested that upper amphibolite conditions have persisted throughout the Cree Lake zone with a very gentle decrease in metamorphic grade towards the eastern and western margins of the zone. The grade

## TABLE I

## TABLE OF STRATIGRAPHIC UNITS (FROM MORRA 1977)

| | | |
|---|---|---|
| Recent and Pleistocene | | Alluvium, lake silt and sand, gravel, eskers, glacial till. |
| | | Major Unconformity |
| Helikian | ATHABASCA GROUP | Athabasca Formation (south of the mapped area). |
| | | Unconformity? |
| | | Martin Formation (west and possibly south of the mapped area). |
| | | Major Unconformity |
| Aphebian | | Pink pegmatite and irregular bodies |
| | | Intrusive contact |
| | CHARLEBOIS LAKE COMPLEX | Quartzite<br>Biotite Gneiss<br>Hornblende Gneiss and Amphibolite<br>Calc-silicates<br>Migmatite<br>Granodioritic Granofels<br>Granitic and Tonalitic Gneiss |

decreases very rapidly within a few kilometers of the margins. In the Virgin River Shear Zone a decrease from granulite facies to lower amphibolite facies takes place within about 13 kilometers. Although the situation in the northern part of the Cree Lake zone is probably not the same as in the areas south of the Athabasca Basin, there are some indications that the metamorphic grade between Charlebois Lake and the Black Lake fault decreases. Johnston (1963,1964) has observed a large volume of schists in the Lytle Lake area. The Grease River area (Costaschuk 1979) which is about 20 km west of the Black Lake fault, has undergone metamorphism in lower amphibolite to greenschist facies. The Grease River area is a part of the Western Craton and not of the Cree Lake zone so this comparison might not be appropriate. Unfortunately there is not enough published evidence to substantiate or disprove similarities between the marginal areas of the Cree Lake zone south and north of the Athabasca sandstone basin.

Based on the pronounced structural concordance of the members of the Charlebois Lake complex, gradational contacts, strong foliation and banding, continuity of the units and the presence of conformably intermixed calc-silicates with all of the other units, Morra (1977) suggested that pre-existing rocks were sediments deposited in dry and shallow marine environments which were subjected to sudden and cyclic changes during the deposition. The

original sedimentary sequence consisted of arkosic arenites, calcareous pelites, sandstones and tuffaceous and pyroclastic material, pelites and feldspathic arenites. The present rocks are mono-metamorphic derivatives of these sediments. The metamorphic potash migration, which has not been on a very large scale, might have been partly responsible for migmatite formation.

The late pink felsic dykes and irregular pegmatitic bodies outcrop at various locations, crosscutting almost all of the other rock units. According to Cumming (1952) and particularly Morra (1977), the contacts between these late rocks and the rest of the units of the Charlebois Lake complex appear to be the only unconformable, intrusive contacts in the area.

No detailed geochronological studies have been carried out so far in the Charlebois Lake or immediately surrounding areas. The only published isotopic data from the Charlebois Lake area are by Cumming et al. (1955), obtained on uranium minerals. Recalculation of original data yields a $^{207}Pb/^{206}Pb$ age of 1765 m.y. and 1785 m.y. for two uranium minerals.

Detailed mineralogical and petrological descriptions of all of the rock units are given by Cumming (1952), Kirkland (1952) and Morra (1977). What follows is only a brief summary of the main features of each of the rock units.

Granitic and tonalitic gneiss

This rock unit represents more than 50% of the exposed rocks in the area. Initially it was described and mapped as "late intrusive formation" or orthogneiss (Mawdsley 1952) and subsequently termed: granite, pegmatite granite, granite gneiss, massive granite etc. It is usually exposed in anticline areas of which a very good example is the overturned Pegasus Lake anticline.

The rock grades from massive, fine-grained, gray gneiss in the center of the anticline to slightly foliated in the outer margins, to strongly foliated (when the biotite content is larger than 8%) near the contacts with the other units.

The gneiss is pinkish in colour, in the more foliated type, and generally K-feldspar content is higher. Grain size varies from 0.5 mm to 1 mm. Concordant amphibolite bands of up to 2 meters thick are present throughout the gneiss but are especially prevalent near the contact with the other units.

The mineralogy is rather monotonous. Quartz, plagioclase, K-feldspar and biotite are the main constituents. The relative proportions of these minerals changes depending on the degree of foliation.

Granodioritic granofels

"Pegmatite granite" (Mawdsley 1950), "young intrusive fine pegmatite" (Cumming 1952) and "granodioritic granofels"

(Morra 1977) are common terms used to describe this rock unit.

It is well represented along the southern shore of Dramnitzke Bay, having a thickness of 30 m to 90 m. It borders the granitic gneiss as a continuous lenticular body which is parallel to the regional foliation. Horizons of granodioritic granofels often alternate with the horizons of migmatite. The contacts are gradational and conformable.

Morra (1977) observes: "Granodioritic granofels does not demonstrate a crosscutting (or intrusive) relationship with the adjacent units anywhere in the area. Its parallelism with the stratigraphically lower granitic to tonalitic gneiss and higher calc-silicate is constant and continuous". He suggests that granofels is the most appropriate term for this rock since it is compatible with the textural and mineralogical characteristics and it does not imply that the rock was either igneous or sedimentary before the metamorphism, while "pegmatite" carries a genetic implication.

Mineralogically, the rock is indistinguishable from a granitic gneiss. Grain size is the main distinguishing feature (3 mm to 30 mm compared to 0.5 mm to 1 mm for granitic gneiss). Granodioritic granofels show very little foliation but the grain size becomes finer and biotite assumes subparallel orientation as one approaches the

contact with the granitic gneiss. The colour is light gray to white, and occasionally dark gray when biotite is very abundant. Besides quartz, plagioclase, K-feldspar and biotite, the rock commonly contains variable amounts of uraninite and secondary uranium minerals, monazite, zircon, sphene and molybdenite.

Migmatite

The migmatites are composed of biotite rich portions and separated lenses of granitic, granodioritic and tonalitic composition. The formation of this rock unit could be due to relatively limited potash migration during the metamorphic event or it could be due to a rather gradual and cyclic change in the depositional environment of the original sediments. Its mineralogical composition is intermediate between two rock types: quartz-feldspathic bands (composition equivalent to granitic gneiss) and biotite rich bands (equivalent to the biotite gneiss). It is suggested (Morra 1977) that in terms of original deposition, migmatites correspond to the transitional period of arkosic and pelitic sedimentation, repeated in short, distinct cycles, which gave rise to conformable and regularly interbedded felsic (arkosic) and mafic (pelitic) bands.

The felsic intercalating bands are mainly composed of quartz, plagioclase and K-feldspar, in various proportions. The mafic bands are biotite-and/or hornblende-rich,

are well foliated and are usually finer grained than felsic bands (approximately 0.5 mm and up to 4 mm, respectively). Garnet rich bands are present and serve as marker-horizons for this unit. Uraninites and molybdenites are common, as well as other accessory minerals such as apatite, sphene, sillimanite, and occasionally pyrite and monazite.

Calc-Silicates

This unit includes amphibole-diopside gneiss, talc-serpentine-carbonate marble and sericite-phlogopite/biotite-diopside gneiss. The horizon of this unit, which stratigraphically occurs between granodioritic granofels and hornblende gneiss, is present on the shore of Charlebois Lake, Sprekley Lake and Dramnitzke Bay. These "softer" gneisses have been gouged away by glaciers and are generally extensively weathered. This rock unit could be up to 400 m thick, appears as a continuous band for several miles and follows the general foliation trend of the area.

Grain size is fine to medium, it generally exhibits a massive habit and is dirty-white to gray-green in colour.

Hornblende gneiss and amphibolite

This unit is best represented north of Dramnitzke Bay where it is closely associated with biotite gneiss in the northeast-southwest trending belt. It contains an increasing amount of biotite towards the contact with

biotite gneiss, suggesting a gradational character between these two units.

The colour of the rock depends on the amount of hornblende and varies from medium gray to dark gray. The grain size is usually fine to very fine (less than 0.5 mm) and habit is massive if the amount of hornblende is more than 50% and little quartz is present. K-feldspar is generally absent or present in small amounts.

Biotite-gneiss

This gneiss is also well represented in the area immediately north and west of Dramnitzke Bay in the northeast-southwest striking belt, and is intimately associated with the hornblende gneiss. The percentage of hornblende increases towards the contact with hornblende gneiss. Morra (1977) states: "This unit is difficult to map because of the presence of numerous granodioritic granofels and hornblende gneiss intercalations. Therefore most of the area mapped as biotite gneiss may also contain hornblende gneiss as well as 3-6 meters thick granodioritic granofels bands". The rock is strongly foliated due to the alignment of biotite grains. It is medium gray in colour and grain size is fine to medium, averaging 0.5 mm. The main constituent minerals are quartz, plagioclase, microcline and biotite. Accessories are metamict zircon, apatite and muscovite, and occasionally sillimanite and sphene.

Quartzite

Stratigraphically this unit should be the youngest member of the Charlebois Lake complex. It is found as small occurrences, beds or lenses within the area, generally following conformable biotite gneiss. The quartzite is not "pure". Quartz content averages 75%, the remaining portion being feldspar with a minor amount of biotite.

Late felsic dykes and irregular bodies

All of the units of the Charlebois Lake complex are crosscut by these late felsic dykes at different localities. The dykes are generally 3-6 meters thick with the grain size ranging from medium to coarse, while irregularly shaped pegmatite bodies occupy substantially larger areas and the grain size is coarse to very coarse (individual grains occasionally reaching 10 cm in diameter). The colour is salmon pink due to the presence of a large amount of microcline. The contact with the other units is sharp and postcrystalline deformation is evident in many areas. Major mineral constituents are microcline, quartz, some plagioclase and very small amounts of biotite.

## CHAPTER III

## RESULTS AND DISCUSSION

A suite, consisting of over forty rock samples was collected during two field trips. First, during the summer of 1976 by Dr. G.L. Cumming of the Physics Department and second, in the fall of 1977, by Dr. Cumming and the author.

Extensive weathering of some of the rock units, transportation and other difficulties did not permit collection of large specimens (by volume), nor did they allow sampling of all the members of the Charlebois Lake complex. The size of the samples ranged from approximately one pound, for the specimens collected along the southern shore and north of Dramnitzke Bay, to a few pounds for the specimens from the center of the Pegasus Lake anticline.

Rock units sampled include granitic to tonalitic gneiss, granodioritic granofels, migmatite, biotite gneiss, hornblende gneiss and late felsic dyke. Sample locations and identification numbers are shown in Figure 4.

For convenience and ease of interpretation, all of the samples are divided and considered as three groups: the "Pegasus Lake Area" group which includes samples 1 to 20, is represented by specimens which range from gray massive granitic to tonalitic gneisses, to more foliated gray to pinkish granitic gneisses and three specimens of

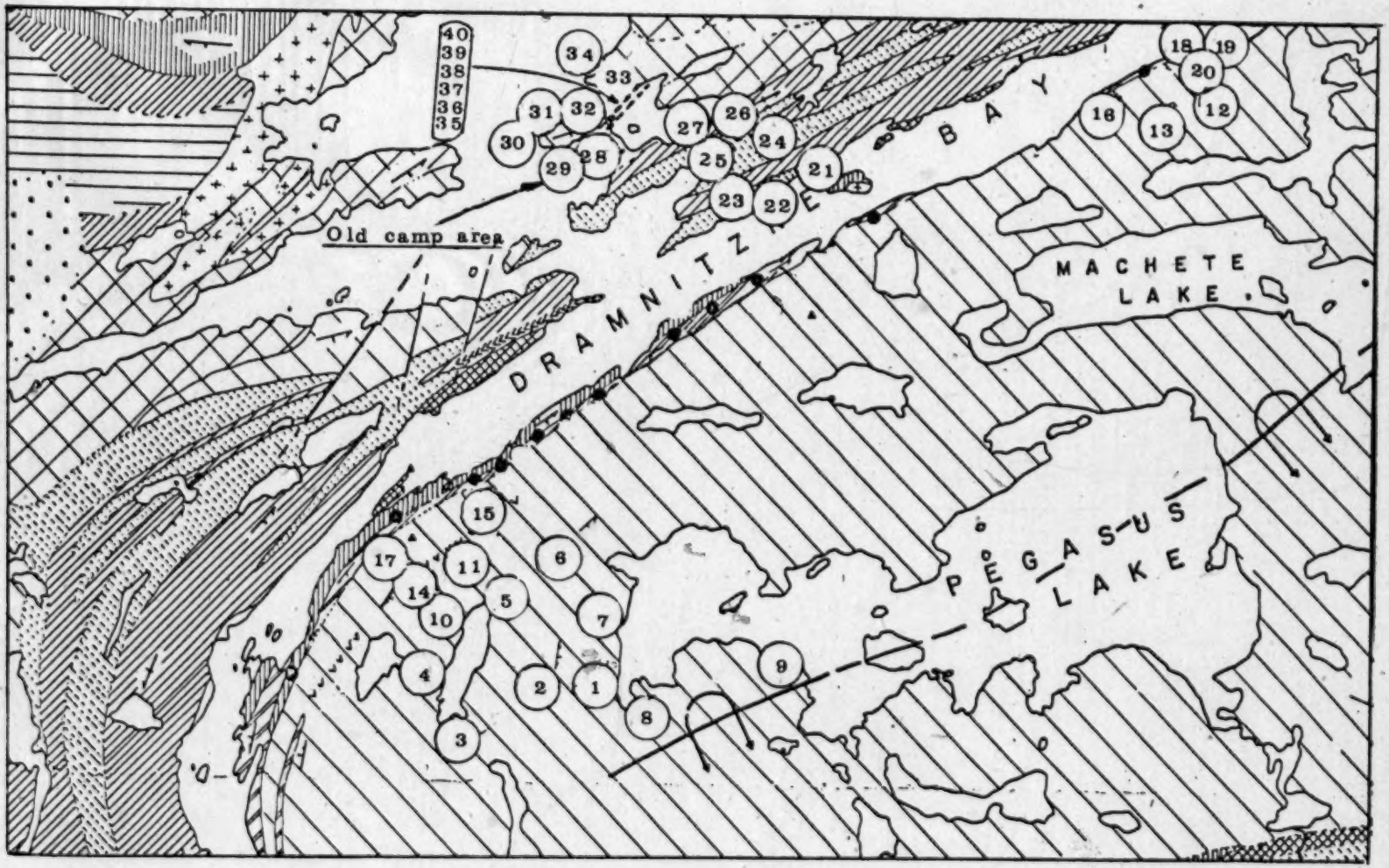


Figure 4. Sample location map.

coarse grained, mineralized granodioritic-granofels.

The area north of Dramnitzke Bay where samples 21 to 34 were collected, was traditionally the field camp area of Mawdsley (1950), Cumming (1952), Kirkland (1952) and Fosago Exploration (Morra 1977). This area will be referred to as the "Old Camp Area". The area is comprised of migmatites along the shore of Dramnitzke Bay, which northward grade to biotite gneiss, hornblende gneiss, culminating with amphibolites, some three to five hundred meters from the shore of Dramnitzke Bay. A not very well defined fault, following the regional and local northeast-southwest trend, appears to be present in the hornblende gneiss-amphibolite area. Northwest of this apparent fault the rocks again grade from gneiss with high mafic content to almost gray granitic gneiss.

The third group of samples (35 to 40) consists of specimens collected from the fifteen foot wide late pink felsic dyke which crosscuts the other rock units in the "Old Camp Area".

The sample size and the fact that not all the members of the Charlebois Lake complex have been represented, have put definite limits on the depth of this study, as will be seen later in this chapter.

Most of the calculations, including isotopic ratios, concentrations, straight line fitting (Cumming et al. 1972), and the drawing of diagrams were done using computer programs written by Dr. G.L. Cumming. Ages and error limits

from the intersections of lines with the concordia or growth curve were calculated using computer programs written by the author.

Whenever a straight line was fitted to a set of points, the errors used in the calculations were at one sigma level. Assigned correlation coefficients were: 0.95 for lead/uranium data, 0.75 for lead/lead data and 0.0 for rubidium/strontium data. Therefore, throughout this study, all the slopes are given at one sigma error level. All the age values obtained from the slope of the line or from the intercepts of lines with the concordia or growth curve, were calculated at two sigma error level including the error resulting from the imperfect fit of the data, as given by MSWD (Mean Squared Weighted Deviates) factor. The MSWD factor is a measure of how well the data points fit the line within the assigned analytical error limits. In the case of a perfect fit, MSWD will have a value of 1. Values higher than 1 suggest that the data points scatter due to "geological" reasons (providing the analytical errors have not been underestimated). Values smaller than 1 indicate that the data points probably fit the line but that the analytical error limits have been overestimated. A very brief treatment of the geochronological theory applicable to the isotopic systems studied in this thesis, along with a set of important general references, are given in Appendix I.

U-Th-Pb Results

Five rock specimens were available for this work. They included three samples of granodioritic granofels (two very coarse grained and one medium grained) from the mineralized area on the southern shore and two samples of migmatite with high whole rock lead-lead ratios from the north shore of Dramnitzke Bay.

The rock samples were crushed and pulverized. Pb-Pb and Rb-Sr analyses were performed on the whole rock powder, after which the heavy minerals were separated. Small relatively clean uraninite grains and monazite-rich fractions were picked out under the microscope from three specimens (18, 19 and 22), "uraninite" from specimen 20 was extracted by leaching the heavy mineral separate with 4N $HNO_3$ and after that the monazite-rich phase was concentrated. Specimen 23 did not contain any visible uraninite so that only a monazite-rich fraction was prepared. One specimen of coarse grained, biotite rich, radioactive pegmatite from Sickle Lake (southwest of Pegasus Lake antiform), collected in 1951 and analysed at the University of Toronto (Cumming 1955) was also available. A polished section was prepared and very small grains of what was assumed to be uranium mineral were separated under the microscope by Dr. R.D. Morton of this department.

The samples were analysed for lead, uranium and some for thorium isotopes. Detailed analytical procedures are

given in Appendix II. The analytical results are presented in Tables II, III and IV. Two sigma errors of 1% were assigned to the $^{207}Pb/^{235}U$, $^{206}Pb/^{238}U$ and $^{208}Pb/^{232}Th$ ratios, as suggested in Appendix II. Lead-uranium ratios are plotted on the standard concordia diagram (Figure 5). The size of the elipses represents the error limits at three sigma level and the subscripts "U" or "M" attached to the sample identification number designates a uraninite or monazite-rich phase.

It should be pointed out that the uranium, thorium and lead concentration results are to be viewed as relative rather than absolute with respect to the analysed specimen. This is particularly so where the total available sample is very small, the phases are impure or where leaching was involved.

The data points in the concordia diagram appear to form two distinctly different trends. One uraninite sample (22U) is concordant and plots on the concordia curve. Two other uraninite separates exhibit normal discordance (18U and 19U), i.e., they plot in the lead loss field. The leached uraninite (20U) exhibits slightly reverse discordance (Baadsgaard 1965). Two monazites plot in the lead loss field (18M and 19M) and the other three show reverse discordance (relatively common behaviour for monazites). The Sickle Lake specimen contains about 30% common lead and shows very high reverse discordance. The high content of common lead makes it

## TABLE II

### U/Th/Pb CONCENTRATION DATA

| No. | Sample | Sample Available mgm | U % | Th % | Total Pb % | Common Pb % of Total Pb |
|---|---|---|---|---|---|---|
| 18U | Uraninite | 0.24 | 69.6 | - | 25.3 | 0.89 |
| 18M | Monazite-Rich Mineral Fraction | 17.2 | 0.512 | 6.60 | 0.678 | 0.82 |
| 19U | Uraninite | 0.39 | 49.4 | - | 16.57 | 0.84 |
| 19M | Monazite-Rich Mineral Fraction | 20.3 | 0.297 | 2.30 | 0.291 | 0.64 |
| 20U | Uraninite | 0.62 | 2.24 | - | 2.24 | 9.32 |
| 20M | Monazite-Rich Mineral Fraction | 4.7 | 0.080 | 0.286 | 1.38 | 2.08 |
| 22U | Uraninite | <0.1 | 5.55 | - | 2.62 | 8.83 |
| 22M | Monazite-Rich Mineral Fraction | 11.6 | 0.621 | 2.243 | 0.575 | 15.9 |
| 23M | Monazite-Rich Mineral Fraction | 8.8 | 0.125 | - | 0.235 | 0.81 |
| Sickle Lake | Uranium Mineral | <0.1 | 0.303 | - | 0.325 | 29.6 |

## TABLE III

### U-Th-Pb APPARENT AGE DATA (m.y.)

| No. | Sample | $^{207}Pb/^{206}Pb$ | $^{206}Pb/^{238}U$ | $^{207}Pb/^{235}U$ | $^{208}Pb/^{232}Th$ |
|---|---|---|---|---|---|
| 18U | Uraninite | 1678 | 1432 | 1534 | -- |
| 18M | Monazite Rich Mineral Fraction | 1791 | 1660 | 1719 | 1716 |
| 19U | Uraninite | 1634 | 1171 | 1345 | -- |
| 19M | Monazite Rich Mineral Fraction | 1797 | 1658 | 1720 | 1905 |
| 20U | Uraninite | 1802 | 1881 | 1844 | -- |
| 20M | Monazite Rich Mineral Fraction | 1799 | 2056 | 1931 | 6969 |
| 22U | Uraninite | 1758 | 1755 | 1757 | -- |
| 22M | Monazite Rich Mineral Fraction | 1804 | 2102 | 1955 | 2396 |
| 23M | Monazite Rich Mineral Fraction | 1802 | 2183 | 1993 | -- |
| Sickle Lake | Uranium Mineral | 1797 | 3598 | 2550 | -- |

TABLE IV

U-Th-Pb ISOTOPIC RATIO DATA

| No. | Sample | $^{207}Pb/^{206}Pb$ | $^{208}Pb/^{206}Pb$ | $^{204}Pb/^{206}Pb$ | $^{207}Pb/^{235}U$ | $^{206}Pb/^{238}U$ | $^{208}Pb/^{232}Th$ |
|---|---|---|---|---|---|---|---|
| 18U | Uraninite | 0.10597 | 0.58164 | 0.000222 | 3.529 | 0.2487 | -- |
| 18M | Monazite Rich Fraction | 0.11800 | 4.03605 | 0.000623 | 4.435 | 0.2937 | 0.08864 |
| 19U | Uraninite | 0.10386 | 0.83999 | 0.000241 | 2.761 | 0.1991 | -- |
| 19M | Monazite Rich Fraction | 0.11481 | 2.72540 | 0.000364 | 4.441 | 0.2932 | 0.09882 |
| 20U | Uraninite | 0.16605 | 1.9792 | 0.004020 | 5.147 | 0.3389 | -- |
| 20M | Monazite Rich Fraction | 0.13145 | 4.02054 | 0.001577 | 5.696 | 0.3757 | 0.4117 |
| 22U | Uraninite | 0.13746 | 0.54743 | 0.002188 | 4.640 | 0.3129 | -- |
| 22M | Monazite Rich Fraction | 0.19022 | 1.32233 | 0.005868 | 5.860 | 0.3854 | 0.1259 |
| 23M | Monazite Rich Fraction | 0.11890 | 4.18823 | 0.000641 | 6.122 | 0.4030 | -- |
| Sickle Lake | Uranium Mineral | 0.19850 | 0.28974 | 0.006502 | 11.32 | 0.7474 | -- |

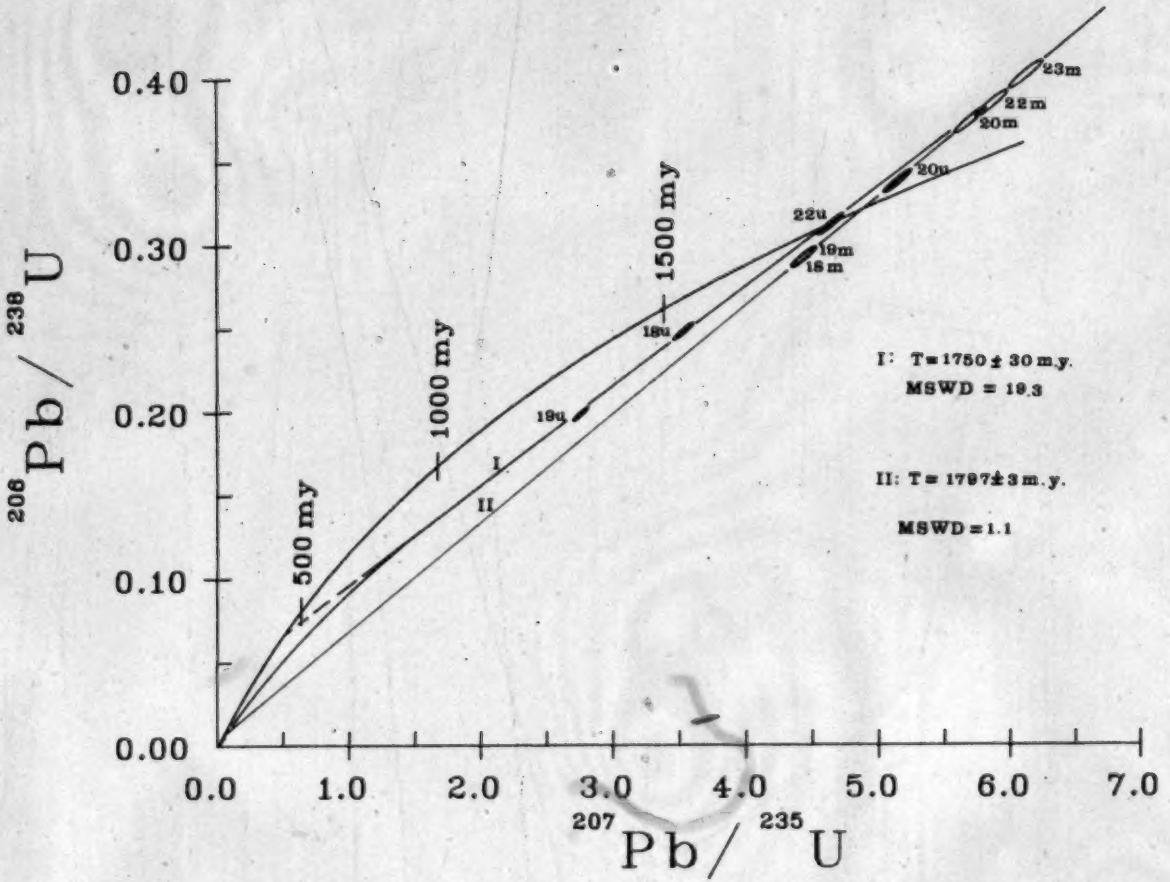


Figure 5. Concordia diagram for the cogenetic uraninite (filled ellipses) and monazite-rich mineral fractions separated from granodioritic granofels and migmatites of the Charlebois Lake complex. For identification of the specimens refer to Figure 4 and Table IV. Data ellipses are drawn at 3σ error level.

very susceptible to error due to the uncertain isotopic composition of common lead, so that any interpretation of U-Pb data becomes highly unreliable. For that reason this sample has not been plotted on the concordia diagram.

Three uraninite data points (excluding leached uraninite 20U) form one group and the monazite-rich phases form the other. Leached uraninite (20U) appears to fall within the monazite group. A straight line fitted through three uraninite samples intersects the concordia curve at 1750±30 m.y. and 368±100 m.y. and passes through the most reversely discordant monazite (23M). The age obtained from the upper intersection is the more reliable one and shows the "true" age of the suite of samples. In this case the upper intersection age is controlled by the concordant uraninite point and is in good agreement with the age obtained from the whole rock lead-lead data (to be discussed later). This could mean that 1750 m.y. represents the completion time of the uranium mineralization which is marked by the closing of the uraninite crystalline system. An age of 368 m.y. obtained from the lower intersection with the concordia curve, suggesting an episodic event that caused the lead loss, is not supported by any geological or geochronological evidence up to this time. Therefore it is assumed that this age is artificial and a probable result of the continuous lead diffusion from the mineral lattice. In fact, the uraninite data define a straight line rather

poorly (MSWD=19.3). Comparing this data to the continuous diffusion curve with the the constant coefficient of diffusion: $D_{(t)}=D_o$ (Wasserberg 1963), for a primary age of 1750 m.y., it becomes apparent that three uraninite points define the continuous diffusion curve much better than the straight line. Unfortunately, since no more uraninite data are available, a statement suggesting that these uraninites might represent a good case of continuous diffusion lead loss would be rather presumptuous.

Monazite-rich fractions on the other hand form an almost perfect line (MSWD=1.1). Leached uraninite (20U) has been excluded from the straight line calculation, although it fits very well with this data and does not alter the results. The line intersects the concordia curve at 1797±3 m.y. and at 55±40 m.y. The immediate implication of this distribution is that U-Pb systems in monazite-rich fractions became closed at 1797 m.y. which is distinctly different from the cogenetic uraninites. The lower intersection at 55±40 m.y. suggests a recent episodic lead-uranium loss or one of the theoretically limiting cases (Wetherill 1963) of continuous diffusions where the intrinsic diffusion coefficient $D_o$ is very small and the radiation damage of the lattice is somehow "frozen in", so that defects will have negligible mobility. In that way, the diffusion coefficient will not increase until the system is raised to a somewhat higher temperature or lower pressure, sometime in the recent past, when

the mobility of the defects becomes significant and therefore the diffusion coefficient is increased. The result of this quasi-episodic loss would be the continuous diffusion curve that approaches the line of recent episodic lead/uranium loss. Whatever the reason for the lower intersection, the upper intersection should reflect the "true" age of these minerals. Referring back to the statement of Lewrey et al. (1978) regarding the duration of the high grade metamorphic condition in the Cree Lake zone (see page 7 of this thesis), two different ages obtained for cogenetic uraninites and monazite-rich phases suggest that parts of the lead-uranium system of the Charlebois Lake area began closing at least 1797 m.y. ago with crystallization of monazites and possibly other high grade minerals. The end of the Hudsonian orogeny in the area was characterized by the formation of uraninites, and probably other late minerals, around 1750 m.y. ago.

There are other possible causes for the observed distribution of data points in the concordia diagram in Figure 5. These other causes are suggested by the experimental studies on the mobility of lead, uranium and thorium in monazites and other uranium minerals (Komlev et al. 1964, Starik and Lazarev 1964, Burger et al. 1967, Shestakov 1972, Cumming and Rimsaite 1979), and the theoretical basis for diffusion of lead and uranium provided by Wetherill (1963) and Wasserburg (1963).

Wetherill (1963) and Wasserburg (1963) have proposed that distinctly different patterns for pure continuous diffusional losses of lead or uranium are to be expected in the concordia diagram, where the slope of the pure lead diffusion line is always greater than that for pure uranium diffusion. Mixed lead and uranium diffusion, where the diffusion coefficients for lead and uranium are proportional, will produce a line of intermediate slope. In a limiting case, if the diffusion coefficient for the parent isotope is equivalent to the diffusion coefficient for the daughter isotope, the resulting data point would be concordant, i.e. plotting on the concordia curve.

Burger et al. (1967) and Komlev et al. (1964) have demonstrated that various amounts of lead, uranium and even thorium can be leached from monazite under very mild laboratory conditions. This seems to be supported, to some extent, in this study by the result of the uraninite sample (20U) which was separated from the rest of the heavy minerals by leaching. This sample appears to have gained some lead (possibly a minor amount of uranium, too) during the leaching process. Its position in the concordia diagram depends on the relative amounts of lead and uranium leached from the monazite and other admixed minerals, and on the total amount of uraninite present. It appears that the amount of leached lead added to the uraninite was larger than the amount of leached uranium, since the addition of lead forces the uraninite towards the uranium

loss/lead gain field, making it reversely discordant. At the same time the monazite-rich fraction (20M) of this sample would move from its original, presumably reversely discordant position along the modern episodic lead loss line. The distance of movement would be determined by the relative proportions of leached lead and uranium.

The other monazite-rich fractions were washed in warm 2N $HNO_3$ for one hour before analysis, without immediate realization that some lead, uranium and possibly thorium might be lost in the process. If an assumption is made that various amounts of lead, uranium and thorium have been indeed leached from the monazite-rich fractions during the washing process, then their presently observed distribution is artificial. Assuming they were originally very closely spaced in the vicinity of the most discordant monazite fraction (23M), being along the lead-uranium continuous diffusion line represented by three uraninite samples, the loss of lead and uranium would alter their position and move them along the modern episodic lead-uranium loss line, possibly achieving the observed distribution.

This suggestion appears to be rather unlikely because it assumes that all monazite-rich fractions had almost the same lead-uranium composition as 23M. The only plausible fact about it is that it does not require monazite-rich fractions to behave as closed systems under still relatively high pressure/temperature conditions for almost fifty million years while U-Pb systems of their cogenetic

uraninites were open.

The thorium-lead ages are discordant and do not substantiate either possibility. It is clear that additional work of this kind is needed to definitely establish the age relationship of these cogenetic minerals.

Lead-Lead Results

The analytical results obtained on the whole rock samples and six feldspar separates are listed in Table V and the data are plotted and presented in Figures 6-13. All of the data have been corrected for fractionation. Two sigma errors of 0.7°/₀₀, 1°/₀₀ and 1.4°/₀₀ have been assigned to $^{206}Pb/^{204}Pb$, $^{207}Pb/^{204}Pb$ and $^{208}Pb/^{204}Pb$ ratios, respectively, based on the repeated measurements of NBS SRM-981 common lead standard. A detailed discussion of error estimates, analytical procedures and fractionation corrections is given in Appendix II. On all of the diagrams, Stacey and Kramers (1975) growth curve is drawn as a reference growth curve. In some of the diagrams the elipses are used for presenting data points. Their size represents the error limits at three sigma level.

A distribution of the $^{206}Pb/^{204}Pb$, $^{207}Pb/^{204}Pb$ and $^{208}Pb/^{204}Pb$ ratios obtained from the samples of the Pegasus Lake area is displayed in Figures 6 and 11. In both of these standard diagrams the data exhibits wide scatter which is far beyond the assigned errors. Some relatively weak correlation between the isotopic ratios and geographical and geological locations appears to be evident

TABLE V

Pb-Pb ANALYTICAL DATA

| No. | Sample | $^{206}Pb/^{204}Pb$ | $^{207}Pb/^{204}Pb$ | $^{208}Pb/^{204}Pb$ |
|---|---|---|---|---|
| 1 | Gray, massive granitic gneiss | 15.617 | 15.181 | 36.999 |
| 1F | Feldspar separate | 14.886 | 15.091 | 35.150 |
| 2 | Gray, massive granitic gneiss | 16.208 | 15.261 | 36.898 |
| 3 | Pinkish-gray, banded granitic gneiss | 18.123 | 15.559 | 36.047 |
| 4 | Pinkish-gray, banded granitic gneiss | 18.902 | 15.634 | 36.844 |
| 5 | Gray, massive granitic gneiss | 15.477 | 15.210 | 35.743 |
| 6 | Gray, slightly banded granitic gneiss | 15.402 | 15.220 | 36.293 |
| 7 | Gray, banded granitic gneiss | 20.184 | 15.697 | 38.530 |
| 8 | Gray, massive granitic gneiss | 15.356 | 15.176 | 35.128 |
| 8F | Feldspar separate | 14.887 | 15.098 | 35.104 |
| 9 | Dark gray, banded granitic gneiss | 16.598 | 15.292 | 37.806 |
| 10 | Gray, banded granitic gneiss | 15.768 | 15.208 | 35.317 |
| 11 | Pinkish, nearly massive granitic gneiss | 18.489 | 15.489 | 37.314 |
| 12 | Light gray, massive granitic gneiss | 19.213 | 15.780 | 36.253 |

TABLE V (cont'd)

| No. | Sample | $^{206}Pb/^{204}Pb$ | $^{207}Pb/^{204}Pb$ | $^{208}Pb/^{204}Pb$ |
|---|---|---|---|---|
| 13 | Gray, massive granitic gneiss | 17.239 | 15.502 | 37.233 |
| 13F | Feldspar separate | 16.232 | 15.387 | 35.566 |
| 13F-R | Leached feldspar separate | 15.905 | 15.394 | 34.549 |
| 14 | Gray, banded granitic gneiss | 15.679 | 15.242 | 35.462 |
| 15 | Gray, banded granitic gneiss | 18.940 | 15.723 | 36.717 |
| 16 | Coarse pink phase of granitic gneiss | 19.692 | 15.754 | 36.472 |
| 17 | Pink band in granitic gneiss | 20.815 | 15.780 | 40.399 |
| 18 | White, coarse grained granodioritic granofels | 240.58 | 39.818 | 60.808 |
| 19 | White, coarse grained granodioritic granofels | 75.832 | 21.968 | 57.81 |
| 20 | Gray, medium grained granodioritic granofels | 23.577 | 16.276 | 40.176 |
| 21 | Felsic band in biotite migmatite | 24.504 | 16.236 | 42.002 |
| 22 | Garnetiferous, felsic band in biotite migmatite | 65.352 | 20.770 | 40.690 |
| 23 | Garnetiferous, felsic band in biotite migmatite | 34.590 | 17.322 | 48.783 |

TABLE V (cont'd)

| No. | Sample | $^{206}Pb/^{204}Pb$ | $^{207}Pb/^{204}Pb$ | $^{208}Pb/^{204}Pb$ |
|---|---|---|---|---|
| 24 | Fine grained biotite-hornblende gneiss | 19.354 | 15.676 | 38.880 |
| 25 | Hornblende gneiss | 18.126 | 15.573 | 37.676 |
| 26 | Fine grained amphibolite | 16.469 | 15.372 | 36.217 |
| 27 | Fine grained amphibolite | 16.232 | 15.289 | 36.152 |
| 27F | Feldspar separate | 15.668 | 15.224 | 35.465 |
| 28 | Biotite gneiss | 20.932 | 15.847 | 41.439 |
| 29 | Pinkish, fine grained biotite gneiss | 17.286 | 15.337 | 37.659 |
| 29F | Feldspar separate | 16.078 | 15.235 | 35.394 |
| 30 | Fine grained, dark gray biotite gneiss | 24.902 | 16.188 | 44.057 |
| 31 | Dark gray, medium grained biotite gneiss | 23.003 | 15.943 | 38.255 |
| 32 | Pinkish-gray, biotite gneiss | 19.161 | 15.568 | 39.799 |
| 33 | Medium grained gray biotite gneiss | 17.890 | 15.436 | 38.741 |
| 34 | Medium grained, well banded granitic gneiss | 18.059 | 15.706 | 36.581 |

TABLE V (cont'd)

| No. | Sample | $^{206}Pb/^{204}Pb$ | $^{207}Pb/^{204}Pb$ | $^{208}Pb/^{204}Pb$ |
|---|---|---|---|---|
| 34F | Feldspar separate | 16.130 | 15.420 | 34.998 |
| 35 | Pink felsic dyke | 18.375 | 15.618 | 36.889 |
| 36 | Pink felsic dyke | 19.057 | 15.662 | 36.773 |
| 37 | Pink felsic dyke | 17.369 | 15.514 | 38.235 |
| 38 | Pink felsic dyke | 19.603 | 15.691 | 43.394 |
| 39 | Pink felsic dyke | 18.018 | 15.556 | 36.715 |
| 40 | Pink felsic dyke | 18.131 | 15.588 | 38.182 |

in Figure 6. Analytical data points obtained on the samples from the central areas of the Pegasus Lake anticline seem to generally plot to the left on the diagram. The radiogenic character of the data points increases towards the shore of the Dramnitzke Bay, i.e. outer margins of the anticline. Samples of the mineralized granodioritic granofels (18,19,20), with $^{206}Pb/^{204}Pb$ ratios of up to 240 plot outside this diagram and lie on line V whose extension is shown as a broken line in this diagram.

The somewhat fan-like distribution of data in Figure 6 is indicative of a complex history for these rocks. Lead-uranium systems from the rocks with a simple history (i.e. rocks which were emplaced sometime in the past and have not been disturbed until the present) exhibit colinear behaviour in the standard lead-lead diagrams. Systems with a more complex history occasionally exhibit straight line patterns and the slopes of these straight lines might often reflect the time of the last metamorphic event but that is only true in a few special cases (discussed in Appendix I). Colinear behaviour is observed only when the changes are brief, episodic and complete, i.e. when the system exhibits closed system behaviour and when all the chemical and isotopic equilibration reactions are completed during a brief metamorphic event. If the system remains open for partial uranium or lead migration across the system's boundaries, colinearity is seldom observed.

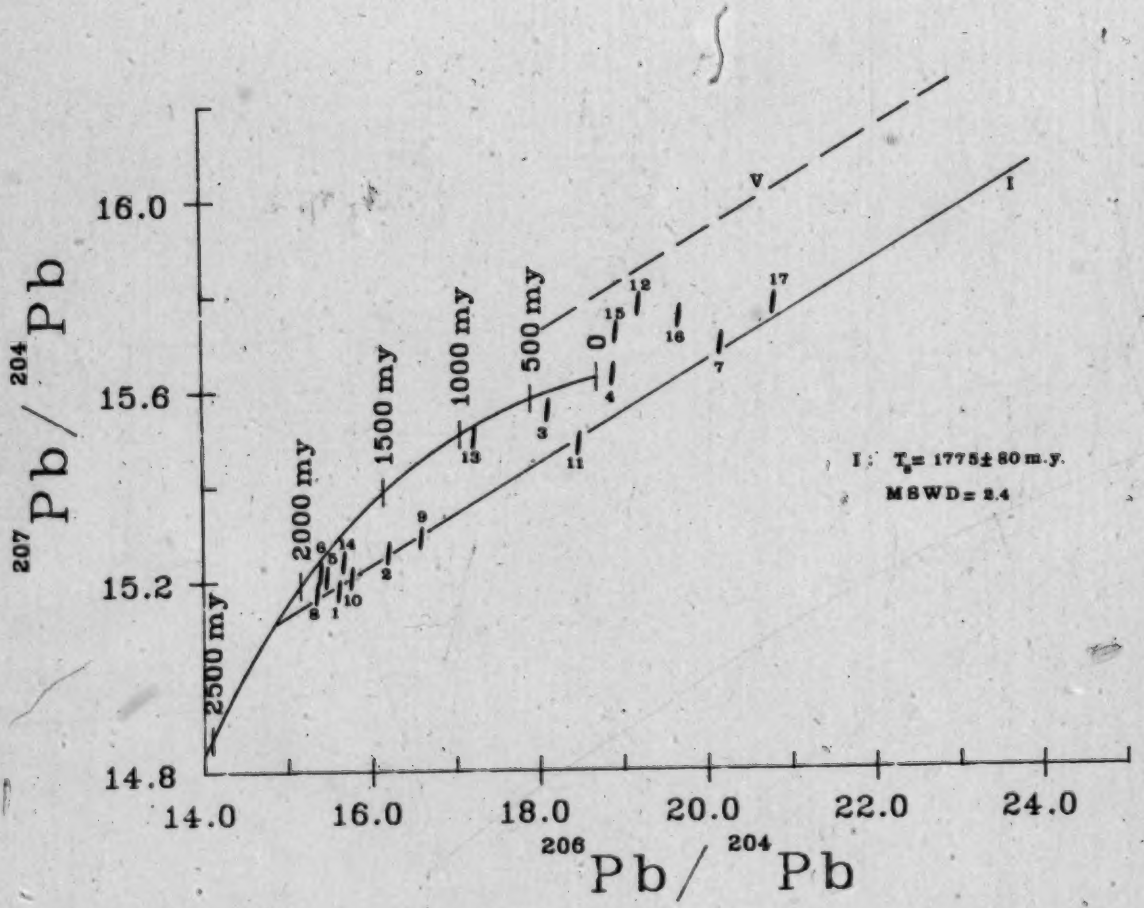


Figure 6. Pb-Pb diagram for the whole rock samples from the "Pegasus Lake Area". For identification of the specimens refer to Figure 4 and Table V. Data ellipses are drawn at 3σ error level.

Providing a sufficient number of data is available, some relatively useful information regarding the history of the system may be derived from the scatter diagram. The slope age calculated from the line representing the lower boundary of the scatter often approaches the time of the last metamorphic event. The distribution of data points around the apex of the "fan" is occasionally indicative of the time of the original formation.

The lower boundary of the scatter in the $^{207}Pb/^{204}Pb$ vs. $^{206}Pb/^{204}Pb$ diagram (Figure 6) is represented by a line fitted through seven points with the slope of 0.10855 and MSWD of 2.45. The corresponding slope age is 1775±80 m.y. at two sigma error level. For reference this line is termed "Line I". The intersection of this line with Stacey and Kramers growth curve at about 2100 m.y. and distribution of the data points suggests that the original emplacement took place sometime before 2100 m.y. ago and subsequent remobilization occurred at around 1775 m.y. ago.

It will only be mentioned now (and discussed later) that three samples of granodioritic granofels (18,19,20) and two samples from the "Old Camp Area" plot on line V which represents the upper limit of the observed distribution in Figures 6 and 7. The slope of this line yields an age of 1772±8 m.y. (Figure 8).

Isotopic results obtained on the gneissic samples from the "Old Camp Area" are plotted in Figures 7 and 11. The data in the $^{207}Pb/^{204}Pb$ vs. $^{206}Pb/^{204}Pb$ diagram is

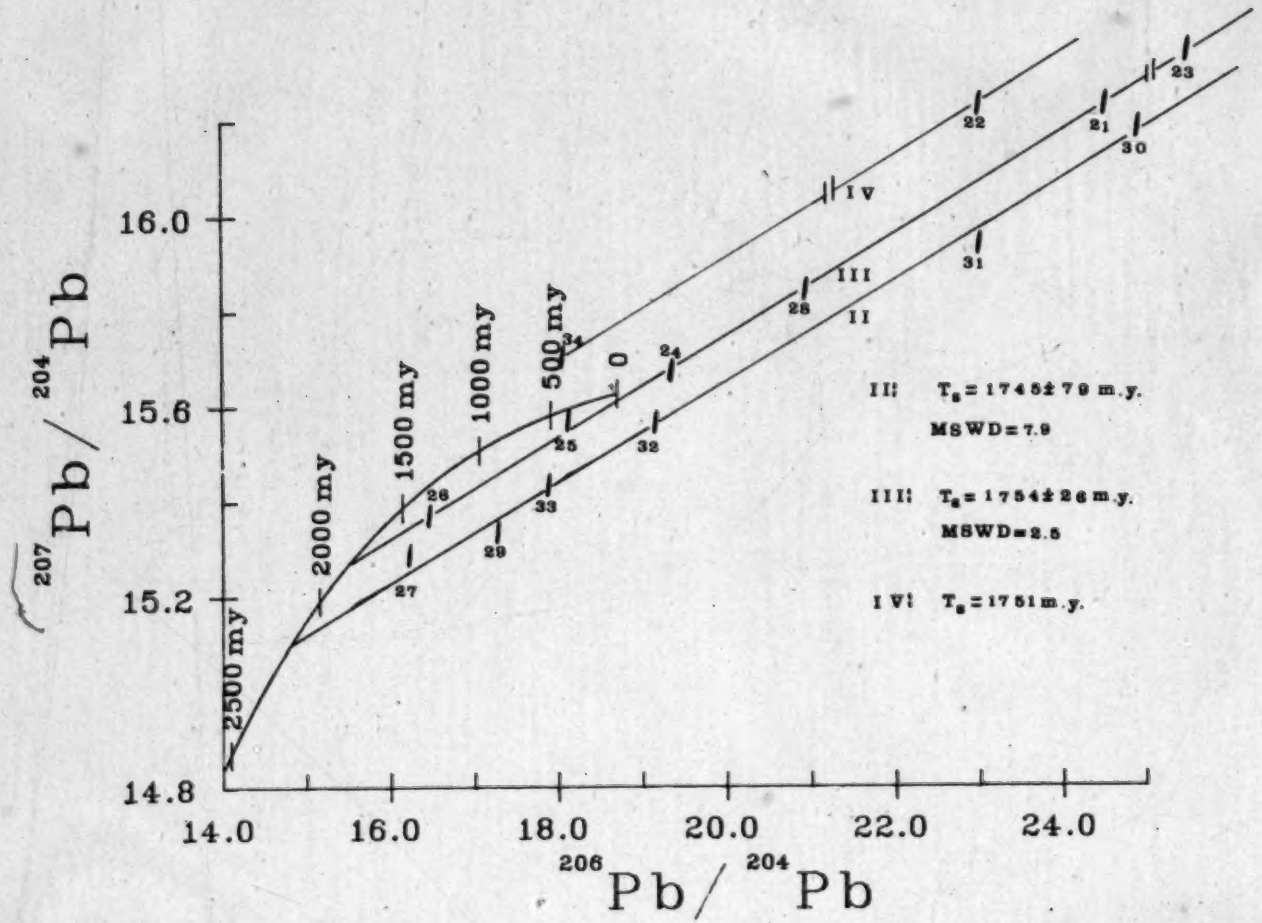


Figure 7. Pb-Pb diagram for the whole rock samples from the "Old Camp Area" showing three parallel line distributions. For identification of the specimens refer to Figure 4 and Table V. Data ellipses are drawn at 3σ error level.

distributed along three parallel trend lines (with the exception of sample 27). Straight line fittings of these data yield:

Line II: Slope=0.10678 MSWD=7.91 $T_s$=1745±79 m.y. (2σ)
Line III: Slope=0.10727 MSWD=2.55 $T_s$=1754±26 m.y. (2σ)
Line IV: Slope=0.10708 Two point line $T_s$=1751 m.y.

As in the case of the "Pegasus Lake Area" some correlation between the distribution of the data in Figure 7 and the geographic-geological location of the samples can be made. Most radiogenic samples were collected along the shore of the Dramnitzke Bay. The radiogenic character of the specimens decreases towards the apparent fault and amphibolite area (samples 26 and 27). Northwest of the apparent fault the correlation is not quite clear, but it seems that the rocks adjacent to the fault area are more radiogenic and the radiogenic character decreases towards the more felsic granitic gneiss (samples 32,33,34). Sample 34 probably owes its position on the $^{207}Pb/^{204}Pb$ vs. $^{206}Pb/^{204}Pb$ diagram to the radiogenic development of its U-Pb system before the last metamorphic event. In order to have such a high $^{207}Pb/^{204}Pb$ ratio and relatively low $^{206}Pb/^{204}Pb$ ratio, the μ value of its Pb-U system before the last metamorphic event must have been higher than 9.74 (which is Stacey and Kramers value for the earth's $\mu_2$ environment (Stacey and Kramers 1975)) and it must have lost most of its uranium during the last metamorphic event.

Therefore, the μ value for this system was low in the last stage of its history.

Samples 22 and 34 form line IV which represents the upper limit to the distribution of the data from the "Old Camp Area". When these data are combined with the granodioritic granofels data (samples 18,19,20) and plotted together (Figure 8) the linear trend with the slope of 0.10840 is obtained (line V). Although the MSWD of 12.58 suggests that the data do not determine the line very well, the calculated slope age at two sigma, taking into account the error due to the imperfect fit, yields an age of 1772±8 m.y.

Three parallel line distributions of data points, the lowest line intersecting the reference growth curve at around 2200 m.y., strongly suggest that these rocks might have developed according to the three stage evolution model with a constant $f_1$ fractionation factor (Gale and Mussett, 1973). The position of the lowest line indicates that the original emplacement of these rocks must have happened more than 2200 m.y. ago and that subsequent remobilization took place between 1700 and 1800 m.y. ago. It appears that the Pb-U system of the "Old Camp Area" was fractionated among at least three major subsystems at the time of the original emplacement and then it was refractionated during the Hudsonian orogeny, producing the presently observed distribution of three parallel lines.

Keeping in mind the conclusions drawn by Morra (1977)

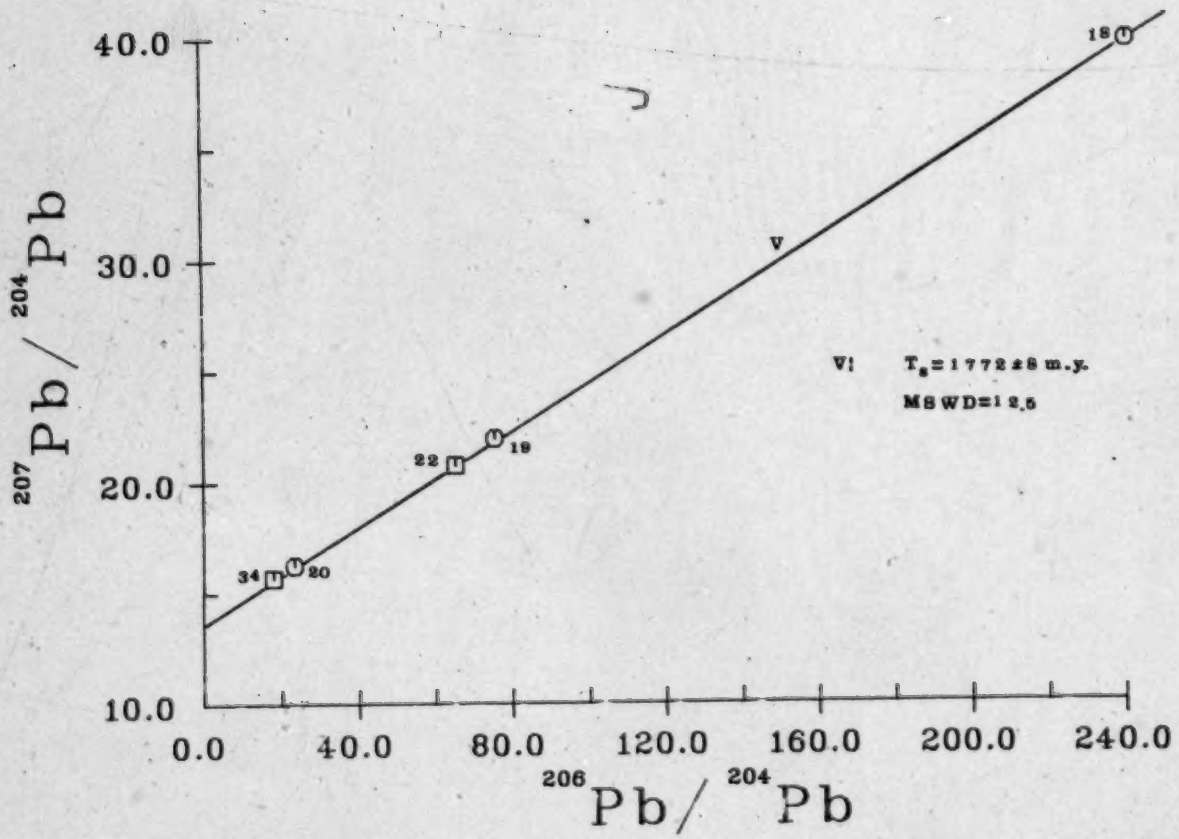


Figure 8. Pb-Pb diagram for the whole rock granodioritic granofels (circles) and some migmatite (squares) members of the Charlebois Lake Complex. For identification of the specimens refer to Figure 4 and Table V.

regarding the integrity of the Charlebois Lake complex, some similarities to the results from the "Pegasus Lake Area" and the "Old Camp Area" are obvious. The slopes and slope ages obtained from line 1 and line 2 (1775±80 m.y. and 1745±79 m.y.) and the intercepts of these lines with reference growth curve (2100 m.y. and 2192 m.y.) are well within the assigned error and in both cases the lines represent the lower limits of the observed distribution in the $^{207}Pb/^{204}Pb$ vs. $^{206}Pb/^{204}Pb$ diagrams. The upper limit of the distribution in both cases is represented by line V with the slope age of 1772±8 m.y. This effectively puts the upper and lower limits on the μ environment of the Charlebois Lake complex for the time period between the present and the Hudsonian metamorphic event. The geologic evidence and above distribution make it reasonable to assume that Pb-U systems, from the "Pegasus Lake Area" and the "Old Camp Area" had also a common history before the Hudsonian time.

In an attempt to gain some information about the time of the original emplacement of the Charlebois Lake complex and the history of the intermediate stage, feldspars from six of the least radiogenic samples were separated and analysed. The chosen samples were: three specimens from the "Pegasus Lake Area" (1, 8 and 13) and three from the "Old Camp Area" (27, 29 and 34).

Under ideal conditions lead isotopic composition in

the feldspars should be representative of the μ environment in the respective Pb-U systems at the beginning of the last evolutionary stage. Low affinity of the feldspar lattice for uranium means that the isotopic composition of lead in the system at time $t_2$, i.e. the Hudsonian metamorphic event, would be "frozen in" and no in situ generation of radiogenic lead would be possible. That means that feldspars behave to some extent as galena (Sinha 1969), i.e. the lead evolution should stop at time $t_2$ and the data points should form a linear trend in the $^{207}Pb/^{204}Pb$ vs. $^{206}Pb/^{204}Pb$ diagram. The slope of this line would be determined by the time of the original emplacement of the rocks ($t_1$) and subsequent metamorphic event ($t_2$).

The slopes of the lines connecting the data points of the whole rocks to that corresponding feldspars should yield the age of the metamorphic event.

Lead isotopic ratios of feldspar-whole rock pairs from the Charlebois Lake complex are plotted in the $^{207}Pb/^{204}Pb$ vs. $^{206}Pb/^{204}Pb$ diagram (Figure 9). All feldspar separates were washed in warm 4N $HNO_3$ for two hours before the lead was separated (described in Appendix II). Samples treated in this manner have the subscript "F" added to the sample I.D. number. Later on, during this study, the remaining amount of one of the feldspar separates (13F) was leached with a warm mixture

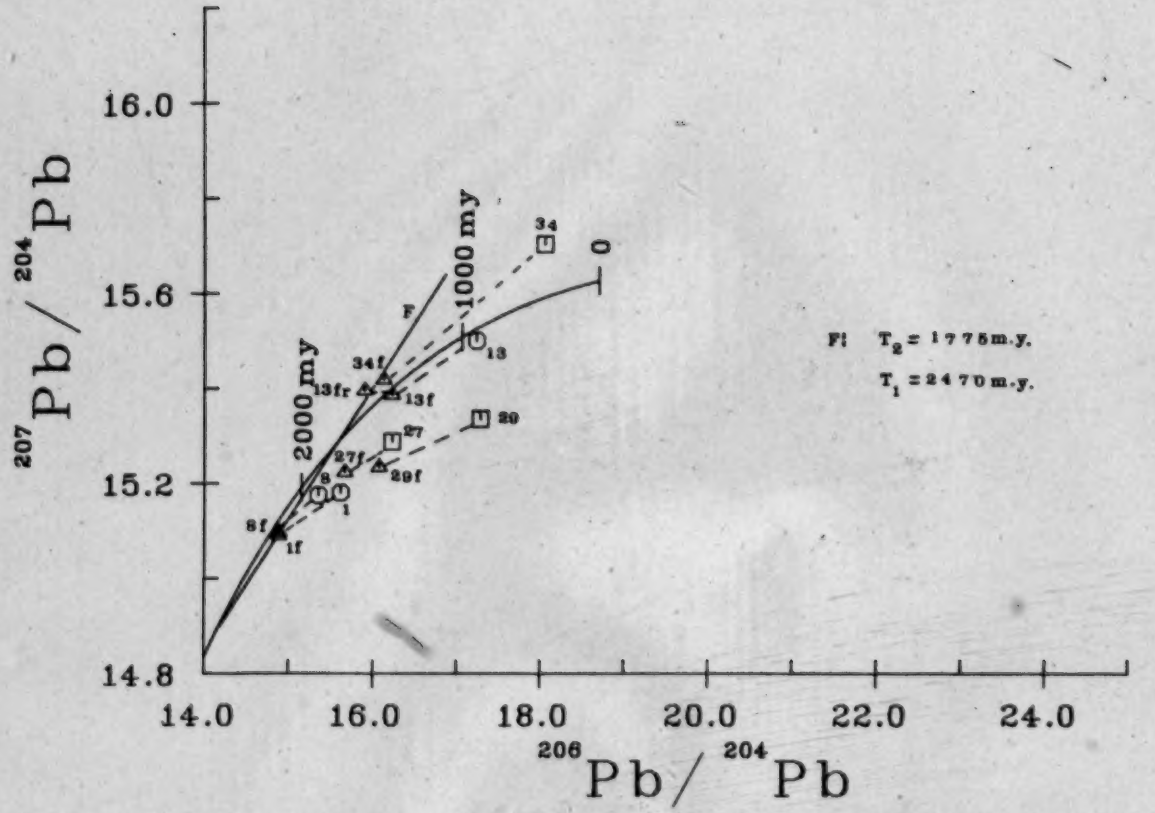


Figure 9. Pb-Pb diagram for the whole rock samples from the "Pegasus Lake Area" (circles), the "Old Camp Area" (squares) and their respective feldspar separates (triangles). For the assigned metamorphic age ($T_2$) of 1775 m.y., the slope of the line F yields the maximum initial emplacement age ($T_1$) of 2470 m.y. ago.

consisting of 20 ml concentrated $HNO_3$ and 0.5 ml concentrated HF for one hour. The residue (13FR) was then analysed for lead isotopes. This data, along with the data from the other feldspars, is presented in Table V.

As expected, all feldspar ratios are less radiogenic than their whole rock counterparts but they exhibit large scatter instead of forming a linear trend. The lines connecting the pairs are far from being parallel and the ages calculated from these lines range from around 1500 m.y. to 2500 m.y. Even though the errors associated with the slopes and therefore with the calculated ages are largely due to the small spread in the feldspar-whole rock $^{206}Pb/^{204}Pb$ ratios, this cannot be considered as the only reason for such a large variation in the calculated slope ages.

Earlier isotopic studies of old Precambrian feldspars have shown that feldspars could be useful in whole rock lead dating (Davis 1978, Vidal et al. 1980) but they often yield younger model ages (Sinha 1969, Catinzaro and Gast 1960, Doe et al. 1965). The lead isotopic composition of feldspars commonly approaches that of associated lead ores, but it is generally more radiogenic. Doe et al. (1965) suggested that gain or exchange of feldspar lead with other rock or mineral lead or admixing of lead from fluids are possible mechanisms causing the increased radiogenic character of the feldspar leads.

Sinha (1969) in the lead volatilization study of feldspars, indicated that radiogenic lead can be easily removed from feldspar by preferential volatilization since this lead is concentrated along the grain boundaries or in distorted lattice sites. Ludwig and Silver (1977) recognized two types of unsupported radiogenic lead present in feldspars. One has normal isotopic composition with relative abundances of $^{206}Pb$, $^{207}Pb$ and $^{208}Pb$ consistent with the age and uranium-thorium content of the rock. The other type of unsupported radiogenic lead is apparently pure $^{206}Pb$ isotope, derived from long-term migration and accumulation of the radioactive daughters of $^{238}U$, namely $^{222}Rn$ and/or $^{226}Ra$.

If it is accepted that various amounts of unsupported lead are present in the analysed feldspars from the Charlebois Lake complex, then it is clear that lead data will not form a linear trend but scattered points. The presence of pure $^{206}Pb$ isotope component would certainly affect the position of the feldspar data points in the $^{207}Pb/^{204}Pb$ vs. $^{206}Pb/^{204}Pb$ diagram and the slopes of the lines connecting these points and their corresponding whole rock data points, the result being the horizontal shift in the feldspar data and higher slopes.

Isotopic ratios obtained from the residue (13FR) of the leached feldspar (13F) seem to support the above argument, since the isotopic results of the residue (13FR)

are less radiogenic than those of the total feldspar separate (13F) and the shift in the $^{206}Pb/^{204}Pb$ appears to be horizontal. Unfortunately there is not enough data of this kind available at present to support this finding. Therefore, it is immaterial whether the observed feldspar distribution in Figure 9 is a result of unsupported radiogenic lead or incomplete equilibration and homogenization of the whole rock Pb-U system with the feldspar Pb-U system during the metamorphic event. Firm conclusions regarding the history of the Charlebois Lake complex before the Hudsonian metamorphic event cannot be drawn from the data presented so far.

Nevertheless, with the few reasonable assumptions regarding the feldspars, a very plausible model history of the Pb-U systems in the Charlebois Lake area can be obtained. It is quite reasonable to assume that the feldspars least affected by the possible presence of unsupported radiogenic lead, i.e. the ones closest to the ideal behaviour, would plot to the far left on the $^{207}Pb/^{204}Pb$ vs. $^{206}Pb/^{204}Pb$ diagram. A slope of 0.27401 (MSWD=8.95) is obtained when the line is fitted through four feldspar points (Figure 9). Since most of the unsupported radiogenic lead is presumably removed from the feldspar 13FR and the other three feldspars might contain some of this lead, the calculated slope very likely represents the maximum possible slope. The slope

of the line is determined by the time of the original emplacement ($t_1$) and the time of the subsequent metamorphic event ($t_2$). Therefore for the assigned metamorphic age $t_2$ = 1775 m.y., the maximum initial age $t_1$ of 2470 m.y. is obtained. Knowing the times $t_1$ and $t_2$ and the slope of the feldspar line, the average $\mu_1$ value is calculated to be 9.85.

A graphical representation of the postulated three stage model history with $f_1$ = const. of the Charlebois Lake complex is given in Figure 10.

The overall Pb-Pb data suggests that during the period before the emplacement of the Charlebois Lake complex, i.e. before 2470 m.y., uranium and lead of this complex were developing in an environment with average $\mu_1$ = 9.85. As early as 2470 m.y. ago $\mu_1$ environment was rehomogenized and refractionated by erosion, deposition, and sedimentation into at least three second-stage $\mu_2$ environments. A Hudsonian metamorphic event, nominally taken here to have occurred 1775 m.y. ago, initiated the third stage of Pb-U evolution and was responsible for the presently observed distribution of data points in the $^{207}Pb/^{204}Pb$ vs. $^{206}Pb/^{204}Pb$ diagram (Figure 10). Deviation from the ideal three-stage, $f_1$ = const. model history, expressed by the imperfect line fit of the data and general scatter could be attributed to the open system behaviour. It was suggested earlier, by the uraninite

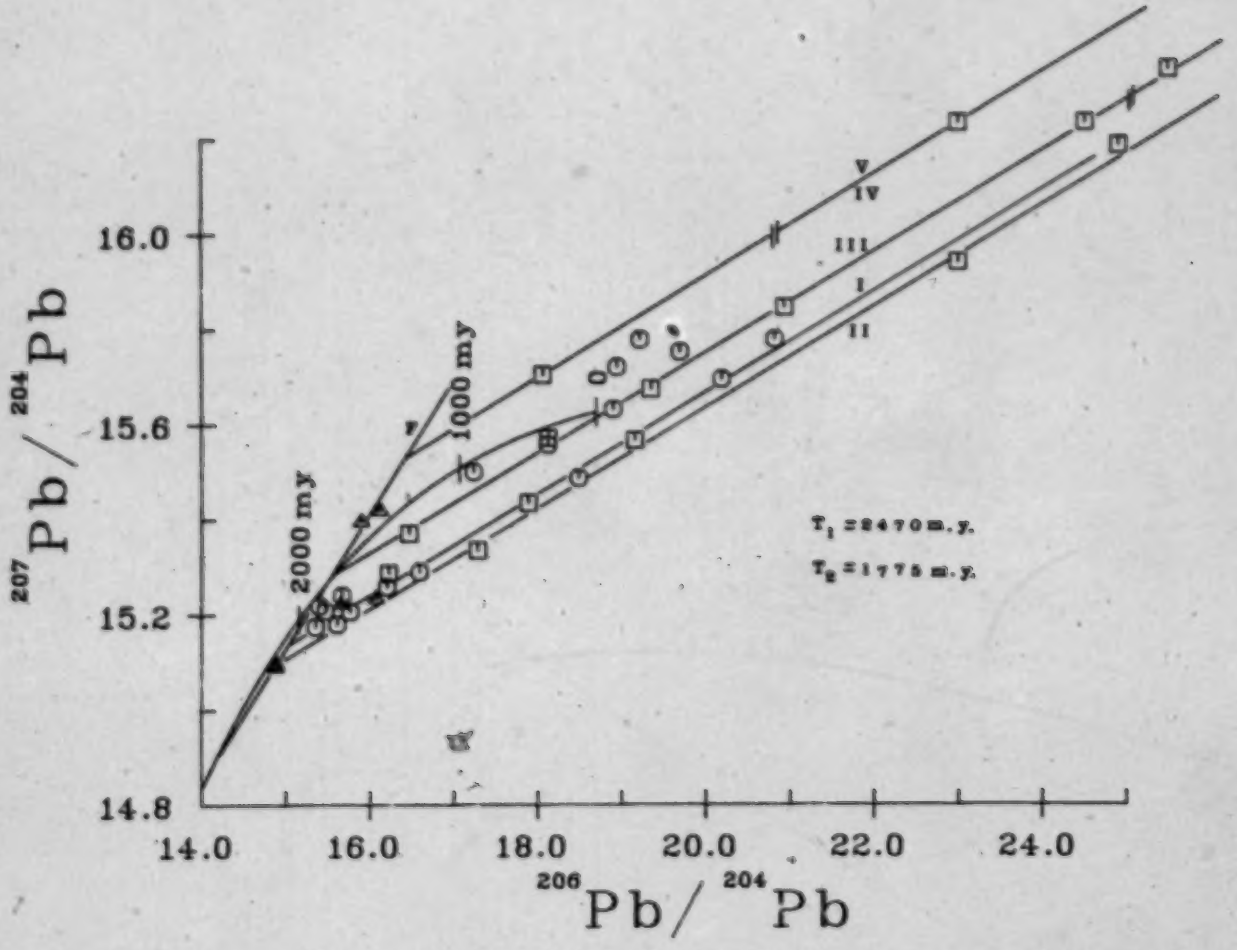


Figure 10. Pb-Pb diagram for the whole rock and feldspar separates from various rock units of the Charlebois Lake Complex indicating three-stage Pb evolution model history. For symbols and line identification refer to Figures 6 to 9.

and monazite U-Pb data, that the global Pb-U system in the Charlebois Lake area had remained partially open for approximately fifty million years during the Hudsonian orogeny. This appears to be particularly evident in the Pegasus Lake area where the data points generally scatter between the limiting line I and line V. It is evident that the most radiogenic samples, i.e. granodioritic granofels and migmatites which plot on line V have partially evolved from the high $\mu_2$ environment of the intermediate stage. That might suggest that the uranium concentration in the original sediments was highest near the boundary between arkosic and more mafic calcareous and tufaceous sediments, and lowest at the bottom of the sedimentary sequence which is seen now as the core of the anticlines in the area. In addition, not very large scale but rather local migration and concentration of uranium during the Hudsonian orogeny has produced uranium mineralization which is associated with granodioritic granofels and migmatites. This seems to be supported by the linearity of the data trends in Figure 10. If large-scale uranium remobilization had taken place during the Hudsonian time, the colinear behaviour of the data would have been destroyed. Partial mixing of the lead and uranium from different subsystems during the migration would have produced general scatter. That might well be the case with some of the granitic gneiss samples from the Pegasus Lake anticline.

Samples from the center of the anticline which evolved in the relatively low $\mu_2$ environment in the intermediate stage, seem to have lost most of their uranium and have also undergone most complete re-equilibration during the last metamorphic event. As a result they form the lower boundary of the distribution. Samples from the outer margins of the anticline have probably been involved in the partial migration of lead and uranium which has resulted in general scatter of the data from that area since rehomogenization has not been completed.

Figure 11 shows the $^{208}Pb/^{204}Pb$ versus $^{206}Pb/^{204}Pb$ ratios of the Charlebois Lake complex. The data show wide scatter as is often the case in trace lead studies. In general the scatter of the data points indicates considerable variation in the Th-U ratio and therefore it is consistent with the proposition made above that several events have affected the development of the lead in the rocks of the Charlebois Lake complex.

Late Felsic Dyke

A fifteen foot wide dyke which crosscuts the rocks in the "Old Camp Area" and grades into the small, very coarse grained pink pegmatitic irregular body on the north side of the bay (Figure 4), was sampled at six locations (35 to 40). Samples 35 and 36 were collected one and three feet, respectively, from the contact with

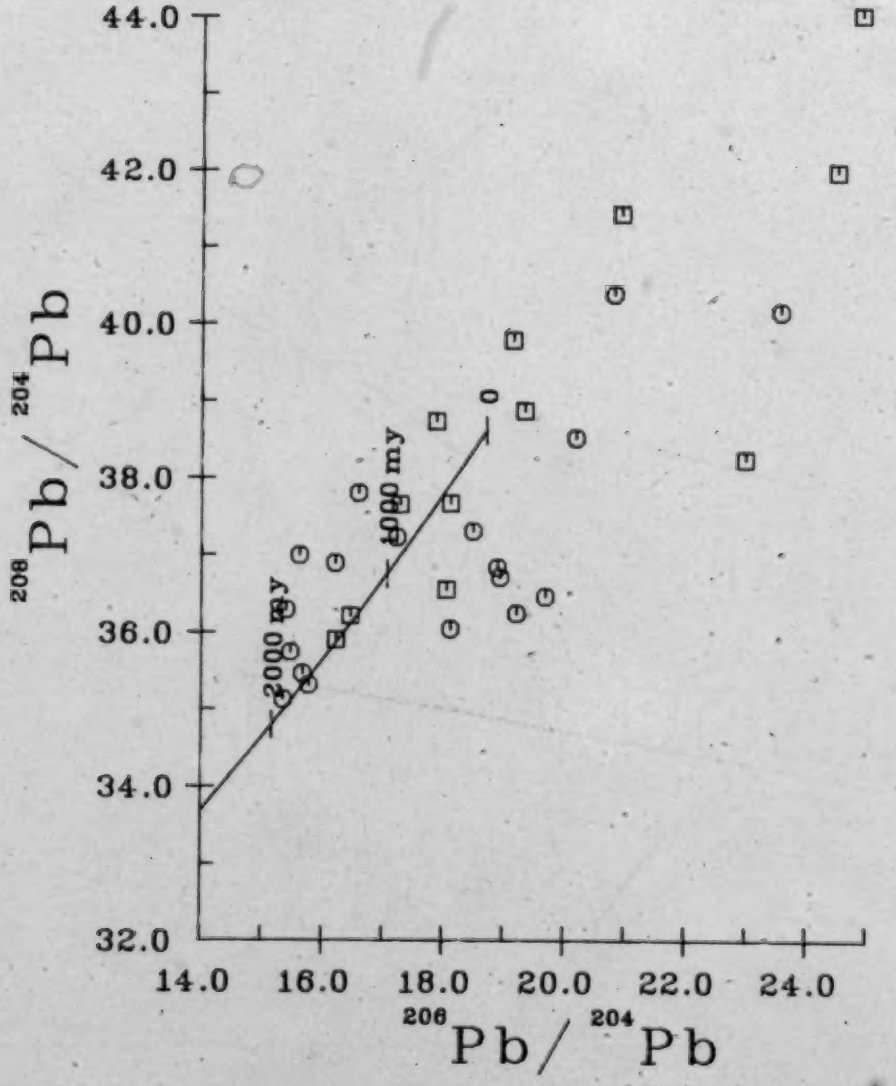


Figure 11. Pb-Pb diagram for the whole rock samples of various rock units from the Charlebois Lake Complex.

the country rock. Sample 37 is from the center of the dyke and the other three samples were collected elsewhere from the dyke.

Lead analytical data are presented in Table V and in Figures 12 and 13. Data plotted in the $^{207}Pb/^{204}Pb$ versus $^{206}Pb/^{204}Pb$ diagram display a linear trend with the range of $^{206}Pb/^{204}Pb$ ratios between 17 and 19.5. When a straight line is fitted to the data it yields a slope of 0.08152 and an MSWD of 3.39. The corresponding slope age is 1235±320 m.y. The line intersects Stacey and Kramers reference growth curve at -8±230 m.y. and 1239±300 m.y. at a two sigma error level. Due to the small spread in the $^{206}Pb/^{204}Pb$ ratios, the small number of samples and general scatter, the data points define the line rather poorly. As a result the calculated slope, slope age and intercepts with the growth curve are associated with fairly large error and the interpretation of this data becomes only tentative.

It is interesting to note that the line intersections with Stacey and Kramers reference growth curve indicate that the source of this dyke has a $\mu$ value very similar to the $\mu$ value of the upper mantle as suggested by Stacey and Kramers (1975). Unfortunately this suggestion is not supported by the distribution of the data points in the $^{208}Pb/^{204}Pb$ versus $^{206}Pb/^{204}Pb$ diagram (Figure 13) nor by Rb-Sr data which will be

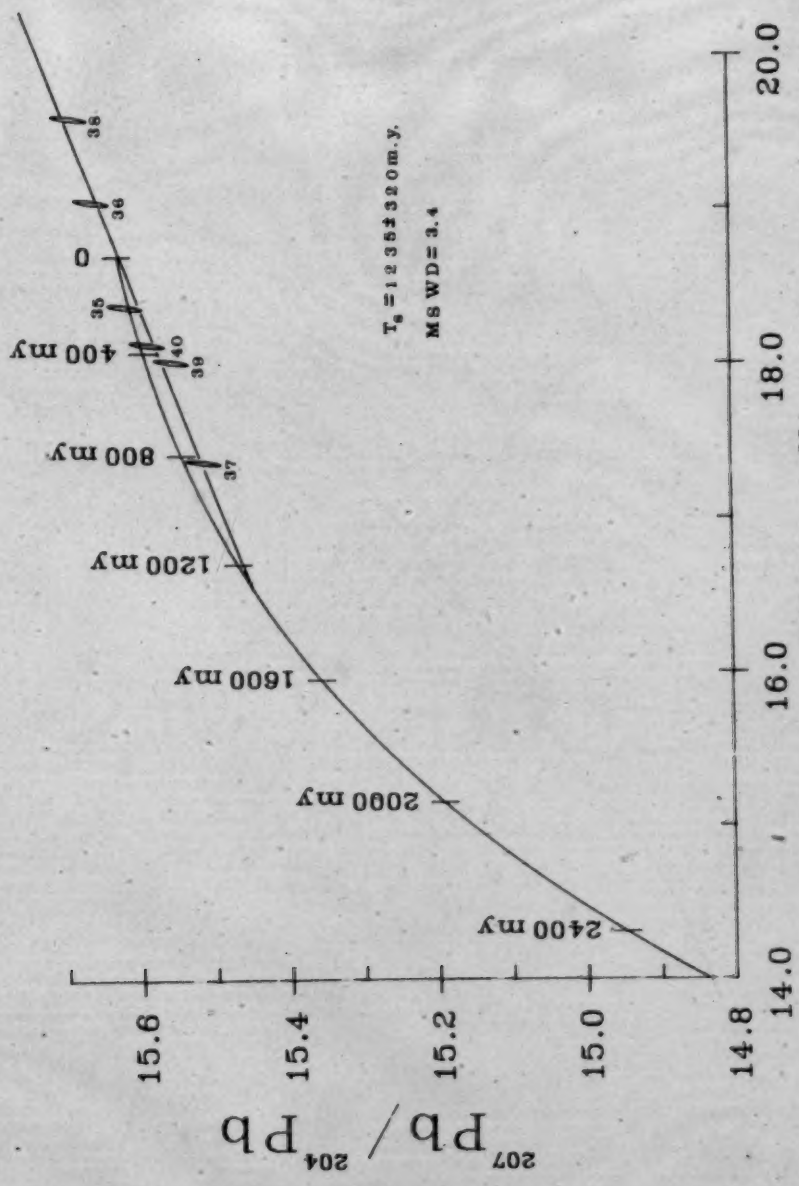


Figure 12. Pb-Pb diagram for the whole rock samples of the pink felsic dyke. For identification of the specimens refer to Figure 4 and Table V. Data ellipses are drawn at 3σ error level.

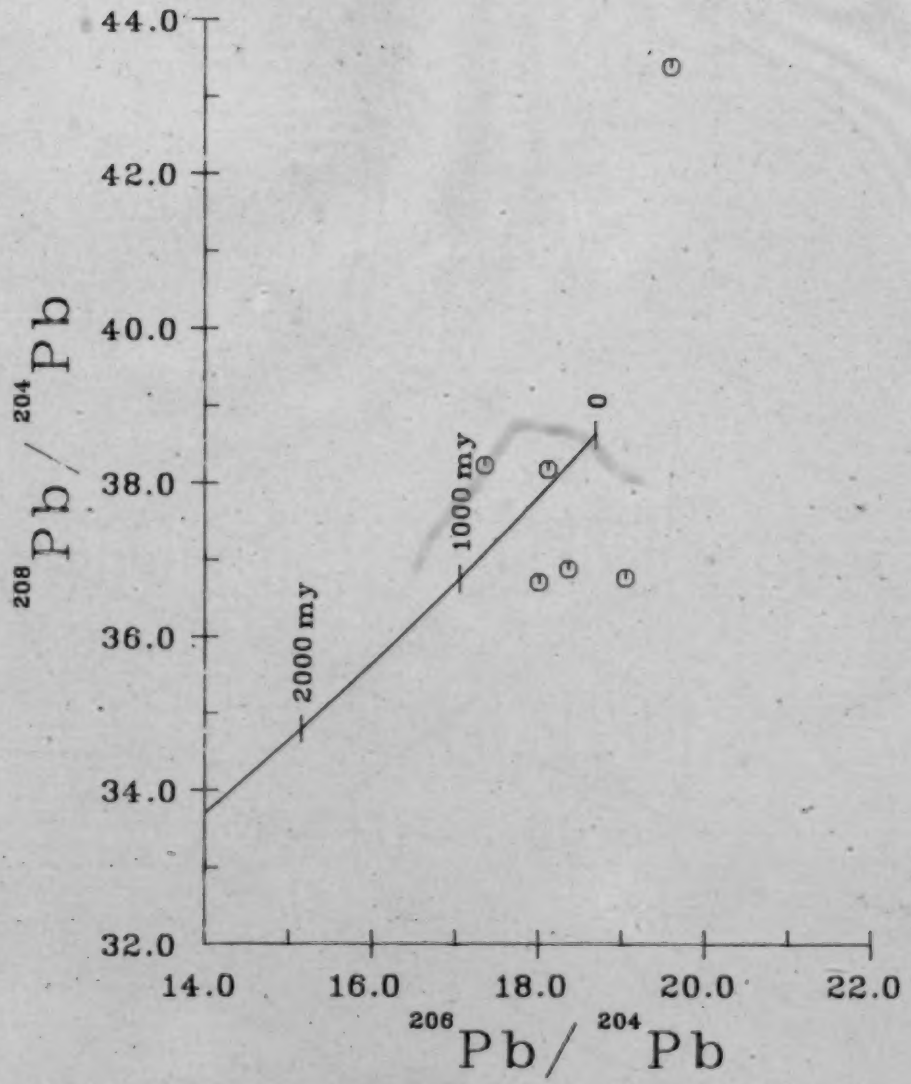


Figure 13. Pb-Pb diagram for the whole rock samples of the pink felsic dyke.

discussed later in this chapter. What might be said is that the source of the felsic dykes and other irregular pegmatitic bodies is probably remelted rocks of the lower crust. The isotopic data confirm the geologic observation that emplacement of this and other similar dykes and pink pegmatitic irregular bodies has happened in the post metamorphic time, possibly as late as around 1200 m.y. ago.

The period of time between 1500 to around 1100 m.y. ago is tectonically a relatively quiescent and economically important period in the history of the Churchill province. It should be pointed out that during this time major uranium deposits of northern Saskatchewan such as Rabbit Lake, Midwest Lake, Key Lake and others have been emplaced (Cumming and Rimsaite 1979, Cumming, Baadsgaard, Hoeve and Morton (in preparation), and Cumming, Worden and Baadsgaard (in preparation)). Some of the diabase dykes of Churchill province have also been emplaced during this period of time (Fahrig and Wanless 1963, Burwash et al. 1962). A detailed, large scale geochronological study of these and felsic dykes from other areas in the Churchill province, along with the diabase dykes, would probably prove to be very beneficial for a clearer understanding of the Churchill province history between 1500 m.y. and 1100 m.y. ago.

Rubidium-Strontium Results

The analytical results obtained on the whole rock samples are listed in Table VI and the data are plotted in Figures 14-16.

Two sigma errors of 0.3°/$_{oo}$ and 1% have been assigned to $^{87}Sr/^{86}Sr$ and $^{87}Rb/^{86}Sr$ ratios, respectively, based on the repeated measurements of NBS SRM-987 common strontium standard and the generally accepted accuracy level in the laboratory. A detailed discussion of error estimates and analytical procedures is given in Appendix II. In some of the diagrams the elipses are used for presenting the data points, their size represents the data with their respective errors at four sigma level.

For ease of interpretation the data are again considered in three groups as was the case with the lead-lead data, i.e. "Pegasus Lake Area", "Old Camp Area" and the late felsic dyke.

All of the rock samples analysed for lead isotopes were also used for Rb-Sr analysis, in an attempt to shed some more light on the history and the nature of the Charlebois Lake complex and its precursors. It was hoped that the whole rock Rb-Sr analysis would provide additional evidence for the age of the precursors and therefore substantiate the claims made on the basis of the lead-lead data. Unfortunately the data presented here exhibits even greater scatter than the lead-lead data.

TABLE VI

Rb-Sr ANALYTICAL DATA

| No. | Sample | $^{87}Sr/^{86}Sr$ | $^{87}Rb/^{86}Sr$ | Rb ppm | Sr ppm |
|---|---|---|---|---|---|
| 1 | Gray, massive granitic gneiss | 0.7169 | 0.4116 | 56.0 | 394.6 |
| 2 | Gray, massive granitic gneiss | 0.7204 | 0.6625 | 73.3 | 434.3 |
| 3 | Pinkish-gray banded granitic gneiss | 0.7172 | 0.5064 | 86.0 | 491.7 |
| 4 | Pinkish-gray, banded granitic gneiss | 0.7174 | 0.4786 | 78.5 | 475.2 |
| 5 | Gray, massive granitic gneiss | 0.7123 | 0.3045 | 64.8 | 615.6 |
| 6 | Gray, slightly-banded granitic gneiss | 0.7157 | 0.3804 | 70.6 | 537.2 |
| 7 | Gray, banded granitic gneiss | 0.7126 | 0.3644 | 68.9 | 547.1 |
| 8 | Gray, massive granitic gneiss | 0.7091 | 0.2386 | 46.7 | 566.8 |
| 9 | Dark gray, banded granitic gneiss | 0.7121 | 0.3772 | 144.7 | 1110.0 |
| 10 | Gray, banded granitic gneiss | 0.7187 | 0.4754 | 81.5 | 496.4 |
| 11 | Pinkish, nearly massive granitic gneiss | 0.7162 | 0.3679 | 62.3 | 490.5 |
| 12 | Light gray massive granitic gneiss | 0.7217 | 0.5957 | 85.5 | 415.8 |
| 13 | Gray, massive granitic gneiss | 0.7196 | 0.4777 | 79.3 | 481.2 |
| 14 | Gray, banded granitic gneiss | 0.7168 | 0.2580 | 72.6 | 815.1 |

TABLE VI (cont'd)

| No. | Sample | $^{87}Sr/^{86}Sr$ | $^{87}Rb/^{86}Sr$ | Rb ppm | Sr ppm |
|---|---|---|---|---|---|
| 15 | Gray, banded granitic gneiss | 0.7116 | 0.1937 | 56.4 | 842.2 |
| 16 | Coarse pink phase of granitic gneiss | 0.7520 | 1.760 | 205.0 | 338.5 |
| 17 | Pink bank in granitic gneiss | 0.8117 | 4.183 | 185.3 | 129.5 |
| 18 | White, coarse-grained granodioritic granofels | 0.7410 | 1.177 | 162.2 | 369.3 |
| 19 | White, coarse-grained granodioritic granofels | 0.7658 | 2.130 | 240.6 | 328.6 |
| 20 | Gray, medium-grained granodioritic granofels | 0.7824 | 2.868 | 185.9 | 188.9 |
| 21 | Felsic band in biotite migmatite | 0.8008 | 3.992 | 186.7 | 136.5 |
| 22 | Garnetiferous felsic band in biotite migmatite | 0.7287 | 0.7784 | 44.9 | 155.9 |
| 23 | Garnetiferous felsic band in biotite migmatite | 0.7200 | 0.4459 | 44.3 | 323.6 |
| 24 | Fine-grained biotite-hornblende gneiss | 0.7541 | 1.760 | 136.7 | 225.9 |
| 25 | Hornblende gneiss | 0.7277 | 0.9600 | 46.7 | 140.9 |
| 26 | Fine-grained amphibolite band | 0.7050 | 0.0547 | 3.02 | 159.8 |

TABLE VI (cont'd)

| No. | Sample | $^{87}Sr/^{86}Sr$ | $^{87}Rb/^{86}Sr$ | Rb ppm | Sr ppm |
|---|---|---|---|---|---|
| 27 | Fine-grained amphibolite band | 0.7085 | 0.2946 | 52.2 | 512.5 |
| 28 | Biotite gneiss | 0.7106 | 0.3446 | 39.1 | 328.2 |
| 29 | Pinkish, fine-grained biotite gneiss | 0.7178 | 0.5979 | 42.0 | 203.3 |
| 30 | Fine-grained, dark gray biotite gneiss | 0.7145 | 0.3298 | 22.8 | 200.3 |
| 31 | Dark gray, medium-grained, biotite gneiss | 0.7146 | 0.4821 | 46.3 | 277.9 |
| 32 | Pinkish gray biotite gneiss | 0.7173 | 0.5093 | 42.2 | 240.0 |
| 33 | Medium gray biotite gneiss | 0.7111 | 0.3191 | 35.9 | 325.8 |
| 34 | Medium-grained, banded granitic gneiss | 0.7249 | 0.9921 | 123.9 | 361.9 |
| 35 | Pink felsic dyke | 1.0247 | 15.27 | 213.9 | 41.7 |
| 36 | Pink felsic dyke | 1.2977 | 32.51 | 214.9 | 29.2 |
| 37 | Pink felsic dyke | 0.9966 | 12.15 | 165.1 | 40.4 |
| 38 | Pink felsic dyke | 0.8723 | 7.430 | 173.7 | 68.7 |
| 39 | Pink felsic dyke | 0.8870 | 7.761 | 168.1 | 63.8 |
| 40 | Pink felsic dyke | 0.9180 | 11.34 | 185.9 | 48.4 |

The Hudsonian metamorphic event appears to have been strong enough to wipe out the record of the time when these rocks were originally emplaced, but not strong enough to completely reset the whole rock Rb-Sr clock in this area.

The Rb-Sr data in all of the standard isochron diagrams exhibits wide scatter so that no firm geochronological conclusions were possible. Close inspection of the data in the scatter diagrams coupled with the evidence obtained from the lead analyses and other geological studies provide some indications of the probable history of the Rb-Sr systems of these rocks. The purpose of the discussion that follows is to see what kind of information can be extracted from highly discordant Rb-Sr data and how closely it correlates with the information obtained from lead-uranium and lead-lead analyses.

The data obtained on the samples from the "Pegasus Lake Area", including three granodioritic granofels specimens (18, 19 and 20) are plotted in Figure 14.

Coarse-grained, mineralized, granodioritic granofels samples exhibit a relatively wide spread in Rb-Sr ratios lying along the trend which would give an initial $^{87}Sr/^{86}Sr$ ratio of around 0.712 and slope age of close to 1750 m.y. As in the case of lead-lead data it again forms the upper limit to the distribution of data in the standard isochron plot.

The rest of the gneissic samples are fairly mono-

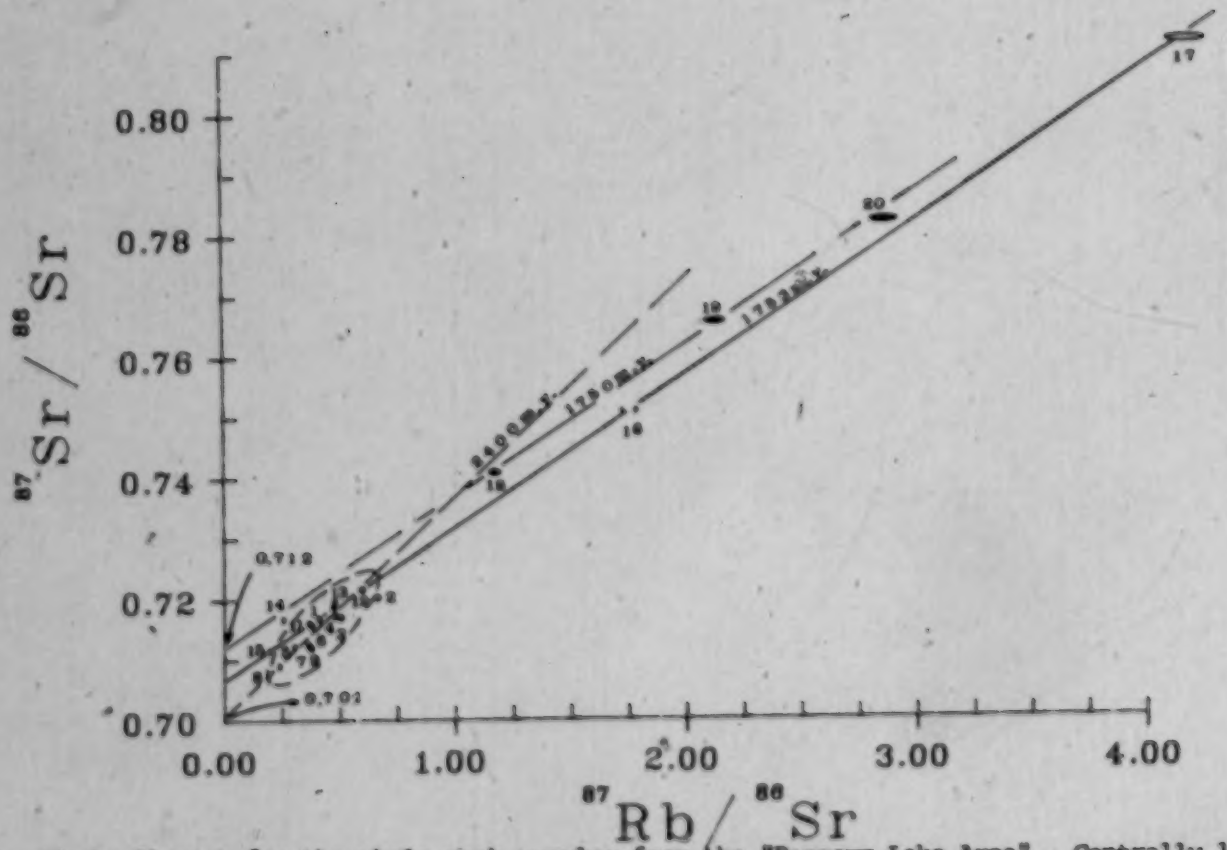


Figure 14. Rb-Sr diagram for the whole rock samples from the "Pegasus Lake Area". Centrally located samples (encircled by the dashed line) show indications of the original emplacement time while the granodioritic granofels (filled ellipses) and the rocks adjacent to the granofels horizons suggest the time of the metamorphism. For identification of the specimens refer to Figure 4 and Table VI. Data ellipses are drawn at 4$\sigma$ error level.

tonous with respect to the Rb-Sr ratios, exhibiting a limited range of values, as would be expected from their mineralogy. This is especially true for samples from the central part of the anticline where the gneiss has a predominantly gray, massive appearance with no foliation or even lineation. The range of $^{87}Rb/^{86}Sr$ values for samples 1 to 13 is 0.23-0.60 (the points within the dashed area in Figure 14). The rest of the points which do not fall into this group were collected from within about 300 meters from the shore of Dramnitzke Bay, i.e. adjacent to the mineralized granodioritic granofels area. The biotite content of these rocks is somewhat higher than in the rocks from the center of the anticline; the colour is predominantly pinkish-gray and the foliation is visible. The range of $^{87}Rb/^{86}Sr$ ratios is wider and sample 17 has the most radiogenic value of 4.2. A line fitted through three of these points (15, 16 and 17) passes through the scatter displayed by the anticline core samples, giving a slope age of 1753 m.y. and a $^{87}Sr/^{86}Sr$ initial ratio of 0.7066. It should be noted that most of the other samples from the scatter that seem to lie along this line are geographically close to the granodioritic granofels area.

An attempt to fit the line through the scatter displayed by the anticline core samples which have a small range of $^{87}Rb/^{86}Sr$ values and are distributed

within the dashed area in Figure 14 (1-13, except #2), would yield a slope age of approximately 2400 m.y. and 0.701 for an initial $^{87}Sr/^{86}Sr$ ratio.

Rb-Sr systems for the rocks from the "Pegasus Lake Area" appear to show some similarities to the U-Pb systems. In both cases the radiogenic character increases towards the outer margins of the anticline. Granodioritic granofels data form the upper limit to the distribution of points in both Pb-Pb and Rb-Sr diagrams. Rubidium and uranium seem to be enriched in granodioritic granofels, while the rocks adjacent to the mineralized area exhibit an intermediate character between centrally located samples and the samples from the mineralized area.

Data obtained from the samples of the "Old Camp Area" clearly do not exhibit closed system behaviour either (Figure 15). $^{87}Rb/^{86}Sr$ values extend to around 3.5 with the majority of points scattering between 0.0 and 1.0. The data do not display any colinearity, therefore any conclusions drawn from this data would be speculative and just an attempt to obtain confirmation of the rock history based on the whole rock lead-lead and uranium-thorium-lead data.

Assuming that the mobility of the elements during the last metamorphic event has been limited to predominantly small-scale migration and exchange, without large

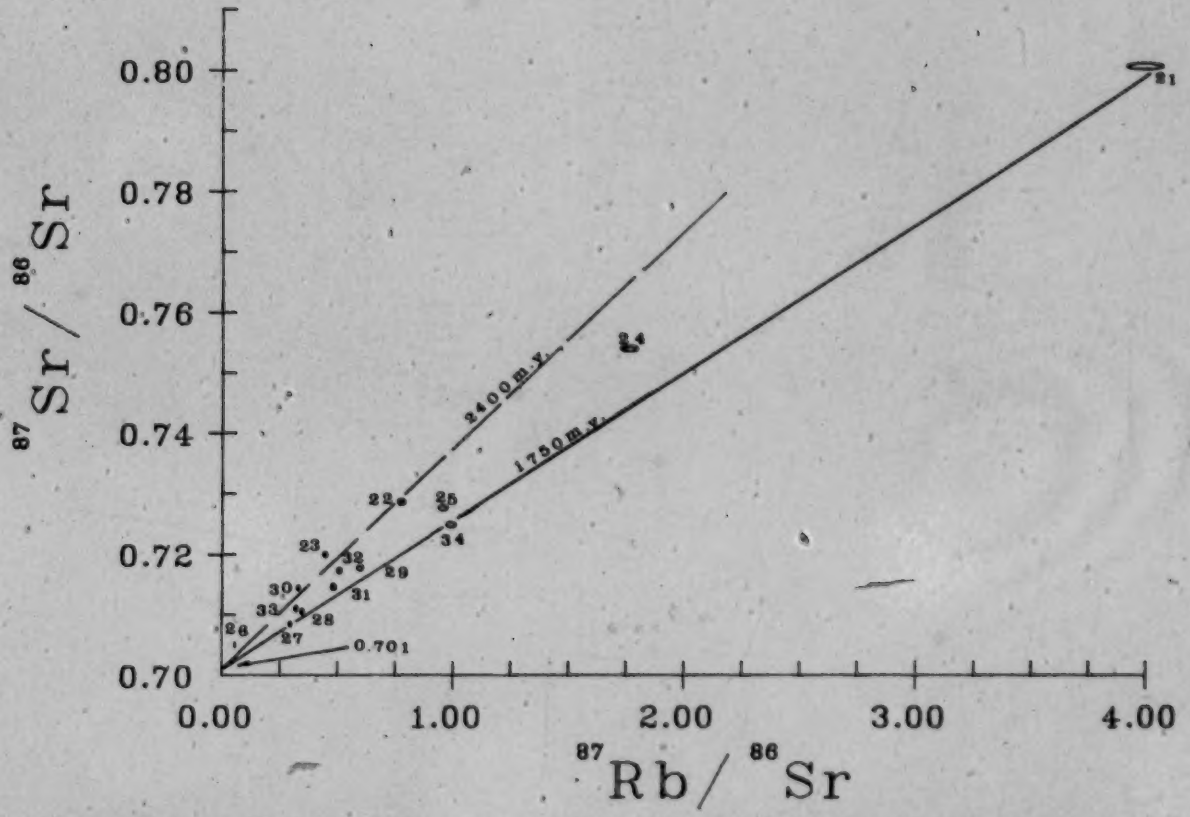


Figure 15. Rb-Sr diagram for the whole rock samples from the "Old Camp Area". "Reference isochrons" indicate the initial age and metamorphic age. For identification of the specimens refer to Figure 4 and Table VI. Data ellipses are drawn at 4σ error level.

contributions of rubidium and strontium from outside, a lower limit to the $^{87}Sr/^{86}Sr$ ratio at the end of the metamorphic event ($t_2$) can be established. This cannot be lower than the ratio of the system when it was first completely rehomogenized ($t_1$). If this value was available, the upper limit to the age of the metamorphic event, which has disturbed the original Rb-Sr system, can be estimated by drawing a reference isochron that starts at this ratio and bounds the lower scatter of the data points. In this study the end of the metamorphic event is fairly well established by the lead-lead and uranium-lead results to be around 1750 m.y. The value sought here is an $^{87}Sr/^{86}Sr$ ratio which might have been the initial $^{87}Sr/^{86}Sr$ ratio during the emplacement of the "Old Camp Area" rocks, i.e. the Charlebois Lake complex. Fitting the line with the slope age of 1750 m.y. to the three points representing the lower boundary of the scatter in Figure 20, an initial ratio of about 0.701 was obtained. Whatever the time of the initial emplacement ($t_1$) of the Charlebois Lake complex was, the average $^{87}Sr/^{86}Sr$ ratio could not have been higher (or much lower for that matter) than 0.701. The same value for initial $^{87}Sr/^{86}Sr$ ratio was obtained from the line fitted to the scatter displayed by the samples from the core of the Pegasus Lake anticline. Since this value, obtained in two different ways, is suggestive of the initial $^{87}Sr/^{86}Sr$

ratio of precursors of the Charlebois Lake complex, further possibilities for deducing the original emplacement age were examined.

For this purpose all of the data were considered together and plotted in Figure 16. Out of the thirty-four samples analysed, twenty-seven had $^{87}Rb/^{86}Sr$ ratios of less than 1.0. The upper and lower boundaries of the data consist of samples of granodioritic granofels and three samples from the "Old Camp Area" respectively. Reference isochrons of 1750 m.y. are drawn through the upper and lower boundaries. This band-like distribution of the Rb-Sr data indicates that at the end of the Hudsonian orogeny, the global Rb-Sr system of the Charlebois Lake complex was probably incompletely homogenized, with the $^{87}Sr/^{86}Sr$ ratio ranging from around 0.701 to 0.712 for the various subsystems of the complex.

It has been already mentioned that metasomatism in the area has not been observed (Morra 1977). If the mobility of rubidium and strontium within the complex as a whole was limited and only local, then from the mean initial $^{87}Sr/^{86}Sr \simeq 0.705$ at the end of the last metamorphic event (about 1750 m.y. ago) and the average $^{87}Rb/^{86}Sr$ of 0.412 for the Charlebois Lake complex, it could be calculated that it would take approximately 680 m.y. to bring the $^{87}Sr/^{86}Sr$ ratio from 0.701 to 0.705. That effectively sets the emplacement time of the Charle-

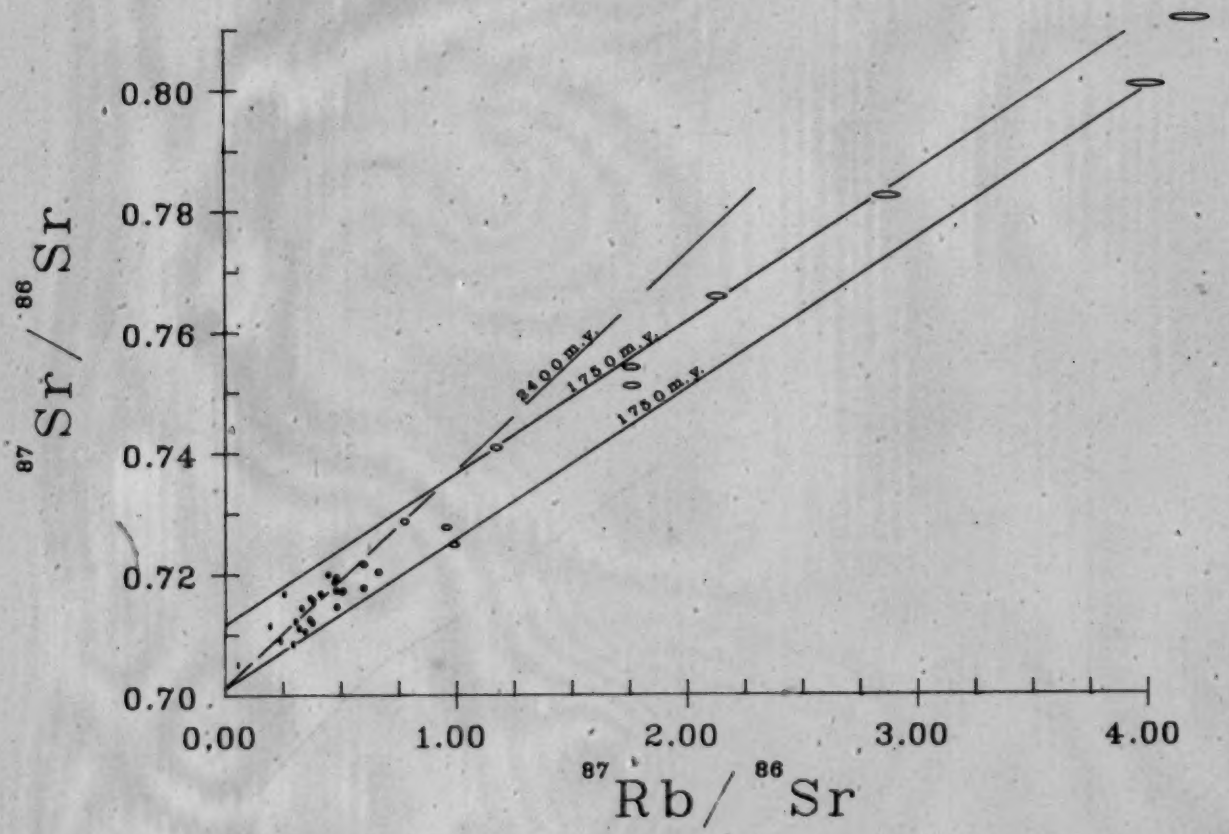


Figure 16. Combined Rb-Sr diagram for the whole rock samples from the "Old Camp Area" and the "Pegasus Lake Area". "Reference isochrons" indicating the age of the precursors and the metamorphic age are shown.

bois Lake complex percursors at about 2440 m.y. ago, which is in good agreement with the age of 2470 m.y. obtained from the feldspar lead-lead data and the 2400 m.y. obtained from the anticline core samples.

The distribution of the Rb-Sr data presented so far clearly demonstrates incomplete homogenization during the last metamorphic event or partial open system behaviour. Various studies dealing with the remobilization effects of rubidium and strontium on mineral systems, under metamorphic conditions, have been carried out (Baadsgaard and van Breemen 1970, Kesmarky 1977). It was shown that micas are readily susceptible to this kind of change. Whether or not the whole rocks are disturbed will depend upon the range of migration of these elements. The relative stability of Rb-Sr systems in whole rocks indicates that under many circumstances rubidium and strontium will become very quickly trapped in minerals having low chemical potential for these elements (such as K-feldspar), before they have a chance to migrate very far. However, other studies have demonstrated that whole rock systems can become partially open (Cumming and Scott 1976, Hoffman 1971, Brooks 1980, Olszewski 1980) or even completely reset during metamorphic events (Taylor 1975, Weber et al. 1975).

Although it has been demonstrated that common strontium can also become mobile under metamorphic

conditions (Baadsgaard and van Breemen 1970), it seems reasonable to assume that under most conditions its mobility on a whole rock scale would be negligible compared to rubidium and radiogenic components of strontium. The bulk of the normal strontium component is usually distributed within the feldspars where it is tightly held in the host lattice, even at elevated temperatures. The radiogenic strontium resulting from decay of $^{87}Rb$ is usually present in a mineral lattice which is a relatively good host for rubidium but not for radiogenic strontium. Radiogenic strontium, being poorly diadochic in this lattice, will have a much greater tendency to diffuse.

It is clear that if the scale of strontium isotope re-equilibration and rubidium migration is much less than the size of the collected and analysed specimens, the whole rock Rb-Sr data should fall on an isochron recording the initial age of the sample. According to Roddick and Compston (1977), the formation of a large rock unit may be imagined as consisting of a set or sub-systems, each of which is large enough to have an Rb-Sr ratio equivalent to that of the rock unit as a whole. If the range of migration is larger than the scale of one such subsystem, then the whole rock Rb-Sr data should fall on an isochron recording the age of the metamorphic event. If, on the other hand, the range of

migration is less than one such subsystem but larger than that of the analysed sample, scatter will be observed in the standard isochron diagram.

It was said at the beginning of this chapter that the size of the collected specimens was on order of 1-2 lb., except the samples collected from the central part of the Pegasus Lake anticline, which were about twice as large. It might not be a coincidence that data obtained on these samples show a tendency to align themselves along the trend line, suggesting the age of initial emplacement of the Charlebois Lake complex precursors (Figure 14). The scatter of these data suggests that the range of migration was probably not much larger than the size of the collected specimens. The other smaller samples collected from the outer areas of the anticline, those of granodioritic granofels and those from the "Old Camp Area", exhibit scatter and some of them show a tendency to align themselves along the isochrons recording the age of the metamorphic event. This behaviour suggests two alternatives. First, the range of migration and re-equilibration was about the same for the centrally located samples from the Pegasus Lake anticline and for the samples from the other areas. However, the samples from the other areas were smaller, resulting in the metamorphic age being "more visible". The other alternative is that although the samples were

smaller, the range of migration in the "Old Camp Area" and other areas close to and including the granodioritic granofels was much larger than in the core of the Pegasus Lake anticline. If this were the case, uranium mineralization, rubidium enrichment in the granodioritic granofels and formation of migmatites could have at least partially been caused by this local, small-scale remobilization and migration of the material during the Hudsonian metamorphic event, as suggested by Morra (1977). Morra's suggestion (1977) that sedimentary precursors of the granodioritic granofels, migmatites and granitic gneiss from the outer margins of the anticline have been originally enriched in uranium and potassium (therefore rubidium also) appears to be supported by the lead-lead and Rb-Sr data presented so far. It is clear from lead-lead and Rb-Sr data that lead and strontium of the granodioritic granofels have evolved in high μ and high Rb-Sr environments during premetamorphic time, while the same elements of the granitic gneisses from the core of the Pegasus Lake anticline have evolved in lower μ and Rb-Sr environments.

Rb-Sr data obtained on six whole rock samples of the 5 m wide late felsic dyke which crosscuts other rock units in the "Old Camp Area" are presented in Table VI and Figure 17. The data exhibit a range of $^{87}Rb/^{86}Sr$ ratios from around 6.0 to over 30.0. All of the points scatter rather

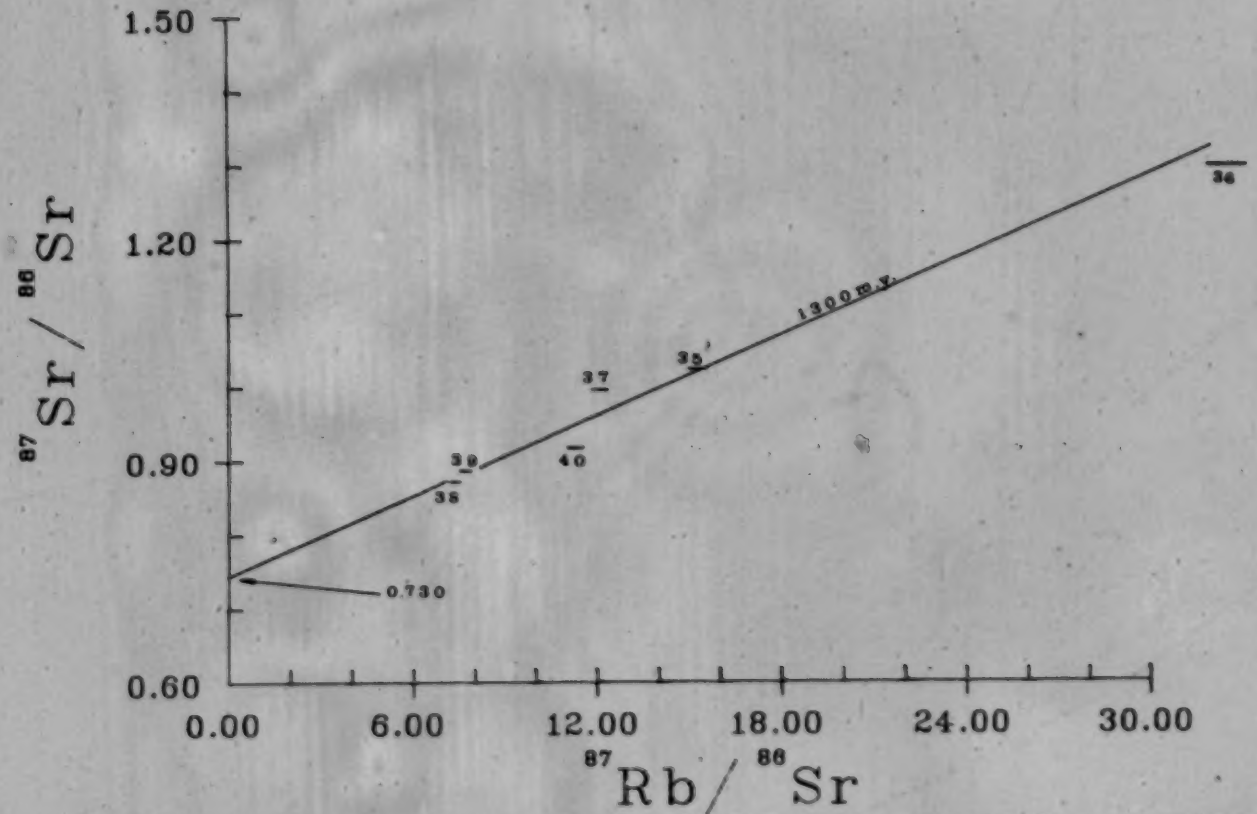


Figure 17. Rb-Sr diagram for the whole rock samples of the pink felsic dyke displays general scatter of data points around the 1300 m.y. reference isochron and high ($^{87}Sr/^{86}Sr$) ratio. For identification of the specimens refer to Figure 4 and Table VI. Data ellipses are drawn at 4σ error level.

badly so that no reasonable isochron may be computed. An approximate line drawn through the scattered points gives an approximate age of about 1300 m.y. and an initial $^{87}Sr/^{86}Sr$ ratio of about 0.730. Although this age does not have a statistical certainty because of very wide scatter, it is strikingly similar to the age obtained from lead-lead data on the same samples. Contamination by the metasedimentary rocks (Baadsgaard and Godfrey 1972) and remelting of the rocks from the lower crust might be responsible for the scatter and high apparent initial $^{87}Sr/^{86}Sr$ ratio.

## CHAPTER IV

## SUMMARY AND CONCLUSIONS

The study was undertaken to establish the age and the history of the area and to possibly glean some information regarding the relationship between the individual members of the complex and the origin of the U-Pb system of the uranium mineralized rock units. It became apparent, early in this study, that interpretation of the geochronological data for this area would be complicated by the open system behaviour and limited migration of elements during the last metamorphic event. For that reason a complete set of lead-lead and rubidium-strontium whole rock analyses was performed on the same specimens. Radiogenic minerals such as uraninite and mineral fractions rich in monazite from the granodioritic granofels and two migmatite samples (i.e. samples with the highest $^{206}Pb/^{204}Pb$ ratios) were separated and analysed for lead, uranium and thorium isotopes. Six feldspar separates from the least radioactive samples, that is, samples with the lowest $^{206}Pb/^{204}Pb$ ratios, were analysed for lead isotopes.

The geochronological data obtained during this study was correlated with the available geological evidence and summarized in Table VII.

The uranium-lead and lead-lead results seem to have been more useful than the rubidium-strontium results, which exhibited general scatter and provided only slight

## TABLE VII

### GENERALIZED PRECAMBRIAN GEOCHRONOLOGY OF THE CHARLEBOIS LAKE AREA

| GENERAL GEOLOGIC HISTORY (after Morra, 1977) | | GEOCHRONOLOGIC EVIDENCE | | |
|---|---|---|---|---|
| GEOLOGIC EVENT | TIME m.y. | METHOD AND MATERIAL STUDIED | DATE m.y. | SPECIFIC ROCKS STUDIED |
| | 1200 | | | |
| HELIKIAN — Intrusion | | Pb-Pb on whole rock samples | 1235 | Late felsic dyke and irregular pegmatitic bodies |
| | | Rb-Sr on whole rock samples | 1300 | |
| | 1500 | | | |
| | 1700 | | | |
| | | U-Pb on uraninite | 1750 | Granodioritic granofels and migmatite |
| HUDSONIAN — Mineralization (Anatexis?) (Faulting) (Folding) Metamorphism | | Pb-Pb on whole rock samples | 1750 | "Old Camp": Bt; Hb; granitic gneisses |
| | | Rb-Sr on whole rock samples | 1753 | Pegasus Lk.: Gneiss from outer margin of anticline |
| | | Pb-Pb on whole rock samples | 1772 | Granodioritic granofels and migmatite |
| | | Pb-Pb on whole rock samples | 1775 | Pegasus Lk: Granitic to tonalitic gneiss |
| | | U-Pb on monazite-rich fractions | 1797 | Separates from granodioritic granofels and migmatite |
| | 1900 | | | |
| APHEBIAN — Subsidence formation of precursors of Charlebois Lake complex | 2400 | Rb-Sr on whole rock samples | 2400 | Pegasus Lk: Granitic gneiss from center of the anticline |
| | | Pb-Pb on feldspars | 2470 | Mineral separates from various rocks of the Charlebois Lake complex |

suggestions of the important events in the history of these rocks. The uranium-lead data for uraninites and monazite-rich fractions show clear indications of a relatively slow and gradual weakening of the Hudsonian metamorphic event beginning, in this area, about 1797 m.y. ago with the closing of the U-Pb system of monazites and possibly other high-grade minerals. U-Pb data obtained on the uraninite separates suggest that the end of the Hudsonian orogeny in the Charlebois Lake area was marked by the closing of the U-Pb system of uraninite 1750 m.y. ago. The ages of 368 m.y. and 55 m.y. obtained from the apparent lower concordia intercepts of the uraninite and monazite discordia lines, respectively, are believed to be spurious since discordance is the result of continuous lead diffusion from these minerals.

The overall history of the Charlebois Lake complex is most completely illustrated by the lead-lead and, to some extent, supported by the rubidium-strontium results. Whole rock and feldspar lead-lead data indicated that lead in this complex approximates the evolution according to the three stage evolution model with $f_1$ = const. (Gale and Mussett 1973). It is suggested that the original emplacement (i.e. formation of the sedimentary precursors) of the Charlebois Lake complex could have taken place as early as 2470 m.y. ago from an environment that had $\mu = 9.85$. This value is slightly higher than Stacey and Kramers (1975) estimate of the earth's $\mu_2$ value. The

rubidium-strontium data obtained on the specimens from the core of the Pegasus Lake anticline show vague signs that 0.701 might have been the initial average $^{87}Sr/^{86}Sr$ ratio of the sedimentary precursors some 2400 m.y. ago. From the overall average $^{87}Rb/^{86}Sr$ of 0.412 for the Charlebois Lake complex, the mean $^{87}Sr/^{86}Sr$ ratio of around 0.705 at the end of the Hudsonian metamorphic event and assuming that the initial $^{87}Sr/^{86}Sr$ could not have been very much different from 0.701, it was estimated that the age of the sedimentary precursors must be around 2440 m.y. It therefore was concluded from all these indications that the Charlebois Lake complex was probably formed 2400-2470 m.y. ago.

Besides the lead-uranium data of the radiogenic minerals, the Hudsonian metamorphic event was well defined by the parallel lead distribution of the lead-lead data with slope ages ranging from 1741 m.y. to 1775 m.y. The rubidium-strontium data also provided some indications of this event, expressed in trend lines formed by granodioritic granofels samples, specimens from the outer margins of the Pegasus Lake anticline and the lower distribution boundary of the "Old Camp Area" data.

Morra (1977) observes that there is no evidence of large scale migration of material in the area, and suggests that uranium mineralization is probably a product of locally remobilized uranium (and possibly thorium) from the uranium and thorium-rich sedimentary layers of the

arkosic arenites. These suggestions are supported by the lead-lead and rubidium-strontium data presented in this study. The distribution of the lead-lead and to some extent the rubidium-strontium data, indicated that direct precursors of the mineralized granodioritic granofels had evolved in high $\mu$, i.e. a high uranium and possibly high rubidium environment during premetamorphic time. Both lead-lead and rubidium-strontium data of the mineralized granodioritic granofels represent the more radiogenic limits of the distribution of the geochronological data. The other samples exhibit a gradual decrease in radiogenic component from mineralized granodioritic granofels, which is adjacent to the calc-silicate layer towards the more massive granitic gneiss at the base of the metasedimentary succession. One may speculate that the increase in pressure during compaction of loose sediments "squeezed out" fluids which served to facilitate migration of uranium upwards. The precursors of the calc-silicates (calcareous and tuffaceous sediments) acted as an impermeable barrier to the migrating solution, resulting in the relatively higher concentration of uranium adjacent to this layer. Later, under metamorphic conditions uranium was locally remobilized producing the observed radioactive anomalies and the distribution of lead-lead data presented in Figure 10.

Due to the insufficient number of collected and analysed samples, the history of the late felsic dykes

and the irregular pegmatitic bodies has not been well determined. Lead-lead and rubidium-strontium data indicate that this rock unit was emplaced in the post-Hudsonian time, possibly some time between 1500 m.y. and 1100 m.y. ago. An extensive geochronological investigation using lead-lead and rubidium-strontium methods of this and other similar late rock units from the surrounding areas and larger Churchill province is strongly suggested. The benefit of such a study would be a better understanding of the history and events taking place in the Churchill province during this time period.

This study, like many others in the literature, has demonstrated the necessity of the multimethod approach in geochronological investigations of disturbed rock systems. Although it was shown that the whole rock Pb-Pb system preserves the history record well, and possibly better than the Rb-Sr system, the use of two or more methods generally reveals more details and allows more confidence in making geochrological conclusions and assumptions. Whenever enough material is available, the use of combined Pb-Pb, Rb-Sr and U-Pb dating technique on whole rock and mineral separates is strongly suggested.

## REFERENCES


Baadsgaard, H., 1965. Geochronology. Meolds. fra Dansk. Geol. Foren, 16, 1-48.

Baadsgaard, H. and Godfrey, J.D., 1972. Geochronology of the Canadian Shield of Northeastern Alberta. II. Charles-Andrew-Colin Lakes area. Can. J. Earth Sci., 9, 863-881.

Baadsgaard, H. and Van Breemen, O., 1970. Thermally induced migration of Rb and Sr in an ademellite. Eclog. Geol. Helv., 63, 31-44.

Beck, L., 1969. Uranium deposits in Athabasca region, Saskatchewan. Sask. Dept. Miner. Resour. Report No. 126.

Brooks, C., 1980. Aphebian overprinting in the Superior Province east of James Bay, Quebec. Can. J. Earth Sci., 17, 526-532.

Burger, A.J., Nicolaysen, L.O. and Ahrens, L.H., 1967. Controlled leaching of monazites. J. Geophys. Res., 75, 3585-3594.

Burwash, R.A., 1978. Metamorphism of the Athabasca mobile belt, a subsurface extension of the Churchill province. Geol. Surv. Paper 78-10, 123-127.

Burwash, R.A., 1979. Uranium and thorium in the Precambrian basement of Western Canada. Part II. Petrologic and tectonic controls. Can. J. Earth Sci., 16, 472-483.

Burwash, R.A., Baadsgaard, H. and Peterman, Z.E., 1962. Precambrian K-Ar dates from the Western Canada Sedimentary Basin. J. Geophys. Res., 67, 1617-1675.

Burwash, R.A. and Krupička, J., 1970. Cratonic reactivation in the Precambrian of Western Canada. Part II. Metasomatism and isostasy. Can. J. Earth Sci., 7, 1275-1294.

Catanzaro, E.J. and Gast, P.W., 1960. Isotopic composition in pegmatitic feldspars. Geochim. Cosmochim. Acta, 19, 113-126.

Costaschuk, S.M., 1979. Uraniferous pegmatites in the Grease River area, Northern Saskatchewan. Unpublished M.Sc. Thesis, University of Alberta.

Cumming, G.L., 1952. A petrographic and radiometric study of the Tazin metasediments of the Charlebois Lake area, Northeastern Saskatchewan. Unpublished M.Sc. Thesis, University of Saskatchewan.

Cumming, G.L. and Richards, J.R., 1975. Ore lead isotope ratios in continuously changing earth. Earth Planet. Sci. Lett., 28, 155-171.

Cumming, G.L. and Rimsaite, J., 1979. Isotopic studies of lead-depleted pitchblende, secondary radioactive minerals and sulphides from the Rabbit Lake uranium deposit, Saskatchewan. Can. J. Earth Sci., 16, 1702-1715.

Cumming, G.L., Rollett, J.S., Rossotti, E.J.C. and Whewell, R.J., 1972. Statistical methods for the computation of stability constants. Part I. Straight line fitting of points with the correlated errors. Journal of the Chemical Soc., Dalton Transactions, 2652-2658.

Cumming, G.L. and Scott, B.D., 1976. Rb/Sr dating of rocks from Wollaston Lake Belt, Saskatchewan. Can. J. Earth Sci., 13, 355-364.

Cumming, G.L., Willson, J.T., Farquhar, R.M. and Russell, R.D., 1955. Some dates and subdivisions of the Canadian Shield. Proc. Geol. Assoc. Canada, 7, Part II. 27-79.

Davis, D.W., 1978. Determination of the $^{87}Rb$ decay constant. An Rb/Sr and Pb/Pb study of the Labrador Archean complex. Unpublished Ph.D. Thesis, University of Alberta.

Davis, D.W., Gray, J., Cumming, G.L. and Baadsgaard, H., 1977. Determination of the $^{87}Rb$ decay constant. Geochim. Cosmochim. Acta, 41, 1745-1749.

Doe, B.R., 1970. Lead Isotopes. Springer-Verlag, New York.

Doe, B.R., Tilton, G.R. and Hopson, C.A., 1965. Lead isotopes in feldspars from selected granitic rocks associated with regional metamorphism. J. Geophys. Res., 70, 1947-1968.

Fahrig, W.F. and Wanless, R.K., 1963. Age and significance of diabase dyke swarms of the Canadian Shield. Nature, 200, 934-937.

Faure, G., 1977. Principles of Isotope Geology. John Wiley and Sons, New York.

Faure, G. and Powell, J.L., 1972. Strontium Isotope Geology. Springer-Verlag, New York.

Gale, N.H. and Mussett, A.E., 1973. Episodic uranium-lead models and the interpretation of variations in the isotopic composition of lead in rocks. Rev. Geophys. Space Phys., 11, 37-86.

Hofman, A., 1971. Effect of regional metamorphism on radiometric ages in pelitic rocks - preliminary results. Carn. Inst. Wash. Yearbook, 70, 242-245.

Johnson, F.J., 1963. Geology of Lytle Lake area. West half Saskatchewan. Sask. Dept. Miner. Resour. Report No. 80.

Johnson, F.J., 1964. Geology of Lytle Lake area. East half Saskatchewan. Sask. Dept. Miner. Resour. Report No. 90.

Kanasewich, E.R., 1968. Interpretation of lead isotopes and their geological significance. In: Radiometric dating for geologists. Eds.: Hamilton, E.I. and Farquhar, R.M. Interscience Publishers.

Kesmarky, S., 1977. Rates of migration of alkali and strontium ions in heated quartz monzonites. Unpublished M.Sc. Thesis, University of Alberta.

Kirkland, S.J.T., 1952. Petrology of the granites and pegmatites, Charlebois Lake area, Northern Saskatchewan. Unpublished M.A. Thesis, University of Saskatchewan.

Koeppel, V., 1968. Age and history of the uranium mineralization of the Beaverlodge area, Saskatchewan. Geol. Surv. Can. Paper 67-31.

Komlev, L.V., Ivanova, K.S. and Savonenkov, V.G., 1964. On the diffusional mobility of lead isotopes and character of the admixed lead. Geokhimiya, 12, 1228-1239.

Koster, F. and Baadsgaard, H., 1970. On the geology and geochronology of Northern Saskatchewan. Part I. Tazin Lake Region. Can. J. Earth Sci., 7, 919-930.

Krogh, T.E., 1973. A low contamination method for hydrothermal decomposition of zircon and extraction of U and Pb for isotopic age determination. Geochim. Cosmochim. Acta, 37, 485-494.

Lewrey, J.F., Sibbald, T.I.T. and Rees, C.J., 1978. Metamorphic patterns and their relationship to tectonism and plutonism in the Churchill province in Northern Saskatchewan. Geol. Surv. Can. Paper 78-10, 139-154.

Ludwig, K.R. and Silver, L.T., 1977. Lead-isotope inhomogeneity in Precambrian igneous K-feldspars. Geochim. Cosmochim. Acta, 41, 1457-1471.

Mattinson, J.M., 1972. Preparation of hydrofluoric, hydrochloric and nitric acids at ulta low lead levels. Anal. Chem., 44, 1715-1718.

Money, P.L., Bear, A.J., Scott, B.P. and Wallis, R.H., 1970. The Wollaston Lake Belt, Saskatchewan, Manitoba, Northwest Territories. Geol. Surv. Can. Paper 70-40, 170-197.

Morra, F.P., 1977. Geology and uranium deposits of the Charlebois-Higginson Lake area, Northeastern Saskatchewan. Unpublished M.Sc. Thesis, University of Alberta.

Mawdsley, J.B., 1950. The geology of the Charlebois Lake area. Athabasca Mining Division, Northern Saskatchewan. Precamb. Geol. Series, Report No. 5.

Mawdsley, J.B., 1952. Uraninite-bearing deposits, Charlebois Lake area, Northeastern Saskatchewan. Can. Mining and Metall. Bull., June, 366-375.

Olszewski, W.J., 1980. The geochronology of some stratified metamorphic rocks in northeastern Massachusetts. Can. J. Earth Sci., 12, 1407-1416.

Roddick, J.C. and Compston, W., 1977. Strontium isotope equilibrium: a solution to paradox. Earth Planet. Sci. Lett., 34, 238-246.

Sassano, G.P., 1972. The nature and the origin of the uranium mineralization of the Fay Mine, Eldorado, Saskatchewan. Unpublished Ph.D. Thesis, University of Alberta.

Sassano, G.P., Baadsgaard, H. and Morton, R.D., 1972. Rb-Sr isotopic systematics of the Foot Bay Gneiss, Donaldson Lake Gneiss and pegmatite dykes from the Fay Mine, Northwestern Saskatchewan. Can. J. Earth Sci., 9, 1368-1381.

Shestakov, G.I., 1972. Diffusion of Pb in monazite, zircon, sphene and apatite. Geokhimiya, 10, 1197-1204.

Sibbald, T.I.T., Munday, R.J.C. and Lewrey, J.F., 1976. The geological setting of uranium mineralization in Northern Saskatchewan, uranium in Saskatchewan. Sask. Geol. Soc., Spec. Publ. No. 3, 51-98.

Sinha, A.K., 1969. Removal of radiogenic lead from potassium feldspars by volatilization. Earth Planet. Sci. Lett., 7, 109-115.

Stacey, J.S. and Kramers, J.D., 1975. Approximation of terrestrial lead isotope evolution by two stage model. Earth Planet. Sci. Lett., 26, 207-221.

Starik, I.E. and Lazarev, K.F., 1964. Study of the comparative leachability of the isotopes of radium, uranium and thorium from monazite. Methody Opredeliniyu Absolyut. Vozrasta. Geol. Obrazov., No. 6, 24-31.

Steiger, R.H. and Jäger, E., 1977. Subcommission geochronology: Convention on the use of decay constants in geo- and cosmochronology. Earth Planet. Sci. Lett., 36, 359-362.

Tatsumoto, M., Knight, R.J. and Allegre, C.J., 1973. Time differences in the formation of meteorites as determined from the ratio of $^{207}Pb$ to $^{206}Pb$. Science, 180, 1279-1283.

Taylor, P.N., 1974. An early Precambrian age for migmatite gneiss from Vikon I Bø, Vesteraalen, North Norway. Earth Planet. Sci. Lett., 27, 35-42.

Taylor, P.N., Moorbath, S., Goodwin, R. and Petrikowski, A.C., 1980. Crustal contamination as an indicator of the extent of early Archean continental crust: Pb isotopic evidence from the late Archean gneisses of West Greenland. Geochim. Cosmochim. Acta, 44, 1437-1453.

Trembley, L.P., 1978. Uranium subprovinces and types of uranium deposits in the Precambrian rocks of Saskatchewan. Geol. Surv. Can. Paper 78-1A, 427-435.

Vidal, Ph., Blais, S., Jahn, B.M., Capdevila, R. and Tilton, G.R., 1980. U-Pb and Rb-Sr systematics of the Suomussalmi Archean greenstone belt (Eastern Finland). Geochim. Cosmochim. Acta, 44, 2033-2044.

Wasserburg, G.J., 1963. Diffusion processes in lead-uranium systems. J. Geophys. Res., 68, 4823-4846.

Weber, W., Anderson, R.K. and Clark, G.S., 1975. Geology and geochronology of the Wollaston Lake fold belt in Northwestern Manitoba. Can. J. Earth Sci., 12, 1749-1759.

Wetherill, G.W., 1963. Discordant uranium-lead ages. J. Geophys. Res., 68, 2957-2965.

Winkler, H.G.F., 1967. Petrogenesis of Metamorphic Rocks. 2nd Edition. Springer-Verlag, New York.

## APPENDIX I

## THEORY OF U-Th-Pb, Pb-Pb AND Rb-Sr SYSTEMATICS

### U-Th-Pb Systematics

Three basic radioactive decay systems are used in U-Th-Pb and Pb-Pb age dating techniques

$$^{238}U \rightarrow {}^{206}Pb + 8\,{}^{4}He + 6\beta^{-}$$

$$^{235}U \rightarrow {}^{207}Pb + 7\,{}^{4}He + 4\beta^{-}$$

$$^{232}Th \rightarrow {}^{208}Pb + 6\,{}^{4}He + 4\beta^{-}.$$

The relationship of the molar concentration of the daughter isotope (corrected for initial daughter contamination) to the molar concentration of the parent isotope, measured in the sample at present (t=0) is given by the following general equation:

$$D = P[\exp(\lambda t) - 1]$$

where D is the molar concentration of the daughter isotope, P is the molar concentration of the parent isotope, presently measured, $\lambda$ is radioactive decay constant and t is the time when the isotopic system became closed to migration of either parent or daughter isotope across the boundaries of the system.

Radioactive decay constants, adopted throughout this study, are (as suggested by Steiger and Jäger 1977):

Decay constant of $^{238}U$: $\lambda = 0.155125\times10^{-9}yr^{-1}$

Decay constant of $^{235}U$: $\lambda' = 0.98485\times10^{-9}yr^{-1}$

Decay constant of $^{232}Th$: $\lambda'' = 0.049475\times10^{-9}yr^{-1}$.

It is immediately obvious that knowing the amounts of parent and daughter isotopes at present, the time when the system became closed can be calculated from the relationship:

$$t = 1/\lambda \ln[\frac{D}{P} + 1].$$

Applying this equation to the three decay systems mentioned at the beginning, three independent ages can be obtained.

Since the present relative isotopic proportions of natural uranium are known ($(^{235}U/^{238}U)_{present} = 137.88$) and are assumed to have varied over geologic time due to the radioactive decay only, it is possible to obtain a fourth useful date, i.e. $^{207}Pb/^{206}Pb$ age.

By a comparison of these ages (i.e. measured daughter to parent ratios of the sample system being investigated) it is possible to derive not only the age of the system but some information regarding the history of the isotopes and therefore the sample system as well. If all the calculated ages are the same within analytical error, the phase being dated has remained closed to changes in the parent-daughter system and such dates are termed "concordant dates".

Theoretical U-Pb systematics are graphically expressed in Figure 18. It shows that the mineral or other investigated phase which has not been subjected to the lead loss or uranium gain (or lead gain or uranium loss) will have concordant $^{207}Pb/^{235}U$, $^{206}Pb/^{238}U$ and $^{207}Pb/^{206}Pb$ ages and that data will be represented by a point that lies on the curved line called "concordia".

If the dated phase has been subjected to the lead loss (or uranium gain) during the short period of time, recently or any time in the past after the original closure of the system, obtained ages will not agree, within the set error limits, i.e. they will be "discordant". U-Pb data obtained on a suite of samples that has experienced such episodic daughter losses (or parent gains) whether recently or in a distant past, will theoretically give a chord of points that determines the straight line which intersects the concordia curve at two places. The upper intersection represents the time of original formation of the phase and the lower intersection, the time of the episodic event which caused the disturbance in the system.

If it is assumed that the lead continuously diffuses from the system over the entire history of the phase, measured Pb-U ratios on a set of samples with this type of history will fall along the continuous diffusion line in the concordia plot (Figure 18).

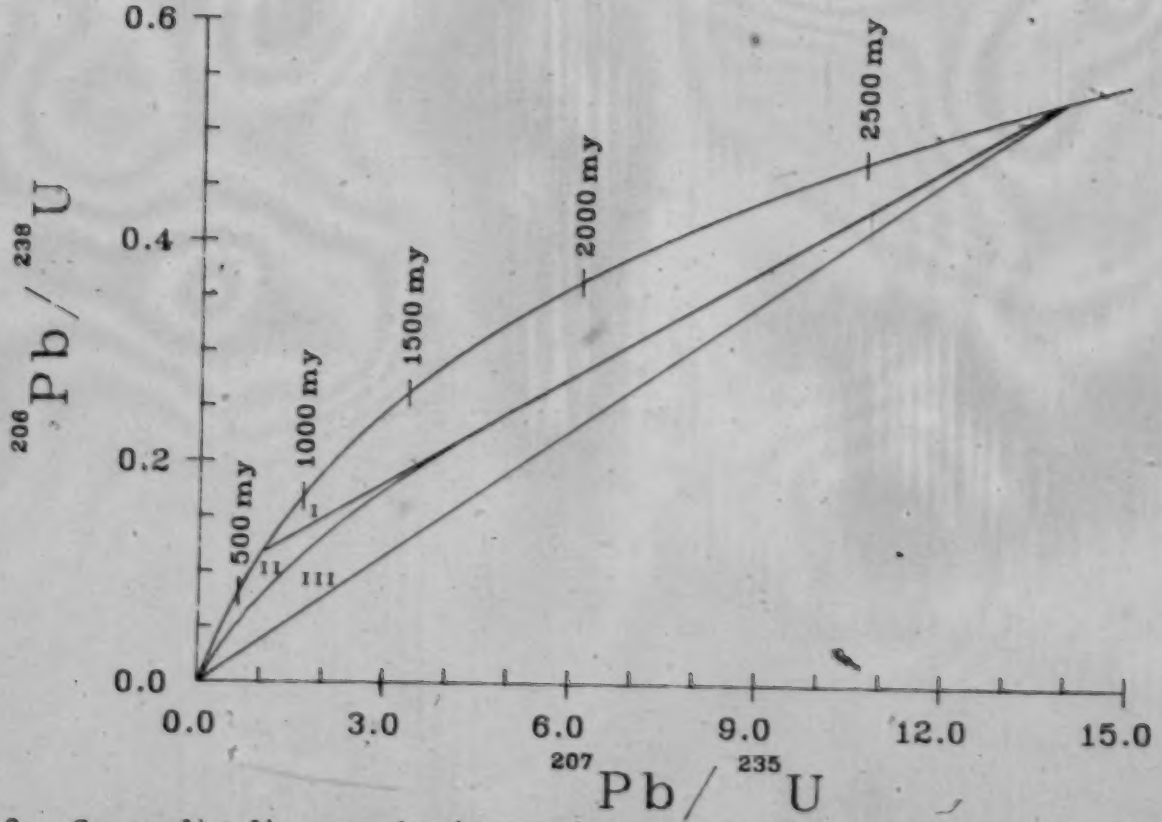


Figure 18. Concordia diagram showing various types of discordance all starting at 2700 m.y. I: episodic lead loss line. II: continuous lead diffusion line. III: recent lead loss (from concordant mineral) line.

A combination of these basic types of parent-daughter histories can greatly complicate the interpretation of the obtained data. A more complete discussion of the U-Th-Pb systematics, along with the set of important references, is given in Faure (1977).

Pb-Pb Systematics

Detailed treatment of Pb-Pb systematics is covered elsewhere in the literature (Faure 1977, Gale and Mussett 1973, Kanasewich 1968, and others) so that only a brief overview of the theory as applied to the whole rock system is given here.

Ratios of the radioactive isotopes $^{206}Pb$, $^{207}Pb$ and $^{208}Pb$ (generated according to the radioactive decay schemes, mentioned in the previous section) to the non-radiogenic $^{204}Pb$ isotope are utilized for interpretation. A more useful way of presenting the data is on a $^{207}Pb/^{204}Pb$ vs. $^{206}Pb/^{204}Pb$ rather than on a $^{208}Pb/^{204}Pb$ vs. $^{206}Pb/^{204}Pb$ diagram. The reason for this is that uranium isotopes (whose products are $^{207}Pb$ and $^{206}Pb$) cannot be significantly separated during the normal geochemical reaction, whereas uranium and thorium (whose decay product is $^{208}Pb$) may be.

The interpretation of the lead isotope distribution in a suite of rock samples basically consists of fitting it to the model which would be described by a set of episodic changes in U-Pb ratio at some discrete time

intervals in the past.

The simplest case of the lead isotope evolution would be if the lead evolved by a simple radioactive decay of uranium to lead over geologic time. This evolution is described by the following equations:

$$x_1 = a_o + \mu[\exp(\lambda t_o) - \exp(\lambda t_1)]$$

$$y_1 = b_o + (\mu/137.88)[\exp(\lambda' t_o) - \exp(\lambda' t_1)]$$

where $x_1 = {}^{206}Pb/{}^{204}Pb$ and $y_1 = {}^{207}Pb/{}^{204}Pb$, both at the time $t_1$; $a_o = {}^{206}Pb/{}^{204}Pb$ and $b_o = {}^{207}Pb/{}^{204}Pb$, both at the time $t_o$; $\mu = {}^{238}U/{}^{204}Pb$ at present time ($t=0$), $\lambda$ and $\lambda'$ are radioactive decay constants with the values given in the previous section. The time $t$ is measured back into time from the present. When plotted on the x-y ($^{207}Pb/^{204}Pb$ versus $^{206}Pb/^{204}Pb$) diagram these two equations are represented by a curve which is termed "lead evolution growth curve" (Figure 19). The values of $a_o$ and $b_o$ are lead isotopic ratios in the triollite phase of the Canyon Diablo meteorite i.e., $a_o$=9.307, $b_o$=10.294, as suggested by Tatsumoto et al. (1973). It is assumed that isotopic composition of the Pb in the earth was equal to $a_o$ and $b_o$ at a time which is referred to as the age of the earth. This term, which is not an easily measurable value, can be estimated in two ways. First, based on the slope of the line which is determined by the $^{207}Pb/^{204}Pb$ and $^{206}Pb/^{204}Pb$ ratios of various meteorites, and second

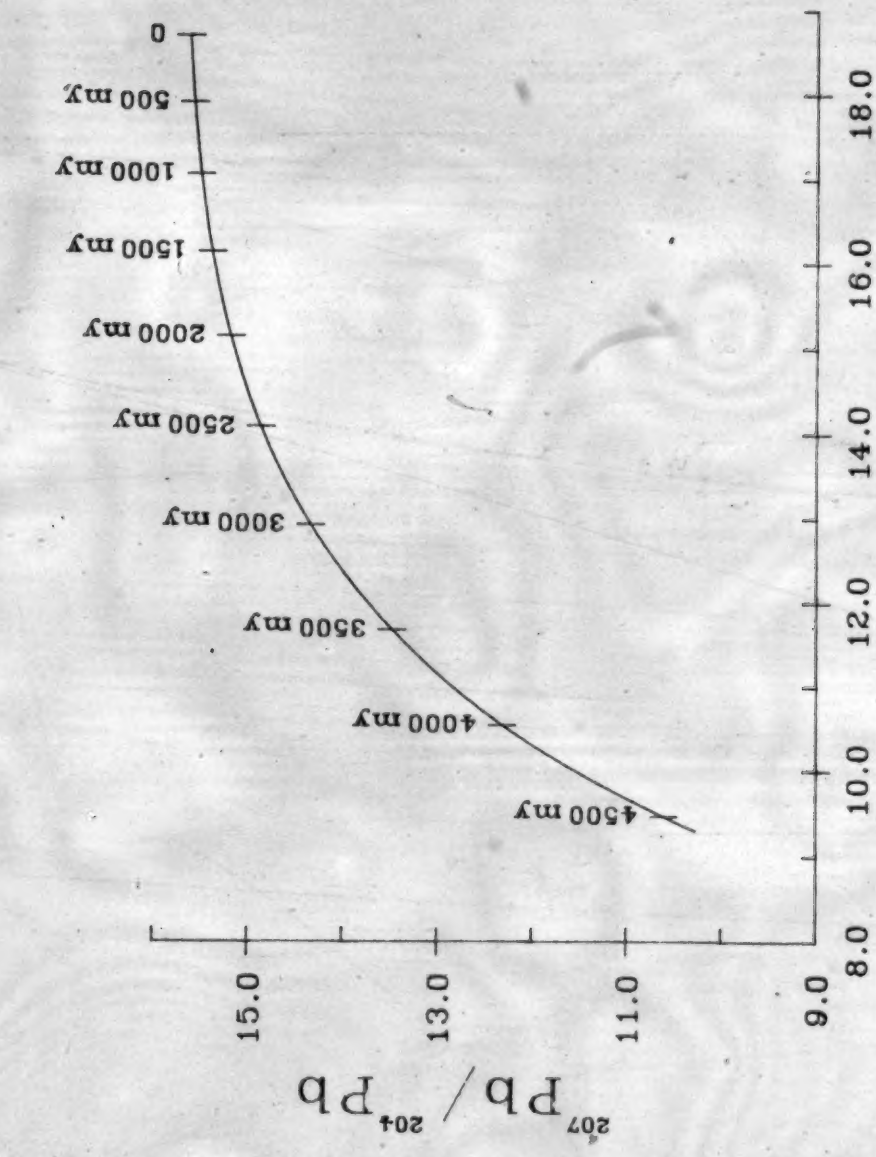


Figure 19. Pb growth curve diagram. $\mu = 9.85$, $a_o = 9.346$, $b_o = 10.218$ and $T_o = 4570$ m.y.

based on the isotopic ratios of conformable lead ore deposits which appear to fall on a single stage growth curve. Their ages, as determined by their position on the lead growth curve, appear to be somewhat younger than their geologic ages determined by other methods. Discrepancies become more pronounced with younger ages, suggesting that the single stage lead evolution growth curve fits the history of these ores only as a first approximation. More sophisticated models of mantle crustal evolution that take into account possible catastrophic changes (Stacey and Kramers 1975) or continuous changes (Cumming and Richards 1975) in the U-Pb system have been devised. From a model with a continuous change in $\mu$ Cumming and Richards estimated the age of the earth to be 4509 m.y. while Stacey and Kramers adopted (from Tatsumoto et al. 1973) 4570 m.y. for the age of the earth and also suggested global scale fractionation of the U-Pb system at 3700 m.y. ago.

In a closed system the only changes taking place in the U-Pb ratio are discrete and episodic. It may be said that the suite of "U-Pb subsystems" which was separated from the global $\mu_1$ system at time $t_1$, with Pb-Pb isotopic composition $x_{(1)}$ and $y_{(1)}$ and then each subsystem evolved in separate $\mu_{2i}$ environments until time $t_2$ (when all the uranium was removed) will distribute themselves along the straight line of slope:

$$\frac{y_{(2)} - y_{(1)}}{x_{(2)} - x_{(1)}} = \frac{1}{137.88} \cdot \frac{\exp(\lambda' t_1) - \exp(\lambda' t_2)}{\exp(\lambda t_1) - \exp(\lambda t_2)} .$$

If the system evolved until the present, then $t_2=0$, and the above slope equation may be solved directly for $t_1$ (Fig. 20). This is a two stage model. The line passes through the primary growth curve of the $\mu_1$ environment at $t=0$ and $t=t_1$. Any of these subsystems can be characterized by two parameters: $\mu_{2i}$ and $f_1 = \mu_1/\mu_{2i}$. The parameter f is the fractionation coefficient and, providing there is no change in the isotopic composition of uranium or lead at the time of differentiation ($t_1$), it is a direct measure of the U-Pb ratio immediately before and after the differentiation.

The general three stage model history involves evolution in the constant $\mu_1$ environment from the formation of the earth to the time ($t_1$) of the first global fractionation of the system into subsystems of different $\mu_{2(i)}$ environments. Each second stage subsystem evolves independently until the new U-Pb fractionation of these individual subsystems takes place at time $t_2$ into the third stage environments which are characterized by the $\mu_{3(ij)}$ values. From then until the present, ($t=0$) each third stage subsystem remains closed and evolution continues by the decay of uranium into lead only.

Each episodic event is characterized by a corresponding fractionation coefficient: at $t_1$ by $f_1 = \mu_1/\mu_2$; and

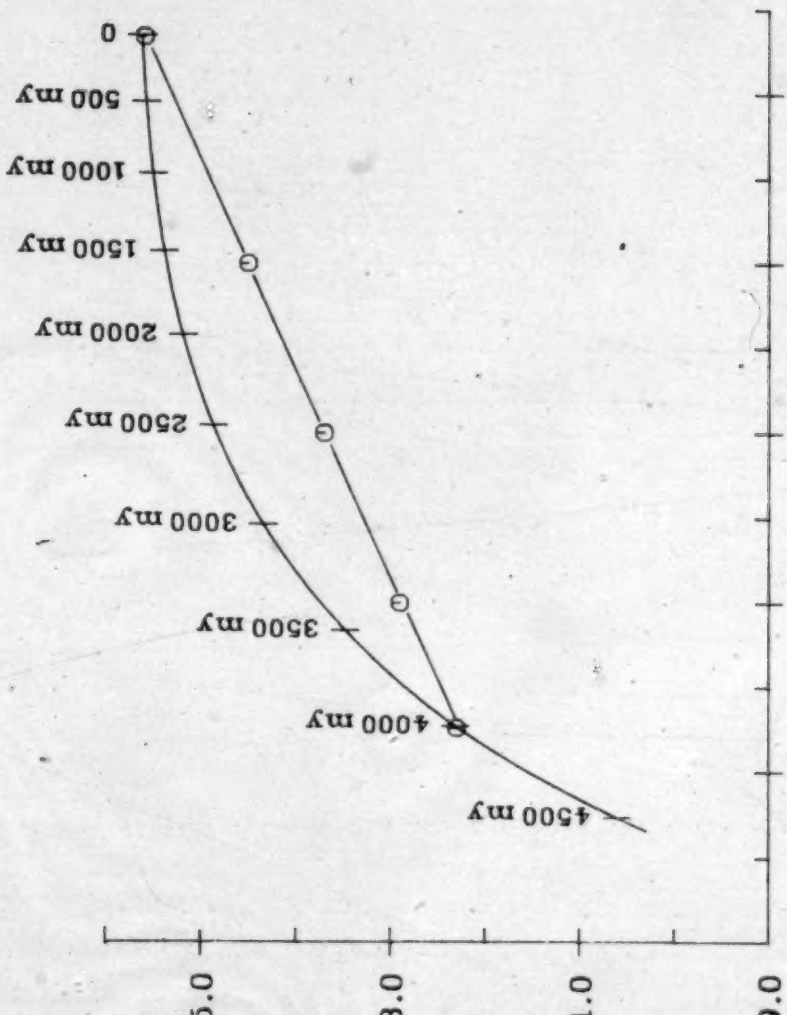


Figure 20. Pb isotopic evolution diagram for the samples which underwent two-stage evolution history. Initial $\mu = 9.85$, $T_o = 4570$ m.y., $t_1 = 4000$ m.y., $a_o = 9.346$ and $b_o = 10.218$.

at $t_2$ by $f_2 = \mu_{2i}/\mu_{3ji}$.

The resulting general distribution of the points in the $^{207}Pb/^{204}Pb$ vs. $^{206}Pb/^{204}Pb$ diagram will be governed by the degree of fractionation at $t_1$ and $t_2$. The most common case will be when $f_1$ and $f_2$ are both variable and the points distribute themselves in a fan-shaped fashion with the apex denoting the lead composition which the system possessed at $t_1$. The lower boundary of the distribution of data points will have a slope age approaching $t_2$ while the upper boundary will, in an ideal situation, intersect the primary growth curve at $t_1$ and $t_2$. This behaviour can be most easily understood by considering Figure 21. Lead evolution according to the three stage model generally results in scattered points on an X-Y diagram. Only in the special cases of $f_1$ = constant or $f_2$ = constant are linear plots obtained. The $f_1$ = const./$f_2$ = variable model is a generally more plausible model from a geological standpoint and theoretically results in a family of parallel straight lines with a constant slope which depends only on $t_2$ (time of the second fractionation) and not on $t_1$ (time of the first U-Pb fractionation). If $f_1 = 1$ there is no fractionation of U-Pb system from $\mu_1$ at time $t_1$, therefore the evolution history reduces to a two-stage model. If $f_1$ becomes very large (i.e. large uranium loss or lead gain (with the same isotopic composition) occurs at time

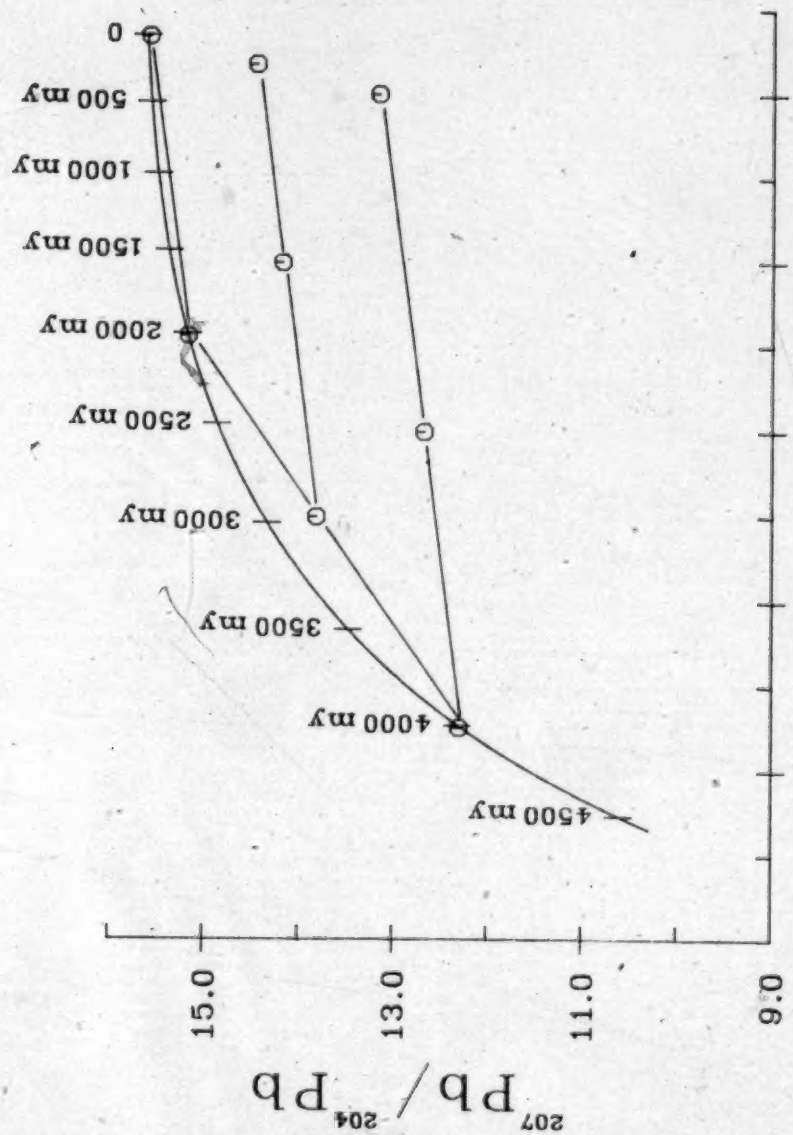


Figure 21. Pb isotopic evolution diagram for the samples which underwent three-stage evolution history. $\mu_1 = 9.85$, $T_o = 4570$ m.y., $a_o = 9.346$, $b_o = 10.218$, $t_1 = 4000$ m.y. and $t_2 = 2000$ m.y.

$t_1$), the limiting straight line will intersect the primary growth curve at $t_1$. Low values of $f_1$ imply uranium gain or lead loss (or both) occurred at the first fractionation event ($t_1$). In the case of $f_1$ = variable/$f_2$ = constant model, theoretically a family of straight lines all passing through the same point, i.e. $t_1$ of $\mu_1$ growth curve will result. The slopes and upper intercepts with the primary growth curve do not have any real meaning. This model is less geologically plausible since it requires constant fractional change for variable $\mu$ environments during the second fractionation event at time $t_2$. It is also somewhat contradictory in the case of the grand system remaining closed. The model allows for lead loss at the second fractionation event but not for a gain of lead with different isotopic compositions. If the global system remains closed and some of the subsystems with different $\mu$'s lose some of their lead (which has a different isotopic composition), other subsystems will be liable to gain that lead, violating the conditions for obtaining a rectilinear plot for a suite of samples analysed at present. A model consisting of more than three episodic stages would produce an overall distribution similar to the three stage model.

Rb-Sr Systematics

The Rb-Sr dating method is based on radioactive decay of the $^{87}Rb$ isotope to the $^{87}Sr$ isotope. The relationship

of the molar concentration of the daughter isotope to the molar concentration of the parent isotope, measured in the sample at present (t=0), is given by the following equation:

$$^{87}Sr = {}^{87}Rb[\exp(\lambda t) - 1] + {}^{87}Sr_o$$

where $^{87}Rb$ is the molar concentration of the $^{87}Rb$ isotope and $^{87}Sr$ is the molar concentration of the $^{87}Sr$ isotope, measured at present. $\lambda$ is the radioactive decay constant of $^{87}Rb = 1.42\times10^{-11} yr^{-1}$ (as suggested by Steiger and Jäger (1977)), t is the time of the initial isotopic homogenization measured positively into the past and $^{87}Sr_o$ is the amount of $^{87}Sr$ originally present.

Because of the presence of the other Sr isotopes and the convenience of handling isotopic ratios, the above equation is modified to include concentration of the $^{86}Sr$ isotope into:

$$^{87}Sr/^{86}Sr = {}^{87}Pb/^{86}Sr[\exp(\lambda t) - 1] + (^{87}Sr/^{86}Sr)_o.$$

This parametric equation (of the type $y = mx + n$) contains two different types of information that could be determined from two or more cogenetic samples, i.e. from the slope and initial $(^{87}Sr/^{86}Sr)$ ratio from the intercept. The model age determination from the single rock or mineral specimen requires an assumption about the initial strontium isotopic composition $(^{87}Sr/^{86}Sr)_o$.

The data from a suite of samples which have been isotopically homogenized at the same time (t) in the past may be evaluated in two ways. The more popular way is by plotting $^{87}Sr/^{86}Sr$ versus $^{87}Rb/^{86}Sr$ values. A cogenetic suite of samples which have been completely homogenized at the time the system was last disturbed should form a straight line known as an isochron (Figure 22).

Another way of representing the data is by following the evolution of $^{87}Sr/^{86}Sr$ with time, i.e. by plotting $^{87}Sr/^{86}Sr$ versus time (Figure 23). This is achieved by calculating the value of $^{87}Sr/^{86}Sr$ at a time approximately equal to the time of formation and joining this point to the presently measured $^{87}Sr/^{86}Sr$ ratio. By doing this for the cogenetic suite of samples, an array of lines will be obtained. The slopes of the lines are proportional to the $^{87}Rb/^{86}Sr$ ratio of each sample since its formation. All the lines intersect at the time equal to the time of isotopic homogenization and at the $^{87}Sr/^{86}Sr$ ratio that the suite had at that time.

The only possible advantage of this treatment over the standard isochron diagram is that it occasionally gives a clearer view of the evolution of the systems which have been disturbed after the initial homogenization. All other information obtained from this diagram is also obtainable from the isochron diagram.

The samples selected for dating may be a set of whole rocks selected from the single formation to give a

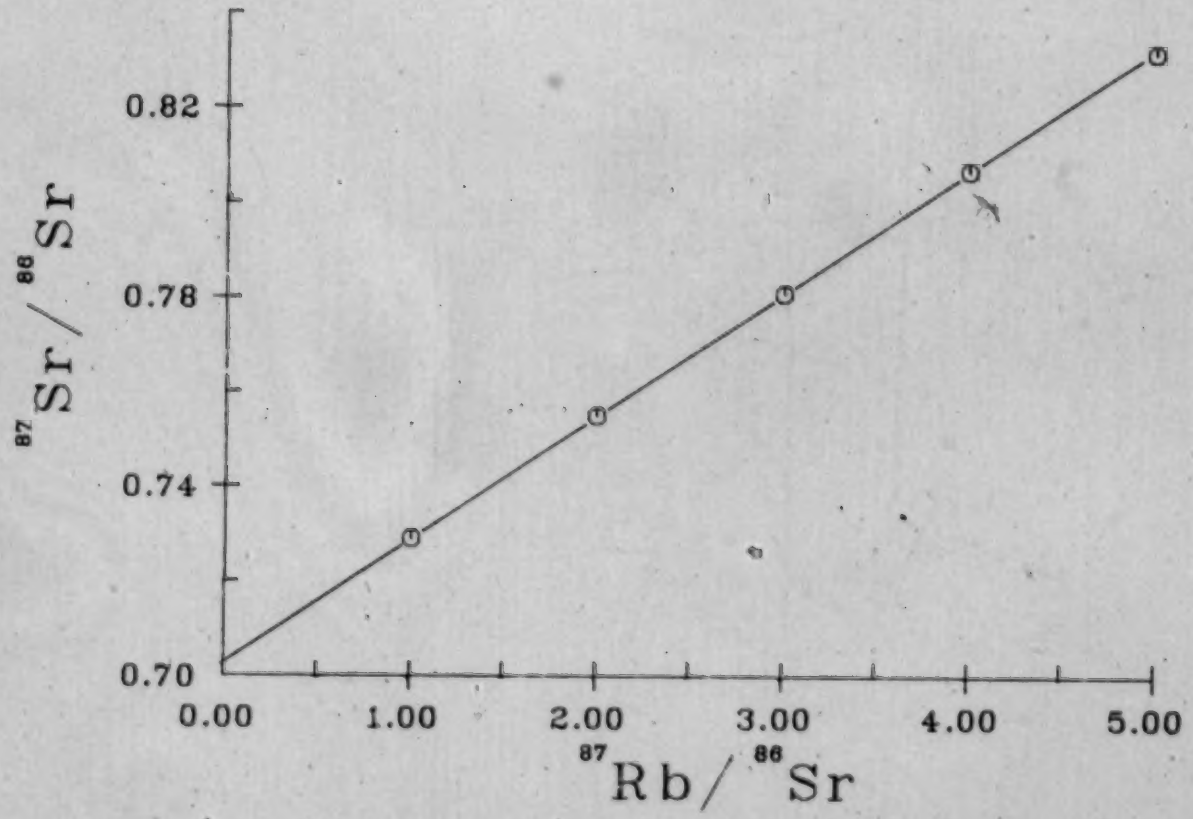


Figure 22. Rb-Sr diagram for the set of samples which were emplaced 1800 m.y. ago with an initial $^{87}Sr/^{86}Sr = 0.703$.

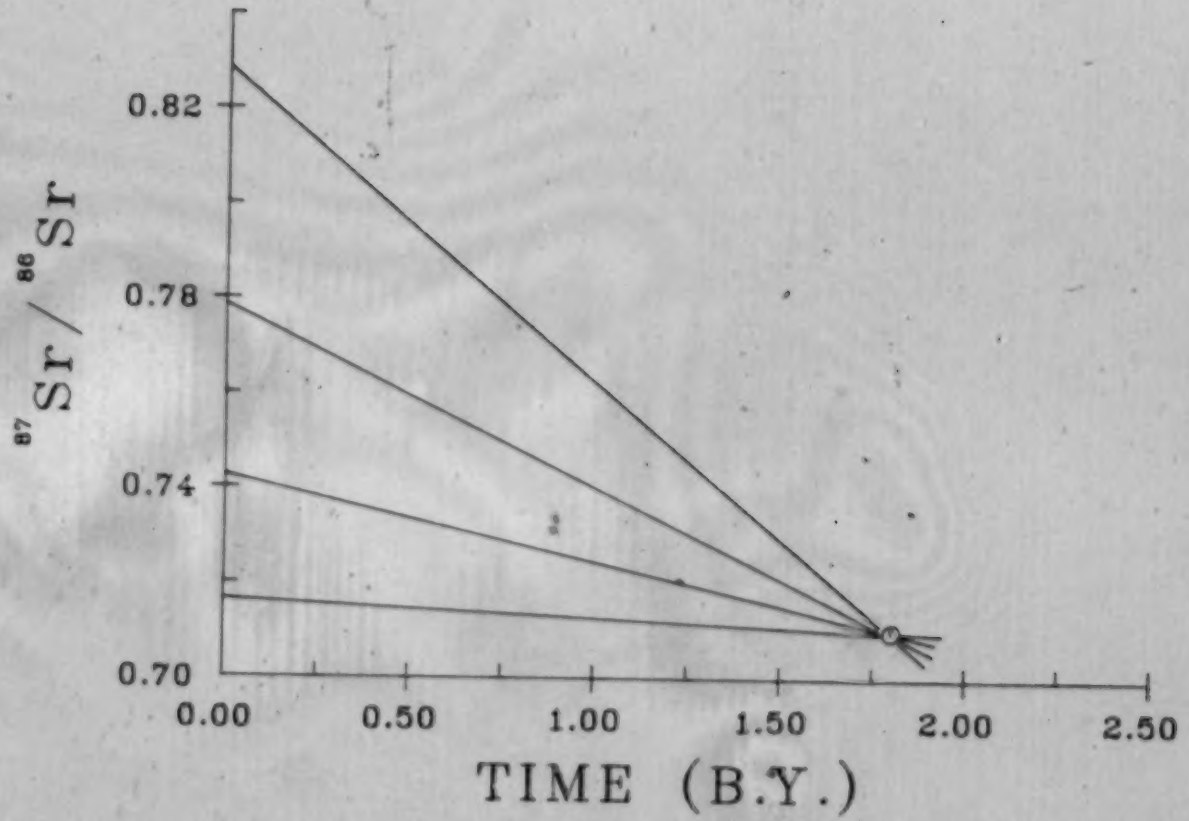


Figure 23. Sr growth lines diagram for the 1800 m.y. old suite of cogenetic samples.

broad range of Rb-Sr values, or they could be mineral separates from a single rock such as low-to-medium Rb-Sr K-feldspars or apatites and high Rb-Sr micas.

The usefulness of the Rb-Sr dating method is entirely dependent on the complete homogenization of the Rb and Sr isotopes at some time in the past and upon minerals and rock remaining closed systems to the migration of Rb and Sr from that time to the present.

If the samples to be dated are crystallized from magma and there was no subsequent disturbance of the system, through thermal or other events, the mineral separates and whole rock samples should give the same true age of the rock.

If the samples have been subjected to metamorphism of sufficient intensity to recrystallize some of the minerals or make them open to diffusion of Rb and Sr, Rb-Sr data of minerals will record the time of metamorphism and the Rb-Sr data of whole rocks the time of initial homogenization. This will hold true providing the range of Rb and/or Sr migration has been limited to an area smaller than the size of the whole rock.

A complete review of Rb-Sr systematics is given in Faure and Powell, 1972 and Faure, 1977.

## APPENDIX II

## ANALYTICAL METHODS

### General Laboratory Procedures

During the course of this work most of the separations, filament loadings and other operations were carried out in the filtered air laboratory or in a laminar flow hood equipped with an HEPA 100+ filter. The water used has been purified by passing through a large mixed bed ion exchange column and then distilling it twice in the sub-boiling stills. The first distillation was done in a glass still; water was fed into the smaller all-quartz still where a second distillation was completed. Nitric and hydrochloric acid, of reagent grade, were purified, first by distillation in an all-quartz sub-boiling still and then in a slow "two teflon bottle" vapour distillation still (Mattinson 1972). Hydrofluoric acid and hydrobromic acid of ARISTAR grade (BDH Chemicals Ltd.) were further purified by distillation in "two teflon bottle" stills. The sulphuric acid and perchloric acid used were of ULTREX grade supplied by J.T. Baker Ltd.

All of the isotope tracers used in this study were obtained from the National Bureau of Standards or Oak Ridge Laboratories and further calibrated and prepared by Dr. H. Baadsgaard of this department.

### Lead-Lead Analyses

One to two grams of finely-ground whole rock or

K-feldspar sample was weighed out in a 150 ml teflon beaker. Ten ml of concentrated HF and 5 ml of concentrated $HNO_3$ were added to the beaker and stirred. The beaker was then covered with a teflon "watch glass" and left overnight at approximately 80°C. The cover was removed, the solution evaporated to dryness and the residue "baked" for one hour at 105°C to remove excess HF. The residue was moistened with a few drops of concentrated $HNO_3$ and "baked" again for one-half hour to convert fluoride salts to nitrate salts. This step was repeated three times.

Ten mls of 8N $HNO_3$ was added to the residue, the beaker was covered and heated at 80°C for two hours. The solution and gelatenous precipitate was transferred to a 15 ml centrifuge tube and the gel was centrifuged off. The solution was poured back into the teflon beaker and evaporated to dryness.

A few drops of 2N HCℓ and 5 ml of 1N HBr were added to the dried residue (for larger samples more HBr is used), the beaker was covered and left overnight. The residual gel (if any) was centrifuged off before anion exchange separation.

The quartz columns used for anion exchange separation of lead were filled with CGA 540-X8, 100-200 mesh, anion exchange resin, supplied by J.T. Baker Ltd. Later on during this study, the resin was replaced with AG 1-X8, 100-200 mesh, anion exchange resin, supplied by BIO-RAD

Laboratories.

A resin bed of 0.4 cm × 12.5 cm was prepared by passing 30 ml of $H_2O$, 30 ml of 9N HCℓ and 30 ml of $H_2O$, and then equilibrated with 30 ml of 1N HBr. The sample solution was passed through the column, followed by 15 ml of 1N HBr and 3 ml of 2N HCℓ. The lead was eluted with 10 ml of 9N HCℓ and collected in the small teflon beaker. While the lead solution was being evaporated to dryness, the column was prepared for HCℓ ion exchange purification of lead by passing through it an additional 20 ml of 9N HCℓ followed by 30 ml of $H_2O$. The resin bed was set with 20 ml of 2N HCℓ.

The residue containing lead in the small teflon beaker was dissolved in 0.5 ml of 2N HCℓ and carefully, without disturbing the resin bed, loaded on the column. The solution was washed in with 3×2 ml of 2N HCℓ and the lead was eluted in the fraction between 6 and 12 ml of 2N HCℓ.

This fraction was evaporated to dryness and lead chloride was redissolved in a few drops of $H_2O$ (preferred concentration at this point is approximately 500 µg Pb/1 ml of solution).

Lead was loaded on a single, zone refined, rhenium filament, using the silica gel technique: first the drop of the aqueous lead solution was gently evaporated onto the rhenium filament (the usual amount of lead on the filament is 2-3 µgm). A large drop of silica gel slurry

in 0.8N $H_3PO_4$ was loaded on top and the reaction observed through the microscope. The current passing through the filament was increased to 1.2 amps. The excess water evaporated, the cloudy gel solution began to liquify and clear up. At 1.4 amps the drop on the filament was completely clear and at 1.6 amps lead-phosphosilicate started precipitating. At around 2.0 amps phosphoric acid was fumed off. The filament was brought, briefly, to "dull red" by increasing the current to approximately 2.5 amps.

Maximum lead blank, for up to 2.5 gm of rock sample, was measured to be not more than 15 nanograms, which is generally well below 0.5 per mil of total lead in the sample and is considered to have a negligible effect on the isotopic ratio in this study.

A filament with lead sample was introduced into ALDERMASTON MICROMASS MM30 solid source mass spectrometer. After the pump-down, the temperature of the filament was raised to 1400°C (as determined by the optical pyrometer). The initially erratic lead beam stabilizes usually after 30 minutes. The mass spectrometer was operated in the peak switching mode and with the Faraday cup collection system. The acceleration voltage used was 8 kv and the data collection and reduction were performed on line by an HP9825 computer. The measuring error of the instrument was better than 0.15 per mil (standard error of the weighted mean ratio).

## TABLE VIII

Isotopic Analyses of NBS SRM-981

| Measured $^{206}Pb/^{204}Pb$ | $F_6 = \frac{\text{measured}}{\text{true}}$ | Measured $^{207}Pb/^{204}Pb$ | $F_7 = \frac{\text{measured}}{\text{true}}$ | Measured $^{208}Pb/^{204}Pb$ | $F_8 = \frac{\text{measured}}{\text{true}}$ |
|---|---|---|---|---|---|
| 16.9371 | NBS value | 15.4913 | NBS value | 36.7213 | NBS value |
| 16.9134 | 0.99862 | 15.4643 | 0.99826 | 36.6339 | 0.99762 |
| 16.9030 | 0.99799 | 15.4447 | 0.99699 | 36.5780 | 0.99612 |
| 16.9014 | 0.99789 | 15.4485 | 0.99742 | 36.6028 | 0.99677 |
| 16.9108 | 0.99845 | 15.4596 | 0.99795 | 36.6116 | 0.99701 |
| 16.9037 | 0.99803 | 15.4476 | 0.99718 | 36.5691 | 0.99586 |
| 16.9036 | 0.99802 | 15.4550 | 0.99766 | 36.6017 | 0.99674 |
| 16.9029 | 0.99798 | 15.4424 | 0.99684 | 36.5780 | 0.99610 |
| 16.8934 | 0.99742 | 15.4481 | 0.99721 | 36.5545 | 0.99546 |
| Mean correction coefficients | 0.99805 ±.00036 | | 0.99742 ±.00050 | | 0.99646 ±.00070 |

Fractionation per mass unit: 0.79°/$_{oo}$

$^{204}Pb$ measuring error: 0.31°/$_{oo}$

Overall 1σ errors assigned to this type of ratio in this study are:

$^{206}Pb/^{204}Pb$ = 0.36°/$_{oo}$ $^{207}Pb/^{204}Pb$ = 0.50°/$_{oo}$ $^{208}Pb/^{204}Pb$ = 0.70°/$_{oo}$

The fractionation correction factors for measured lead ratios, the overall error assigned to the studied samples and the reproducibility of measurements were determined by repetitive analyses of NBS SRM-981 common lead standard. The obtained results are given in Table VIII.

Lead-Uranium-Thorium Analyses

The samples analysed for lead-uranium or lead-uranium-thorium were uraninites and monazite-rich mineral fractions.

The minerals were originally separated from their respective powdered whole rock samples utilizing magnetic and heavy liquid mineral separation. Three of the samples contained uraninite grains large enough to be picked under the microscope. The fourth sample contained some uraninite intergrown with monazite and the fifth sample did not have any visible uraninite. Intergrown uraninite was leached with cold 4H $HNO_3$ for three hours.

From the remainder of the heavy minerals, impurities such as pryite, molybdenite, occasional biotite flakes and other mineral grains were removed under the microscope so that a mineral concentrate containing more than 50% monazite was obtained. The total amount of the samples available ranged from less than 0.1 mg for tiny uraninite cubes to up to 30 mg for large monazite concentrates.

The uraninite samples were dissolved in 4N $HNO_3$ and

monazite-rich fractions (after washing in warm 2N $HNO_3$) and were dissolved in 5 ml of concentrated HF and 2 ml of concentrated $HNO_3$ in a teflon decomposition vessel similar to that of Krogh (1973). The monazite solution was evaporated to dryness and the residue converted to nitrate form by treating it with a few drops of concentrated $HNO_3$ and then it was redissolved in 4N $HNO_3$. Both uraninite and monazite solutions were divided into two aliquots. The larger ones were used for Pb-IR determination and the smaller ones for Pb-U-Th concentration determination. To this aliquot $^{208}Pb$, $^{235}U$ and $^{230}Th$ tracers of known amounts were added and the solution evaporated to dryness and redissolved in a drop of 2N HCℓ and 2 ml of 1N HBr.

Lead from both Pb-IR and Pb-U-Th-ID aliquots was purified in the same manner as described previously in the section on whole rock lead separations. The mixture of Pb, U and Th from the isotope dilution aliquot was loaded on the HBr column, the column was eluted with 1N HBr and 2N HCℓ (lead was "stripped" later with 9N HCℓ) and the collected solution containing U and Th was evaporated to dryness. The residue was carefully converted to nitrate form with a few drops of concentrated $HNO_3$ and again evaporated to dryness.

In the meantime, a glass column was filled with AG1-X8, 100-200 mesh, anion exchange resin in nitrate form. A resin bed of 0.8 cm × 12.5 cm was prepared by passing

50 ml of $H_2O$, 30 ml of 7N $HNO_3$ and 50 ml of $H_2O$ and finally equilibrated with 30 ml of 7N $HNO_3$.

The dry residue containing uranium and thorium was picked up in a few drops of 7N $HNO_3$ and carefully loaded on the resin bed. The column was eluted with 6×2 ml of 7N $HNO_3$, after which uranium and thorium were "stripped" off the column with 20 ml of $H_2O$. This solution was evaporated to dryness, the uranium and thorium were redissolved in a drop of $H_2O$ and the drop was carefully evaporated on the rhenium side filament of the bead equipped with a double filament. On the center filament the corresponding Pb-ID was loaded, so that all three concentration measurements were performed using one double filament bead.

The bead was introduced in the source chamber of the MM30 mass spectrometer. After the lead analysis (from the center filament) was completed, the center filament temperature was raised to 2130°C. The current flowing through the side filament was increased until a steady uranium beam was obtained. Uranium peak switching data collection and reduction were done by an HP9825 computer.

In order to obtain a thorium beam, uranium was "burned off" by increasing the side filament current by about one additional ampere. The ionization of thorium began when the center filament temperature was raised to 2230°C. Data collection starts as soon as the thorium beam reaches 20% intensity on a "GAINX100" scale.

Overall errors on $^{207}Pb/^{235}U$, $^{206}Pb/^{238}U$ and $^{208}Pb/^{232}Th$ are relatively difficult to assess, due to the many possible sources of random and systematic error, such as mass discrimination, blank, etc.

Radiogenic lead measurements have not been corrected for mass discrimination since it is negligible for highly radiogenic samples. The presently assumed level of accuracy for the Pb/U and Pb/Th ratios in the laboratory is better than 1% at two sigma. These error limits have been assigned to all the measurements in this study and therefore have been used for line fittings and age calculations.

Rubidium-Strontium Analyses

Powdered whole rock samples were analysed by X-ray fluorescence spectrometry to give an estimate of Rb and Sr concentrations. From these results enough sample was used to provide about 15-20 µg of strontium and 15-20 µg of rubidium for analyses.

Rubidium separation:

Enough sample was weighed out into a teflon beaker to provide approximately 15 µg of rubidium, $^{87}Rb$ tracer was added along with 10.0 ml of concentrated HF and a few drops of concentrated $HNO_3$. The beaker was covered with teflon "watch glass" and heated for a few hours at approximately 80°C. After the decomposition of the sample was completed, the solution was transferred to

the platinum dish, 5 drops of concentrated $H_2SO_4$ were added and the solution was evaporated to dryness. The temperature was raised, excess $H_2SO_4$ was fumed off and the sample was ignited at 800°C for 30 minutes with the Bunsen burner. When cooled, the residue was leached with a few drops of $H_2O$ and the solution (0.25-0.5 ml in total) was transferred to a 3 ml centrifuge tube. Several drops of pure concentrated $HClO_4$ were added, resulting in the precipitate of $HClO_4$ and coprecipitated $RbClO_4$. The tube was centrifuged and the supernate was poured off. The walls of the tube were then rinsed carefully with water. A drop or two of water was added to the precipitate so that some of it dissolves. A small amount of this solution was carefully evaporated, and then fused on the rhenium side filament.

Strontium separation:

The powdered rock sample was weighed out into a 150 ml teflon beaker, the sides of the beaker were rinsed with several ml of water to bring down material which might have clung electrostatically to the walls. A preweighed $^{84}Sr$ tracer was quantitatively added to the sample in the teflon beaker. The beaker was then left uncovered at low heat so that the water would slowly evaporate. When the residue was dry, 10 ml of concentrated HF and 5 ml of concentrated $HNO_3$ were added to the beaker and after stirring gently the beaker was covered

with teflon "watch glass" and left overnight at approximately 80°C. The cover was then removed, the solution evaporated to dryness and the residue was "baked" at 105°C for one hour. The fluoride salts were converted to nitrate form by moistening the residue with concentrated $HNO_3$ and evaporating it to dryness. This step was repeated three times. Ten mls of 8N $HNO_3$ were added to the beaker and heated gently for a few hours, stirring occasionally to redissolve the residue. The solution was evaporated to half of its original volume, transferred to the centrifuge tube, the undissolved silica gel (if any) was centrifuged off. The supernate was temporarily transferred to its teflon beaker, the gel from the tube was discarded, the tube was rinsed and the supernate was returned to the centrifuge tube.

Three drops of concentrated $Ba(NO_3)_2$ solution were added to the sample solution, stirred, and the total volume made up to 10 ml with concentrated $HNO_3$. The sides of the centrifuge tube were rubbed with the teflon rod to initiate precipitation of fine $Ba(NO_3)_2$ crystals, which coprecipitate strontium ions. After standing for two hours, the $Ba(NO_3)_2$ was centrifuged off and the supernate was discarded.

During the latter part of this study Rb-Sr analyses were performed using mixed Rb-Sr "spiking" techniques. This involves adding mixed tracer to the powdered rock sample and following the strontium separation procedure to the point of centrifuging off $Ba(NO_3)_2$. The supernate

containing rubidium is transferred to a platinum dish, 5 drops of $H_2SO_4$ are added and the rubidium separation procedure is followed.

The $Ba(NO_3)_2$ precipitate was washed with concentrated $HNO_3$ and then recrystallized by dissolving it first in a minimum amount of $H_2O$ and reprecipitating it by adding 8 ml of concentrated $HNO_3$ and rubbing the walls of the tube with a teflon rod. After standing for two hours, the precipitate was centrifuged off, the supernate was discarded, the tube was washed carefully with 2N HCℓ so that the precipitate is not disturbed, and finally the precipitate was dissolved in approximately 0.5 ml of 2N HCℓ.

A quartz cation exchange column was prepared to separate barium and strontium. An 0.4 cm × 16 cm column bed (approx. 2 ml by volume) of DOWEX 50W-X12, 100-200 mesh cation exchange resin was prepared by passing 30 ml of $H_2O$, 30 ml of 9N HCℓ, 30 ml of $H_2O$ and finally 30 ml of 2N HCℓ. The solution containing barium and strontium was carefully loaded on the column without disturbing the resin bed. The column was eluted with 2N HCℓ and strontium was collected in the eluted fraction between 12 ml and 20 ml.

The strontium solution was evaporated to dryness, $SrCℓ_2$ was picked up in a small drop of water and gently evaporated on a rhenium side filament of a double filament.

Mass spectrometric analyses were performed using an ALDERMASTON MM30 mass spectrometer. Later, rubidium measurements were made using a home-built 12 inch, 90° magnet sector, solid source mass spectrometer with an on line TI 980A minicomputer. This instrument was operated in the peak switching mode, with 5 KV acceleration voltage and a Faraday cup collection system.

Strontium and rubidium blanks for the initial samples which were done by spiking separate aliquots of samples, were measured to be a 2 ng strontium blank and a 4 ng rubidium blank. Blank measurements on the mixed spike procedure produced a 5 ng strontium blank and an 8 ng rubidium blank. In both cases the effect of the blank was considered negligible and no blank corrections were applied to the results.

$^{87}Sr/^{86}Sr$ measuring precision and overall errors, assigned to the $^{87}Sr/^{86}Sr$ ratios of the analysed samples, were determined by repetitive analyses of NBS SRM-987 strontium carbonate standard and by comparing the obtained results with the NBS suggested values. It was found that the results obtained in this study were slightly higher than values suggested by NBS (Table IX). Since the discrepancies are very small, no corrections of the measured $^{87}Sr/^{86}Sr$ ratios were made.

Rubidium fractionation correction coefficient and reproducibility were determined by repetitive measurements of isotopic ratios performed on the NBS SRM-984

rubidium chloride standard and on rubidium extracted from the common granite sample (Table IX).

The individual errors for $^{87}Rb/^{86}Sr$ are somewhat difficult to determine precisely because of the many possible sources of systematic error such as mass discrimination, blank, etc.

The accepted laboratory accuracy for $^{87}Rb/^{86}Sr$ during this study was 1% at two sigma level.

TABLE IX

Isotopic Analyses of Rubidium and Strontium Standards

| NBS suggested value: $^{87}Rb/^{85}Rb = 0.3856$ | | NBS suggested value: $^{87}Sr/^{86}Sr = 0.71014 \pm .0002$ | |
|---|---|---|---|
| Measured $^{87}Rb/^{85}Rb$ | | Measured $^{87}Sr/^{86}Sr$ | |
| 0.38513 | SRM-984 | 0.71034 | SRM-987 |
| 0.38533 | " | 0.71019 | " |
| 0.38488 | " | 0.71033 | " |
| 0.38500 | " | 0.71024 | " |
| 0.38429 | " | 0.71032 | " |
| 0.38523 | Common Granite Sample | 0.71011 | " |
| 0.38401 | " | 0.71010 | " |
| 0.38433 | " | 0.71007 | " |
| 0.38477 | " | 0.71007 | " |
| Mean: 0.38477 ±.00048 | | 0.71021 ±.00011 | |
| 1σ error: 1.25°/₀₀ | | 1σ error: 0.15°/₀₀ | |

Rubidium fractionation correction factor:

$$\frac{(^{87}Rb/^{85}Rb)_{measured}}{(^{87}Rb/^{85}Rb)_{true}} = \frac{0.38477}{0.3856} = 0.99772$$